

# The Assessment of Bullet Wound Trauma Dynamics and the Potential Role of Anatomical Models

Nicholas Russell Maiden

Discipline of Anatomy and Pathology  
School of Medical Sciences  
The University of Adelaide

A thesis submitted in partial fulfilment of the requirements for the  
Degree of Doctor of Philosophy

## DEDICATION

This thesis is dedicated to my late wife Wendy without whose love, support and patience, this fascinating journey and academic milestone would not have been possible. She suffered through many lonely days and evenings as I effectively worked two jobs, as a police forensic firearms examiner and attending to my doctoral studies. Sadly cancer took her life all too early, and we never got to spend the quality time together that we had planned post thesis. However, I have kept my promise to her to complete this work after she passed on. There is still further follow up research I would like to complete on a post doctoral basis, and I know she would support the next phase of this academic journey as well.

*“The advancement of science is slow; it is affected only by virtue of hard work and perseverance. And when a result is attained, should we not in recognition connect it with the efforts of those who have preceded us, who have struggled and suffered in advance? Is it not truly a duty to recall the difficulties which they vanquished, the thoughts which guided them; and how men of different nations, ideas, positions and characters, moved solely by the love of science, have bequeathed to us the unsolved problem? Should not the last comer recall the researches of his predecessors while adding in his turn his contribution of intelligence and of labor? Here is an intellectual collaboration consecrated entirely to the search for truth, and which continues from century to century”.*

Henri Moissan (1852-1907)

## TABLE OF CONTENTS

<b>1. The Science of Wound Ballistics .....</b>	<b>25</b>
1.1 Introduction .....	25
1.2 Aim .....	25
1.3 Hypothesis .....	26
1.4 Historical Overview of Wound Ballistics Research.....	27
1.4.1 Introduction.....	27
1.4.2 Historical Developments .....	28
1.4.3 Explosive effects.....	28
1.4.4 Stopping power.....	29
1.4.5 Mechanisms .....	30
1.4.6 Forensic Applications and Models .....	31
1.4.7 Conclusion.....	32
1.5 Mechanisms of Bullet Wound Trauma .....	32
1.5.1 Introduction.....	32
1.5.2 Physiological Responses .....	33
1.5.3 Tissue Damage .....	34
1.5.4 Shock Wave Injuries .....	36
1.5.5 Bullet Design .....	37
1.5.6 Military Rifle Bullet Design .....	38
1.5.7 Calibre 5.56x45mmNATO.....	38
1.5.8 Calibre 7.62x39mmSoviet.....	40
1.5.9 Calibre 9mm Luger .....	41
1.5.10 Conclusion.....	42
1.6 The Use of Tissue Simulants in Wound Ballistics Research.....	43
1.6.1 Introduction.....	43
1.6.2 General Benefits and Properties of Tissue Simulants .....	44
1.6.3 Cadaver Testing .....	45
1.6.4 Animal Testing.....	46
1.6.5 Ballistics Ordnance Gelatine.....	46
1.6.6 New Synthetic Simulants .....	49
1.6.7 Computational Models and Physical Surrogates.....	51
1.6.8 Conclusion.....	52

1.7 Mechanical Properties of Selected Human Tissue .....	53
1.7.1 Introduction.....	53
1.7.2 Bio-mechanical Properties of Tissue.....	53
1.7.3 High and Low Velocity Impact Characteristics .....	59
1.7.4 Conclusion.....	62
1.8 Methods of Injury Assessment in Bullet Wound Trauma – A Military and Police Perspective .....	63
1.8.1 Introduction.....	63
1.8.2 Measures and Indices.....	64
1.8.3 Lethality versus Incapacitation .....	64
1.8.4 Abbreviated Injury Scale .....	65
1.8.5 Other Injury Scoring Systems .....	67
1.8.6 Injury Severity Score (ISS).....	68
1.8.7 New Injury Severity Score (NISS) .....	69
1.8.8 Trauma Injury Severity Score (TRISS).....	69
1.8.9 International Classification of Disease Injury Severity Score (ICISS) .....	70
1.8.10 Trauma Registry Abbreviated Injury Scale Score (TRAIS).....	71
1.8.11 Anatomic Profile Score (APS).....	71
1.8.12 Maximum Abbreviated Injury Score (MAXAIS).....	72
1.9 Previous Wound Trauma Models .....	73
1.9.1 Kinetic Energy Models .....	73
1.9.2 Stopping Power Model.....	74
1.9.3 Relative Incapacitation Index (RII) .....	76
1.9.4 Federal Bureau of Investigation (FBI) Test Program.....	77
1.9.5 The Verwundungsmodell Schütze (VeMo-S).....	77
1.9.6 Knock Down Power .....	77
1.9.7 Mathematical models .....	78
1.9.8 Combat and Street Shooting Data Modelling .....	78
1.9.9 Conclusion.....	79
<b>2. Materials and Methods .....</b>	<b>81</b>
2.1 Human and Animal Ethics .....	81
2.2 Data Collection and Experimental Procedures .....	81
2.2.1 An Analysis of the Characteristics of Thoracic and Abdominal Injuries and Ballistic Data in Gunshot Homicides in Israel .....	81

2.2.2	Tensile Strength Biomechanics of Thawed Cadavers and the Implications for Wound Ballistics Research.....	82
2.2.3	Pig Organ Energy Loss Comparison Experiments Using BB Rifle Pellets.....	83
2.2.4	Statistical Analysis .....	89
2.2.5	Ballistics Ordnance Gelatine – How Different Concentrations, Temperatures and Curing Times Affect Calibration Results .....	90
2.2.6	Statistical Analysis .....	91
2.2.7	Anatomical Model Pilot Study .....	91
<b>3.</b>	<b>An Analysis of the Characteristics of Thoracic and Abdominal Injuries and Ballistic Data in Gunshot Homicides in Israel.....</b>	<b>98</b>
3.1	Introduction .....	98
3.2	Data Collection Study .....	98
3.3	Results .....	98
3.4	Discussion.....	105
3.5	Conclusion .....	109
<b>4.</b>	<b>Tensile Strength Biomechanics of Thawed Cadavers and the Implications for Wound Ballistics Research .....</b>	<b>111</b>
4.1	Introduction .....	111
4.2	Experimental Design .....	111
4.3	Results.....	111
4.4	Discussion.....	113
4.5	Conclusion .....	116
<b>5.</b>	<b>Pig Organ Energy Loss Comparison Experiments Using BB Rifle Pellets .....</b>	<b>118</b>
5.1	Introduction .....	118
5.2	Experimental Design .....	118
5.3	Results.....	119
5.3.1	Energy Loss – Ordnance Gelatine Formulations and Simulant ‘A’ .....	119
5.3.2	Energy Loss – Organs/Tissues at Room Temperature .....	119
5.3.3	Energy Loss – Organs/Tissues at 37°C.....	119
5.3.4	Energy Loss – Organs/Tissues at 4°C .....	120
5.4	Sample Decomposition.....	120
5.5	Energy Grouping Results Summary .....	120

5.6 Discussion .....	129
5.7 Limitations of Study .....	134
5.8 Conclusion .....	134
<b>6. Ballistics Ordnance Gelatine – How Different Concentrations, Temperatures and Curing Times Affect Calibration Results .....</b>	<b>137</b>
6.1 Introduction .....	137
6.2 Experimental Design .....	137
6.3 Results.....	137
6.3.1 10% Ordnance Gelatine at 4°C 250 Bloom (FBI Standard).....	137
(a) 21 Hours Curing Time .....	137
(b) 100 Hours Curing Time .....	138
(c) 3 Weeks Curing Time.....	138
6.3.2 20% Ordnance Gelatine at 10°C 250 Bloom (NATO Standard).....	138
(a) 21 Hours Curing Time.....	138
(b) 100 Hours Curing Time .....	138
6.3.3 20% Ordnance Gelatine at 10°C using 285 Bloom .....	138
(a) 21 Hours Curing Time .....	138
6.3.4 20% Ordnance Gelatine at 20°C using 285 Bloom .....	139
(a) 100 Hours Curing Time .....	139
6.4 Discussion .....	142
6.5 Conclusion .....	146
<b>7. Anatomical Model Pilot Study.....</b>	<b>148</b>
7.1 Introduction .....	148
7.2 Experimental Design .....	148
7.3 Results.....	149
7.3.1 Test 1 (Bare gelatine control block) .....	149
7.3.2 Test 1A (Repeat - bare gelatine control block).....	149
7.3.3 Test 2 (Bare gelatine plate with air gap and gelatine block).....	152
7.3.4 Test 3 (Repeat - bare gelatine plate with air gap and gelatine witness block) .....	153
7.3.5 Test 4 (Skin simulatant attached to gelatine witness block).....	154
7.3.6 Test 5 (Gelatine plate with skin and bone composite, air gap and gelatine block).....	155
7.3.7 Test 6 (Gelatine plate with skin and bone composite, bubble wrap, air gap, bubble wrap and a gelatine block) .....	158

7.3.8	Test 7 (Gelatine plate with skin and bone composite, bubble wrap, air gap, bubble wrap, followed by a second gelatine plate with skin and bone composite, and a gelatine block) .....	161
7.4	Discussion.....	171
7.5	Conclusion .....	175
<b>8.</b>	<b>Conclusions .....</b>	<b>178</b>
8.1	An Analysis of the Characteristics of Thoracic and Abdominal Injuries and Ballistic Data in Gunshot Homicides in Israel.....	178
8.2	Unpredictable Tensile Strength Biomechanics May Limit Thawed Cadaver Use in Wound Ballistics Research.....	178
8.3	Porcine Organ Energy Loss Comparison Experiments Using BB Rifle Pellets .....	179
8.4	Ballistics Ordnance Gelatine – How Different Concentrations, Temperatures and Curing Times Affect Calibration Results .....	180
8.5	Anatomical Model Pilot Study.....	180
8.6	Thesis Hypothesis Conclusion.....	181
8.7	Future Directions .....	182
8.7.1	Anthropometric Data.....	182
8.7.2	High Velocity and Energy Retardation Tests.....	183
8.7.3	Develop Candidate Simulants.....	183
8.7.4	Model Validation .....	184
8.7.5	Scoring System .....	184
8.7.6	Finite Element Analysis Model .....	184

**References**

## ABSTRACT

### Background

It is hypothesised that an anatomical simulant model, that replicates the heterogeneous nature of human organs and tissues, will provide a more reliable and accurate method of evaluating the pathological features and incapacitation potential of ammunition in a weapons system than homogeneous bare ordnance gelatine alone. The use of frozen and thawed cadavers for simulant development was also examined. To develop a model, the most critical organs and tissues that sustain bullet wound trauma within the thorax and abdomen must be determined. Next a suitable method for establishing and matching the relevant biomechanical properties with candidate simulant materials must be developed, and an appropriate scoring system adopted.

### Method

De-identified wound trauma data from 197 homicidal gunshot post mortem examinations in Israel were obtained between 2000-2001 and 2004-2008. The corresponding forensic ballistics data was only available for the cases between 2004 and 2008. The major organs involved, type of wounds, cause of death (COD), most common bullet paths, distances involved, firearm calibres and bullet types were established.

Tensile strength tests were undertaken on selected tissue samples from an un-embalmed cadaver that had been frozen and thawed five times, which maximised the effects of repeated cycles. The universal test equipment Hounsfield H50KM machine was used to apply uniaxial tension until tissue failure occurred. The maximum tensile strength results in  $\text{g/mm}^2$  were compared against corresponding data from the literature.

Energy loss tests were conducted on fresh porcine organs/tissues using steel 4.5mm BB pellets fired from a Daisy® brand air rifle. Each organ/tissue was tested at room temperature and 37°C (body temperature). They were compared to Federal Bureau of Investigation (FBI) and North Atlantic Treaty Organisation (NATO) specification ordnance gelatine, as well as a candidate simulant material. A limited number of tests were also conducted at 4°C for further comparison purposes. Two chronographs



measured BB pellet velocity before and after each test material was perforated and the difference was established in m/s. The resulting energy loss was established using the formula  $KE = \frac{1}{2} mv^2$ .

FBI and NATO specified ordnance gelatine of 250 and 285 Bloom strengths were manufactured using tap water, reverse osmosis (RO) water and de-ionized water. They were allowed to cure for 21 hours, 100 hours and 3 weeks. The FBI calibration standard was used for all formulations as there is no separate standard for the NATO formulation in the literature.

An Australian Defence Force (ADF) AUSTEYR model F88 ICW (individual combat weapon) in calibre 5.56x45mm NATO was used with standard issue ASF1 ball ammunition. Large FBI specification ordnance gelatine blocks were manufactured and thin gelatine/composite plates were used to simulate subcutaneous tissue and fat, as well as to provide a platform for the attachment of a skin simulant and to embed bone/rib composite within. A 250mm air gap and bubble wrap was used to simulate an expanded lung. The gelatine/composite plates were secured to a wooden cradle and the gelatine blocks were positioned behind it. The F88 ICW was fixed in a remote firing device 50m from the target and a chronograph 3m in front of the rifle measured bullet velocity. Test results were recorded using two high speed 'Photron Fastcam' digital cameras. Maximum three dimensional permanent cavity dimensions were obtained using a vernier gauge, and temporary cavity measurements were taken from high speed video images.

## **Results**

The homicide study established that males represent 91% of gunshot victims. Of the 999 bullet wounds recorded, males were struck in the body an average of 5.2 occasions, with 2.2 of these bullets striking the thorax and/or abdomen. A contributing factor to the frequency of bullet strikes was the type of firearms involved, namely semi automatic pistols in the predominant calibre 9mm Luger, and assault rifles in calibre 5.56x45mm and calibre 7.62x39mm Soviet. Full metal jacket bullets were used in most instances and the majority of shootings (N=124) occurred at ranges estimated at 1m or greater. The most common bullet path was front to back in 66% of cases, followed by back to front in 27% of cases. Entry wounds occurred more often on the left side of the thorax, abdomen and back (N=253) compared to the right (N=172). The most common

critical organs/tissues to sustain bullet trauma in descending order were; heart, lungs, liver, aorta, spleen, kidneys and vena cava. Ribs were struck by most bullets that entered the thorax. Multiple organ injury was listed in 146 of the 192 cases where a specific COD was determined by the pathologist.

The following tensile strength results were achieved from the cadaver study: heart 3.56g/mm<sup>2</sup>, kidney 10.27g/mm<sup>2</sup>, oesophagus 22.08g/mm<sup>2</sup>, skeletal muscle 29.46g/mm<sup>2</sup>, ascending aorta 59.98g/mm<sup>2</sup>, trachea 155.40g/mm<sup>2</sup>, spleen 4.65g/mm<sup>2</sup>, liver 10.83g/mm<sup>2</sup>, pancreas 15.18g/mm<sup>2</sup>, lung 29.94g/mm<sup>2</sup>, pericardium 136.84g/mm<sup>2</sup>, skin (abdomen) 355.26 g/mm<sup>2</sup> and skin (thorax) 407.88g/mm<sup>2</sup>. These data were compared to published results obtained from non-frozen tissues from elderly persons, recognising that tensile strength values were only available for the following organs and tissues at the 95% degree of confidence: heart 9.2±0.95g/mm<sup>2</sup>; kidney 4±0.20g/mm<sup>2</sup>, oesophagus 51±1.1g/mm<sup>2</sup>, skeletal muscle 9±0.30g/mm<sup>2</sup>, ascending aorta 68±2.4g/mm<sup>2</sup>, trachea 150±6.5g/mm<sup>2</sup>. It can be seen that some results from the test cadaver were higher and some lower than the published results, with trachea recording the only similar result. This indicates that the freezing and thawing process may change the tensile strength of tissues in unpredictable ways. Therefore, bio-mechanical research should avoid the use of frozen/thawed tissues and organs.

The major agreement between the porcine energy loss tests were: FBI specification gelatine was similar ( $p>0.05$ ) to heart and lung at room temperature and 37°C; spleen was similar to NATO specification gelatine at room temperature and 37°C; candidate Simulant 'A' was similar to hindquarter muscle at room temperature and 37°C and hindquarter muscle, kidney and spleen were similar to each other at room temperature and 37°C. Liver and kidney, and liver and fat were similar to each other at 4°C.

The use of different water types had no effect upon ordnance gelatine calibration results. However, different temperatures, concentrations and curing times did have a significant effect. Neither of the two NATO 20% formulations met the same calibration standard as the FBI 10% formulation. The penetration depths achieved for the FBI formulations at both 3°C and 4°C were closest to the recommended calibration standard after 3 weeks curing time. A 20% concentration of 285 Bloom at 20°C met the same FBI calibration standard after 100 hours of curing and can be considered comparable.

The anatomical model pilot tests demonstrated the benefit of using simulants that are more representative of the heterogeneous nature of human organs/tissues. It was found that by combining skin, bone and other simulant materials with ordnance gelatine, the behaviour of a military full metal jacket (FMJ) rifle bullet changes with regard to the earlier onset of temporary cavitation, reduced penetration depth and a higher degree of bullet yaw compared to simulations using only bare FBI specification ordnance gelatine. This occurs because more energy is consumed negotiating the various anatomical simulants, which means wounding is likely to occur much earlier, and organs that are deeper within the body may not be affected to the same degree. These factors will impact significantly upon injury severity in real tactical scenarios.

### **Conclusion**

The experimental studies provide the framework for the development of a heterogeneous model for bullet trauma simulations of the thorax and abdomen. This model would be more representative of actual wound trauma than bare ordnance gelatine alone. This conclusion was arrived at by identifying the most critical organs/tissues for modelling purposes. Their energy loss values (J/m) were established and the method adopted allows for comparable simulants to be developed. Porcine energy loss tests showed that FBI specification gelatine is similar to heart and lung, but different to hind quarter muscle and most of the other 'critical' organs and tissues within the thorax and abdomen. NATO specification gelatine is a suitable simulant for spleen, and test Simulant 'A' is a suitable simulant for both hindquarter muscle and kidney. A separate simulant would be required for liver, fat and aorta.

Frozen and thawed cadaveric tissue was shown to produce unpredictable tensile strength data and is therefore unsuitable for simulant development. The limitations of using FBI and NATO specification ordnance gelatine was highlighted when changes to bloom number, temperature and curing times altered calibration results. Therefore, temperature stable synthetic simulants such as Simulant 'A' are preferable.

The anatomical model pilot tests clearly demonstrated that the addition of simulant materials directly affects wound severity simulations compared with bare ordnance gelatine alone. This in turn affects interpretation of real life situations. The AIS 2005/2008 and MAXISS scoring systems are deemed appropriate to grade the lethality potential of model simulations. Therefore, the original hypothesis has been validated.

**DECLARATION**

I certify that this work contains no material which has been accepted for the award of any other degree or diploma in my name in any university or other tertiary institution and, to the best of my knowledge and belief, contains no material previously published or written by another person, except where due reference has been made in the text. In addition, I certify that no part of this work will, in the future, be used in a submission in my name, for any other degree or diploma in any university or other tertiary institution without the prior approval of the University of Adelaide and where applicable, any partner institution responsible for the joint-award of this degree.

I give consent to this copy of my thesis, when deposited in the University Library, being made available for loan and photocopying, subject to the provisions of the Copyright Act 1968.

I also give permission for the digital version of my thesis to be made available on the web, via the University's digital research repository, the Library Search and also through web search engines, unless permission has been granted by the University to restrict access for a period of time.

*Signed* .....

Nicholas Russell Maiden

*On this day the .....of ..... 2014*

## **PAPERS AND GRANTS DURING PERIOD OF CANDIDATURE**

**Portions of the work contained in this thesis have been published in the literature or submitted for publication.**

### **Published**

Maiden N. Historical overview of wound ballistics research. *Forensic Sci Med Pathol.* 2009;5:85-89.

Maiden N. Ballistic reviews: mechanisms of bullet wound trauma. *Forensic Sci Med Pathol.* 2009;5:204-209.

### **Submitted**

Maiden N, Byard RW. Unpredictable tensile strength biomechanics may limit thawed cadaver use in wound ballistics research. *Aust J Forensic Sci* 2014.

Maiden N, Hiss J, Gipps H, Hocherman G, Levin N, Trubina O, Vinokurov A, Zelkowicz A, Byard RW. An analysis of the characteristics of thoracic and abdominal injuries due to gunshot homicides in Israel. *J Forensic Sci.* 2014.

Maiden N, Fisk W, Wachsberger C, Byard RW. Ballistics ordnance gelatine – how different concentrations, temperatures and curing times affect calibration results. *J Med Sci Law.* 2014.

### **Awaiting Submission**

Maiden N, Fisk W, Byard RW. How porcine organs compare to FBI and NATO ordnance gelatine formulations using energy loss experiments.

### **Other papers published during period of candidature**

Maiden NR. Serial Number Restoration: Firearm. In: Jamieson A, Moenssens A, editors. *Wiley Encyclopedia of Forensic Science.* John Wiley & Sons, New Jersey. 2009.

Maiden NR. Firearms: Scene Investigation. In: Jamieson A, Moenssens A, editors. *Wiley Encyclopedia of Forensic Science.* John Wiley & Sons, New Jersey. 2009.

### **Development of National Training Program for Forensic Firearm Examiners**

Davies E, Dutton G, Jackson M, Maiden N. National Training Curriculum for Forensic Firearm Examiners. National Institute of Forensic Science. 2007.

### **Research Grants Awarded**

Australia-Israel Scientific Foundation \$5,000 travel grant, 2010.

## **ACKNOWLEDGEMENTS**

Wound ballistics is a subject that has fascinated me for many years. This project has provided the opportunity to explore this subject and related areas in greater detail and potentially contribute to the science. I would never have thought this possible a relatively short time ago.

Commitment is important in achieving the aims of the project, but commitment alone is unlikely to succeed without the support of key individuals and the organisations they represent. I would therefore like to recognise the following:

This work is supported in part by the Defence Science and Technology Organisation (DSTO). I would like to express my sincere gratitude to the DSTO and in particular my co-supervisor Mr. Christian Wachsberger and his team from the Weapons Systems Division. From the very beginning Chris supported my research and provided invaluable guidance and assistance. He provided materials, the ballistic range, high speed photography, Doppler radar and personnel necessary to conduct ordnance gelatine and other simulant tests. Without this support, the project could not be undertaken.

I would like to express my deep appreciation and gratitude to my supervisor Professor Roger Byard from the Discipline of Anatomy and Pathology, who is also internationally recognised for his work as a forensic pathologist. Despite a punishing workload, he encouraged me to pursue my academic dreams and acknowledged the value of my background experience and other qualifications. He was enthusiastic about the subject matter of this thesis and keen to assist my progress. He also introduced me to the world of academic publishing. In addition, he accompanied me to Israel to conduct the gunshot homicide study. This was one of the most fascinating and rewarding overseas trips I have ever undertaken. His expertise, support, advice and encouragement have been invaluable throughout this project.

I would also like to express my deep appreciation to Professor Robert Vink, my principal supervisor and Head of the School of Medical Sciences. His oversight role, experience, direction and encouragement during challenging periods of my candidature were instrumental in achieving my ultimate goal.

To Mr. Wesley Fisk, Manager of the Ray Last Anatomy Laboratory, I wish to express my deep appreciation and gratitude for his friendship, support and the many hours spent assisting me to conduct various gelatine and tissue related tests. I would also like to thank the other members of the laboratory, (past and present) namely Michael Hodges, Stelios Michas and Corey Loyd for assisting me throughout my studies.

I would like to sincerely thank Dr. Ian Musgrave, Discipline of Pharmacology, for his assistance and guidance with the statistical aspects of this thesis.

I would like to pass on a special thankyou to Dr. Andrew Buchanan, Discipline of Anatomy and Pathology, whose patience, keen sense of humour and unique style of teaching human anatomy and dissection, was pivotal to achieving the underpinning knowledge I required in this area.

I would also like to thank the Australia-Israel Scientific foundation for the grant I was awarded to travel to Israel to collect pathology and forensic ballistics data from the National Centre of Forensic Medicine and the Israel Police Division of Identification and Forensic Science. This grant allowed me the opportunity to meet and work with many dedicated and skilled people, who were incredibly helpful and hospitable.

To the staff and post graduate students within the Discipline of Anatomy and Pathology, I wish to say thank you for having made me feel so welcome within what is a truly fascinating and diverse area of the university.

Last, but by no means least, I wish to express my sincere gratitude to all my family and in particular my late and beautiful wife Wendy. Without her love and support, understanding and patience, I would not have been able to embark on this journey and pursue my academic goals.

## ABBREVIATIONS

ADF	australian defence force
AIS	abbreviated injury score
AP	anatomic profile
APS	anatomic profile score
BB	4.5 mm steel pellet fired from compressed air operated BB rifle
BMI	body mass index
CNS	central nervous system
COD	cause of death
CQB	close quarter battle
CT	computed tomography
DSTO	defence science & technology organisation
DTO	dithiooxamide
FBI	federal bureau of investigation
FEA	finite element analysis
FMJ	full metal jacket
fps	feet per second
f-lb	foot pound of energy
FSL	frangible surrogate leg
GCS	glasgow coma scale
g/mL	grams per millilitre
gr	grains
GSR	gunshot residue
HSHM	human surrogate head model
HTSM	human torso surrogate model
ICD-9	international classification of disease-9
ICISS	international classification of disease injury severity score
ICW	individual combat weapon
IDF	Israel defence force
IECC	international early conflict care (database)
IED	improvised explosive device
ISS	injury severity score
J	joules of energy
JHP	jacketed hollow point
KE	kinetic energy
$KE = \frac{1}{2}$	formula for kinetic energy equals half mass
$MV^2$	(M) multiplied by velocity (V) squared
$kg/m^3$	kilogram per metre cubed



KmVAB	formula for 'relative stopping power' equals scaling constant (K) multiplied by bullet mass (m) multiplied by bullet velocity (V) multiplied by bullet cross sectional area (A) multiplied by bullet shape (form) factor (B)
MAXAIS	maximum abbreviated injury score
MGT	modified griess test
m/s	metres per second
ME	muzzle energy
m <sup>2</sup> /kg	metre squared per kilogram
MV	muzzle velocity
N	Newton
N>	Number greater than
NATO	north atlantic treaty organisation
NIJ	national institute of justice
N/m <sup>2</sup>	newton metres squared
NISS	new injury severity score
N/S	not specified
PAG	physical associating gels
PI	polyisoprene
PS	polystyrene
Ps	probability of survival
PS-PS	diblock
RII	relative incapacitation index
RO	reverse osmosis water
RR	respiratory rate
RSP	relative stopping power
RTS	revised trauma score
SBP	systemic blood pressure
Spitzer	pointed rifle shaped bullets
SRRs	survival risk ratios
SRT	sodium rhodizonate test
STANAG	NATO standardization agreement
TBI	traumatic brain injury
TRAIS	trauma registry abbreviated injury scale
TRISS	trauma injury severity score
WB2D	two dimensional mathematical wound ballistics computer program developed by Crucq
WDMET	Wound data and munitions effectiveness team
w/w	Weight to weight

## TABLE OF FIGURES

- Figure 1 Main features of the Spitzer shaped ASF1 ball bullet.
- Figure 2 Anterior view of the thorax and abdomen showing some of the major organs within the 'centre of mass.'
- Figure 3 Overall view of pig organ and simulant velocity testing equipment and set-up.
- Figure 4 Closer view of velocity testing equipment (chronographs) and tissue/organ/simulant apparatus.
- Figure 5 Side view of the test rig set up within the DSTO ballistic range.
- Figure 6 Sample of the skin simulant.
- Figure 7 Sample of the bone composite embedded within a thin gelatine plate.
- Figure 8 An overhead view of the simulant test rig.
- Figure 9 Number of bullet entry impacts into regions of the thorax and abdomen.
- Figure 10 Number of bullet impacts into major organs/tissues within the thorax and abdomen.
- Figure 11 Comparison of tissue and organ tensile strength values ( $\text{g}/\text{mm}^2$ ) from the frozen and thawed elderly test cadaver, to published standards for non frozen elderly cadavers.
- Figure 12 Tensile strength values ( $\text{g}/\text{mm}^2$ ) from other tissues and organs obtained from the elderly frozen and thawed test cadavers that are not mentioned in published literature.
- Figure 13 Aging rates for adult human respiratory and digestive organs and Tissues
- Figure 14 Energy loss comparison between FBI and NATO gelatine formulations, Simulant 'A' and pig organs/tissues at room temperature.
- Figure 15 Energy loss comparison between FBI and NATO gelatine formulations, Simulant 'A' and pig organs/tissues at  $37^\circ\text{C}$ .

- Figure 16 Energy loss comparison between FBI and NATO gelatine formulations, Simulant 'A' and pig organs/tissues at 4°C.
- Figure 17 Energy loss comparison between FBI and NATO gelatine formulations, Simulant 'A' and pig organs/tissues at room temperature, 37°C and 4°C.
- Figure 18 Energy loss comparison for pig fat at 4°C, room temperature and 37°C, showing its anti-thixotropic nature.
- Figure 19 Comparison of mean BB pellet penetration depths for 10% ordnance gelatine at 4°C 250 Bloom using three different water types and curing times. In addition, the same formulation at 3°C was tested to compare results.
- Figure 20 Comparison of mean BB pellet penetration depths for 20% ordnance gelatine at 10°C 250 Bloom using three different water types and two different curing times.
- Figure 21 Comparison of mean BB pellet penetration depths for 20% ordnance gelatine at 10°C 250 Bloom and 20% ordnance gelatine at 20°C 285 Bloom, using two different water types and a different curing time.
- Figure 22 Overall comparison of mean BB pellet penetration depths for 10% ordnance gelatine at 3° and 4°C 250 Bloom, 20 ordnance gelatine at 10°C 250 Bloom, 20% ordnance gelatine at 10°C 285 Bloom, and 20% ordnance gelatine at 20°C 285 Bloom, using a combination of three different water types and three different curing times.
- Figure 23 Test 1A. The ASF1 ball bullet in flight and about to penetrate the bare gelatine block. In this position the bullet has no significant yaw angle.
- Figure 24 Test 1A. The ASF1 ball bullet penetrated 70mm into the bare gelatine block. Point A indicates the position at which the bullet has a significant upward yaw angle, indicating a loss of stability just prior to the commencement of the temporary cavity.
- Figure 25 Test 1A. Shows the temporary cavity forming, including backwards along the shot line, and the high upward departure angle of the ASF1 ball bullet as it exits the bare gelatine block.

- Figure 26 Test 1A. Point at which the maximum temporary cavity has formed within the bare gelatine block.
- Figure 27 Test 2. Shows the ASF1 ball bullet having exited the rear of the bare gelatine plate and in flight within the 250mm air gap with no significant yaw angle at this time.
- Figure 28 Test 2. Point at which maximum temporary cavitation has occurred within the bare gelatine block.
- Figure 29 Test 4. Skin simulant attached to the anterior surface of the bare Gelatine block. Also shows the ASF1 ball bullet entry point relative to the aim point drawn in black.
- Figure 30 Test 5. Shows the damage to the back of the gelatine plate containing the skin simulant and embedded bone composite. Also shows the ASF1 ball bullet in flight within the 250mm air gap with an angled upward trajectory.
- Figure 31 Test 5. Shows maximum temporary cavitation and the upward departure angle of the ASF1 ball bullet.
- Figure 32 Test 5. Shows the entry point of the ASF1 ball bullet into the gelatine block and the permanent cavity that was formed.
- Figure 33 Test 5. Bone composite that was embedded within the gelatine plate showing a large area of damage.
- Figure 34 Test 6. The ASF1 ball bullet in flight after exiting the gelatine plate, which has kin simulant attached to the anterior surface and bone composite embedded within it. Also shows the exit hole and the slight downward trajectory and yaw angle of the bullet.
- Figure 35 Test 6. Maximum temporary cavitation is shown, as well as the dynamic nature of this cavitation extending backwards along the shot line into the air gap. The resting position of the ASF1 ball bullet is also shown.
- Figure 36 Test 6. Damage sustained by the bone composite embedded within the gelatine plate.

- Figure 37 Test 7. The ASF1 ball bullet in flight within the air gap after exiting the anterior gelatine plate, which has skin simulant attached to the anterior surface and bone composite embedded within it. Also shown is the exit point through the gelatine plate and the high yaw angle of the ASF1 ball bullet just prior to entering the posterior gelatine plate.
- Figure 38 Test 7. An overhead view of the immediate temporary cavitation which occurred in the gelatine block.
- Figure 39 Test 7. A side view of the dynamic nature of the damage caused by the ASF1 ball bullet.
- Figure 40 Test 7. Entry point of the ASF1 ball bullet through the bone composite embedded within the anterior gelatine plate.
- Figure 41 Test 7. Exit point of the ASF1 ball bullet through the bone composite which was embedded within the anterior gelatine plate. Also shows the remote damage caused by the transfer of kinetic energy.
- Figure 42 Test 7. The extensive damage caused by the ASF1 ball bullet to the bone composite embedded within the posterior gelatine plate.
- Figure 43 Test 7. The extensive damage caused by the ASF1 ball bullet at maximum yaw as it exited the skin simulant attached to the back of the posterior gelatine plate.
- Figure 44 Test 7. Shows the permanent cavity and the upward trajectory of the ASF1 ball bullet through the gelatine block.
- Figure 45 Unfired ASF1 ball bullet with its features described.
- Figure 46 Test 2. Recovered ASF1 ball bullet showing damage.
- Figure 47 Test 6. Recovered ASF1 ball bullet showing damage.
- Figure 48 Test 7. Recovered ASF 1 ball bullet showing damage.
- Figure 49 Temporary cavitation commencement depths for each anatomical simulant model compared to the two gelatine control blocks.
- Figure 50 Bullet penetration depths for each of the anatomical simulant models compared to the two gelatine control blocks.

Figure 51 Comparison of the volume (L) of the temporary cavity for those anatomical model tests where the volume could be determined, compared to gelatine control block 1A.

## **TABLES**

Table 1	Results of published tissue and simulant penetration tests.
Table 2	Comparison between the published densities of some biological tissues and simulant media.
Table 3	Scale of values used for the AIS severity code classification.
Table 4	Bullet path through victims from the homicide study.
Table 5	The approximate distances over which shootings occurred in the homicide study.
Table 6	Number of bullet impacts to the sternum and each rib from the homicide study.
Table 7	Statistical significance ( $p < 0.05$ )* of the FBI gelatine formulation compared to the NATO gelatine formulation, Simulant 'A' and the pig organs/tissues at room temperature, 37°C and 4°C.
Table 8	Statistical significance ( $p < 0.05$ )* of the NATO gelatine formulation compared to Simulant 'A' and the pig organs/tissues at room temperature, 37°C and 4°C
Table 9	Statistical significance ( $p < 0.05$ )* of Simulant 'A' compared to the pig organs/tissues at room temperature, 37°C and 4°C.
Table 10	Statistical significance ( $p < 0.05$ )* of pig organs/tissues compared to each other at room temperature, 37°C and 4°C.

**1. THE SCIENCE OF WOUND BALLISTICS**

**LITERATURE REVIEW**



## 1. **The Science of Wound Ballistics**

### 1.1 **Introduction**

This thesis explores the fundamental difficulty of reliably evaluating the terminal (wound ballistics) actions of ammunition in human tissues. Ballistic ordnance gelatine is one of the most widely used simulants for this type of small arms testing as it has similar properties to soft tissues. However, being a homogenous material, it cannot represent the heterogeneous nature of human bodily structure comprising hard and soft tissues of various consistencies. Therefore, ballistic ordnance gelatine does not accurately represent bullet wound trauma in all types of human tissue, and so the conclusions drawn from its use must be qualified.

Anatomically correct models will provide a viable alternative to conventional evaluation methods, by using materials that have similar biomechanical properties to human tissues and organs. Their use may provide an objective means by which the physiological effects of bullet wounding can be studied and the lethality or incapacitation potential of a particular bullet type evaluated. The thorax and abdomen are the principal anatomical regions that would need to be replicated, as soldiers and police officers are trained to shoot at the 'centre of mass.'

This study also focuses on the terminal (wound ballistics) performance of calibre 5.56x45mm North Atlantic Treaty Organisation (NATO). This calibre has been chosen because of concerns raised in both the Afghanistan and Iraq conflicts regarding the effectiveness of this type of ammunition. This NATO Standardized Agreement (STANAG) 4172 calibre is used by the Australian Defence Force (ADF) and specialised units of Australian law enforcement agencies in what can be broadly categorised as assault rifles. Two other calibres will also be discussed namely 9mm Luger, which is used by the ADF in semi-automatic pistols and 7.62x39mm Soviet, commonly used by forces opposed to the ADF and other coalition forces.

### 1.2 **Aim**

The primary aim of this thesis was to determine the validity of anatomical simulants to evaluate the dynamics of wound trauma caused by military style full metal jacket (FMJ) bullets, in particular calibre 5.56x45mm NATO.

A series of experimental and data collection studies were undertaken to demonstrate the complexity of issues surrounding ballistic tissue simulant research. They also enabled:

- An analysis of the characteristics of homicidal gunshot wounds where FMJ bullets are predominantly used.
- A comparison of relevant tissue tensile strength data from a selected cadaver against published data, to highlight the limitations of using frozen cadaveric material for simulant research.
- Collection of velocity and energy loss data from tests using BB rifle pellets on selected pig organs, in order to establish a baseline for the development of suitable anatomical simulants.
- Variance of ballistic ordnance gelatine manufacturing conditions to determine their effect upon calibration results and highlight the deficiencies of this simulant material.
- The development of basic anatomical models in order to test fire calibre 5.56x45mmNATO and compare the results achieved with those obtained from FBI specification bare ordnance gelatine.

### 1.3 Hypothesis

There is currently no accurate method to assess the dynamics of bullet wound trauma in the human thorax and abdomen. Ballistics ordnance gelatine is the most widely used simulant, but it is a homogeneous material. It is hypothesised that anatomical simulants that replicate the heterogeneous nature of relevant human organs and tissues will provide a more reliable and accurate method to evaluate the effects of ammunition than FBI or NATO specification bare ordnance gelatine. Specifically:-

- That an analysis of homicide cases due to thoracic and abdominal gunshot wounds will provide data on which organs and tissues are most vulnerable to ballistic trauma.

- Readily available cadaveric tissue for ballistic research has often been frozen and thawed. It is hypothesised that this will result in tissue changes that render it unsuitable for injury interpretation.
- Different animal organs will show different ballistic characteristics and this will be temperature dependant. Also, ordnance gelatine at various temperatures will be comparable to different animal tissue in terms of its ballistic characteristics such as projectile penetrability.
- Different concentrations, temperatures and curing times will affect the physical characteristics and properties of ballistics ordnance gelatine.
- The addition of tissue simulant materials to FBI specification ordnance gelatine will significantly change the behaviour of calibre 5.56x45mm NATO bullets compared to bare FBI specification ordnance gelatine. The interpretation of wounding features will therefore also change.

#### **1.4 Historical Overview of Wound Ballistics Research**

##### **1.4.1 Introduction**

Ballistics is the science behind the motion of projectiles. It is divided into four primary areas; internal ballistics, the study of the projectile in a firearm; intermediate ballistics, the behaviour of projectiles as they leave a barrel; exterior ballistics, the behaviour of a projectile in flight, and terminal ballistics, the study of the penetration of a medium denser than air by projectiles (1-3). Wound ballistics is a part of terminal ballistics and refers to the study of the effects of projectiles that penetrate the human or animal body (4). It can also be described as the scientific study of injuries caused by projectiles and the behaviour of these projectiles within human biological tissues (1).

This review focuses on the theories behind, and major advances in, the field of wound ballistics, which has played an important role in the development of better performing firearms and ammunition. Wound ballistics is also used extensively in forensic science to assist in the re-construction of crimes and this aspect has largely dominated contemporary scientific literature on the subject. As a result, although it is not the primary focus of this thesis, the forensic aspects of wound ballistics will be discussed briefly.

### 1.4.2 Historical Developments

The science of wound ballistics dates back to the 1830's, but major advances did not occur until the 1870's when Kocher evolved a hydrodynamic theory for the effect of gunshot wounds. This refers to the pressure wave that is created when a liquid is displaced by a high explosive or high velocity projectile. He also identified the importance of projectile deformation in the wounding process by predicting a decrease in soft tissue disruption with the introduction of smaller calibre copper jacketed bullets, despite an increase in velocity. A bullet's calibre is a numerical term used to describe the bullet's nominal diameter. It is commonly expressed in both imperial and metric terms (4). This decrease in wounding effects noted by Kocher occurred because these types of bullets did not deform as did the large calibre lead bullets commonly in use at that time (5-7). Kocher was also the first to use soap and gelatine as tissue simulants (1, 7, 8).

In the 1890's La Garde confirmed that a faster, harder, smaller-diameter bullet produced less severe wounds than larger calibre soft lead bullets which deformed when they hit a body (9, 10). In 1901 La Garde and Thompson (who invented the Thompson machine gun), established that the permanent cavity (path taken by the bullet while crushing tissue) is of primary importance in handgun wound ballistics and that kinetic energy is not always the main factor in deciding the wounding potential of a bullet (9, 11-18). They also established that a larger calibre is more effective in creating wound trauma when using similar types of bullets (9, 17).

### 1.4.3 Explosive effects

La Garde also examined what was commonly called the 'explosive effects' of rifle bullets, meaning the devastating injuries sustained from high velocity rifle bullet impacts. A number of theories had been previously put forward to explain these effects such as the theory of compressed air, hydraulic pressure, the velocity of rotation and heating of the bullet. After experimentation, La Garde discounted these theories and concluded that the real cause was the transfer of energy from the bullet, which was dependent upon the velocity at the time of impact (9).

In 1907 Journee became the first researcher to study the penetrability of human skin and the relationship between kinetic energy and the extent of the wounds inflicted. He

reviewed the state of bodies on the battlefield as well as performing controlled experiments with horses (16, 19, 20).

Hatcher was another notable researcher in the field of wound ballistics. He served in the United States Army Ordnance Department, where he became chief of machine gun and small arms engineering and design in 1917. He was tasked with determining what calibre of rifle ammunition would provide the highest degree of lethal force, while still conforming to the humanitarian considerations outlined in The Hague Convention Guidelines of 1899. He established this by conducting an exhaustive series of tests on animals and examining the wound tracks and tissue damage sustained (21, 22).

#### 1.4.4 **Stopping power**

Hatcher (21) developed a model and formula for what he called “Stopping Power”, which refers to incapacitation. Incapacitation is a term used to describe the extent of human functional impairment with respect to a specified task. The task generally relates to an aggressive action designed to cause harm. Incapacitation has been variously defined by authors as: the physiological inability to perform complex movements independent of consciousness or intention (23, 24), instant incapacitation will render an assailant incapable of posing a continued threat (16), and immediate incapacitation is the sudden physical or mental inability to cause injury or pose any further risk to another person (25, 26). The terms instant and immediate incapacitation have the same meaning and indicate that the threat has been removed with no discernible time delay. The term ‘rapid’ incapacitation is not instant or immediate, but refers to incapacitation within a short time frame. This could be in the order of 30 seconds to approximately 5 minutes and is usually achieved following significant haemorrhage from a major vessel or the heart (23, 26).

Hatcher’s model was based on momentum as he saw flaws with energy-based models. He recognised that handgun bullets do not cause appreciable damage outside a narrow wound path formed by the permanent cavity. He also identified bullet placement as a critical factor in the wounding process, as well as penetration to reach a vital organ or structure. Bullet placement is the process of aiming and achieving impact with a vital area of the body. Hatcher was also one of the first researchers to identify psychological factors and their role in the wounding process (17, 21, 22, 27).

#### 1.4.5 Mechanisms

There is considerable misinformation about the mechanisms of bullet wound trauma (11, 28), and one of the researchers responsible for clarifying many of the misconceptions was Fackler. In 1982, he was the first to compare ballistics gelatine with living tissue. He determined that 10% ordnance gelatine was an acceptable human muscle simulant after conducting comparative tests with pig legs (29-31). In the mid 1980's, he was also the first researcher to introduce calibration into ordnance gelatine testing, which potentially rendered previous results with non-calibrated gelatine invalid (17). In addition, he followed on from the work of Hatcher and refuted the kinetic energy wounding theory, which stated that kinetic energy transfer from high velocity bullets to tissue was the primary mechanism of wounding. He demonstrated that kinetic energy was not a reliable measure through a series of gelatine wound profiles covering many common calibres. He also showed that fragmentation was the most effective means of inflicting wounds from a military rifle round (6, 8, 28, 31-33).

In 1991 MacPherson a mechanical engineer and rocket scientist, formed a partnership with Fackler to assist with ballistic analysis. He later developed a bullet penetration model based on mathematical formulae, which predicted the type of injury that might be sustained (17, 33). While the merits of this model are not challenged, the fact that it is mathematically based has meant that most researchers do not use it, preferring to experiment with simulant materials that provide an optical result.

In 1994, Sellier from the Institute of Forensic Science, University of Bonn, Germany, and Kneubuehl from the Defense Technology and Procurement Agency, Switzerland, collaborated in an attempt to rationalise the scientific basis behind many wound ballistics theories. Their book (27) covers a wide range of subject matter including the underpinning laws of physics, the behaviour of projectiles in a dense medium, the mechanisms of wounding and the use of simulant materials for wound ballistics research. They created some controversy when they claimed that the remote effects seen in tissue were the result of pressure changes from shock waves rather than temporary cavitation. A more detailed discussion of this issue is contained under section 1.5.4.

#### 1.4.6 Forensic Applications and Models

The forensic application of wound ballistics is commonly used by forensic firearm examiners and pathologists to assist in re-constructing shooting scenes. Correct interpretation of bullet wound features combined with experimental research, has enabled this field of study to become an important tool in the investigation of criminal acts involving firearms.

Differentiating between an entrance wound and an exit wound can have a significant impact on the interpretation of circumstances or charges relating to a criminal case. Contact wounds, which are common in suicides, are characterised by a dense pattern of combusted propellant residue or soot within and around the margin of the wound. They may also display stellate (star shaped) tearing of the skin over bony structures. An abrasion collar is also common (2). In 1967 Sellier proved that superficial tissue particles that had been thrown back against the direction of the bullet were the cause of the abrasion collar, also known as a contusion ring. Prior to this, it was thought that friction, indenting or overstretching of the skin were the causes. Unfortunately, in many English speaking countries, the incorrect causes of the abrasion collar are still maintained today, because many in the international scientific community are not familiar with publications written in German (34).

Gunshot residue (GSR) analysis is another method of determining range of shot and is most commonly used on the clothing of a victim. Gunshot residue is generally made up of the elements lead, barium and antimony, which form the basis of most modern primers used in ammunition (35, 36).

Crucq (1) from the Netherlands developed a computer based model for the prediction of wound trauma involving various types of ammunition and their terminal performance. The model is used by a number of NATO countries for military purposes, but has also been used by law enforcement agencies for forensic applications.

Most recently, German medicolegal research has concentrated on three main areas namely, investigating bullet and biological tissue interactions by using simulants and composite body models, examining the mechanisms of incapacitation from gunshot wounds and identifying methods for determining if a gunshot wound was accidental, deliberate, or the result of suicidal intent (23-25, 27, 34, 37, 38).

Swiss researchers have also investigated bullet and biological tissue interactions by using composite body models such as the skull-brain model, skin, skull, brain model and a finger model as an intermediate target. These have demonstrated that ballistic models and body part substitutes can reproduce the trauma seen in actual gunshot cases without using animal substitutes. This helps to avoid the ethical dilemmas associated with using animals or cadavers (39-42).

The combined efforts of German and Swiss researchers has advanced the use of simulant materials beyond the traditional use of ballistics ordnance gelatine and transparent glycerine soap, by developing limited models that simulate organs, blood vessels and bone or involve embedding nerves or bones within gelatine to show the effects of permanent and/or temporary cavitation. These experimental models have shown that wound trauma resulting from shootings can be reconstructed with considerable accuracy (34, 39, 41, 43). However, data on penetrating wounds to the thorax and abdomen are lacking.

#### 1.4.7 **Conclusion**

There have been significant advances in the understanding of wound trauma caused by bullets over the past 100 years, but this field of study is complicated by the diverse nature of the human body and its response to high velocity bullet impact. In addition, with continuing advances in the development of firearms and ammunition, the nature of the wounds themselves can and will change. Therefore, there is still much which remains uncertain about this subject, but with the aid of suitable biological simulants, it is hoped that future researchers will provide answers to these questions.

### 1.5 **Mechanisms of Bullet Wound Trauma**

#### 1.5.1 **Introduction**

Bullet placement is the single most important factor influencing the capacity of a bullet to cause immediate or rapid physiological incapacitation. This is because incapacitation is determined by the anatomical structures the bullet penetrates and the severity of the damage caused. For example, even a small calibre bullet such as calibre 22 Rimfire can be lethal if it strikes certain regions of the body (21, 44, 45). However, immediate incapacitation occurs only if a projectile strikes the upper portion of the central nervous system (CNS), comprising the brain and/or upper cervical spinal cord (6, 23, 46). It is



also possible to cause indirect CNS tissue damage by bullets that do not strike the CNS, through the mechanism of temporary cavitation in the vicinity of the spine. In this instance the spine would be moved suddenly and violently within the spinal canal. This would have a similar effect to the spinal cord being cut and could cause immediate incapacitation to the muscles innervated by the nerves that emerge from the spinal cord at or below the level of the concussion (47).

The other cause of rapid incapacitation is massive tissue destruction, or collapse of the circulatory system from severe disruption of vital organs and blood vessels in the torso. This also causes cerebral hypoxia from haemorrhage (14, 23, 46).

### 1.5.2 Physiological Responses

The rate of blood loss will be determined by the size of the bullet wound through the relevant blood vessels, as well as the pressure in the vessel at that time (47). For example, an average human male weighs approximately 80kg and has a cardiac output of 5.5L of blood per minute. The total blood volume of this person will be 60mL per kg of body weight or a total of 4,800mL. However, if a person is subjected to severe stress, cardiac output can double and aortic blood flow may reach 11.0L per minute. If a gunshot wound severs the ascending aorta, it will take only 4.6 seconds to lose 20% of the blood volume, which is close to the maximum amount the body can lose before a person is rendered unconscious. A scenario of this type would be classed as one of the best examples of rapid incapacitation for a bullet wound outside the CNS, because although not immediate, incapacitation has occurred within a very short time frame (46).

The centre of the torso is one of the most vulnerable areas outside the CNS because of the abundance of vital structures such as the heart, aorta, other major arteries and veins as well as the liver. In addition, because it is a larger target area, there is an increased hit probability compared with the smaller head. It is for these reasons that soldiers, police and other law enforcement officers are trained to shoot at the 'centre of mass.'

There are factors which can reduce the amount of blood loss a person sustains involving the 'flight or fight response' which describes the process of increasing blood circulation, promoting energy production and restricting non-essential physiological activities. While the body may be able to compensate for approximately 25% of blood

loss or about 1L of total volume in a healthy person, losses of amounts above this cannot be sustained and the brain and heart will become deprived of oxygen resulting in unconsciousness and eventually death, if left untreated (46, 48-50). Endorphins are also released from the pituitary gland and hypothalamus into the blood, spinal cord and brain that help inhibit the perception of pain and allow a person to keep functioning for longer (1). Therefore, it can be seen that the body's compensatory mechanisms are designed to save a person's life after sustaining a significant wound. In situations of armed combat this means that an adversary, although severely wounded, may still be capable of presenting a threat unless immediately incapacitated.

### 1.5.3 Tissue Damage

There are two components to bullet wound trauma. The first is the permanent wound cavity, which is the path taken by the bullet while crushing and effectively destroying tissue (11, 13, 14, 51). The mass of tissue damaged is proportional to the effective volume of the permanent wound cavity. The cross-sectional area of this cavity is also equal to the bullet's cross-section modified by a shape factor derived from the bullet's configuration and the amount of resistance offered to it by tissue (17). The second is the radial stretching of tissue around the bullet's track, which momentarily leaves an empty space called the temporary wound cavity (11, 14, 16, 52, 53). This cavitation effect is caused by high pressures surrounding the projectile that accelerate material away from its path. Harvey (13), Janzon (15, 54), Sellier and Kneubuehl (27) state that the temporary cavity is the most important factor in wound ballistics of high velocity rifle bullets, and that almost all biological phenomena can be explained by it. While the importance of the temporary cavity is recognised by all other contemporary researchers, most do not place its importance above that of the permanent cavity. This is because temporary cavity tissue damage is far less predictable (17, 45, 46, 55). The temporary cavity also has little or no wounding potential with handgun bullets because the amount of kinetic energy transferred to the tissue is insufficient to cause remote injuries (2, 17, 56). The size of the temporary cavity is approximately proportional to the kinetic energy of the striking bullet and also the amount of resistance that the tissue has to stress. Therefore, the maximum volume of the temporary cavity represents the amount of stored strain energy, which is the potential energy stored in a body by virtue of elastic deformation and is equal to the work that must be done to produce this deformation.

The potential for this energy to cause wound trauma depends upon the following factors:-

- Magnitude of the stored energy that results from the drag force affecting the bullet. This force arises from pressure differences at the bullet's surface, caused by the streaming of tissue against it during flight.
- Sensitivity of the tissue to strain.
- The size of the tissue or organ structure.
- The anatomical constraints on tissue movement due to adjacent structures (17).

The temporary cavity may be 11 to 12.5 times as large as the diameter of the centre-fire rifle bullet, but lasts only 5 to 10 milliseconds from its initial rapid growth until its collapse (2). Because much of the body's tissue is elastic, the temporary cavity quickly subsides as the elastic recoil of the stretched tissue returns towards the permanent wound track. Flexible elastic soft tissues such as muscle, intestine, skin and blood vessels, are good energy absorbers and are highly resistant to the type of blunt trauma caused by tissue stretch (45). Therefore, depending on the tissue that was subject to these stresses, there may be no damage or a reduced amount of tissue damage. Again, this is an example of why the temporary cavity is not always a reliable wounding mechanism (46). However, certain organs within the body are more susceptible to damage than others, such as the liver, kidneys, spleen, pancreas and completely fluid filled organs such as the bladder. This is because of their relatively low tensile strength and the high fluid content that deforms in a plastic manner (57). These organs are therefore highly susceptible to splitting, tearing or rupturing as a result of temporary cavitation. Tests conducted by Amato et al. (58) found that the same amount of bullet energy caused greater damage to liver than to muscle. If enough energy was transferred, the liver may in fact disintegrate (54). In addition, the displacement of tissue as a result of the temporary cavity can disrupt blood vessels, particularly arteries, or fracture bones some distance from the projectile path (31, 54). Bone fragments can also function as secondary projectiles causing further tissue disruption (2, 56, 59).

Patrick (26) indicates that the outward velocity of tissue forced aside by temporary cavitation represents not more than one tenth of the velocity of the bullet. This appears to be an over-simplification, because the dynamics at the projectile-tissue contact surface involve explosive radial displacement of the tissues. The velocity of the tissue that is forced aside will vary depending on the type of bullet involved i.e. pointed rifle bullets (Spitzer shaped) versus a bullet with a large contact face such as a flat nose or expanding style of hunting bullet, as well as the tissue type. In addition, the velocity of tissue will decrease with increased radial distance from the shot line.

Penetration is one of the most important functions of a bullet, and a minimum penetration of 300mm in soft tissue is usually required to reach the centre of vital organs from any angle. This became the accepted standard within the United States of America (USA) following the first Wound Ballistics Workshop at the Federal Bureau of Investigation (FBI) Academy in September 1987. This was set up to assess the need to better arm FBI agents following an incident in Miami in 1986 where two agents were killed and five others wounded by two armed offenders who had already sustained multiple gunshot wounds that had failed to incapacitate them (17, 60, 61). While it is acknowledged that many vital organs are far less than 300mm from the anterior chest wall, this minimum standard allows for unexpected bullet paths such as laterally through an upper limb or through unusually fat or muscular bodies where vital organs are under increased amounts of tissue.

#### 1.5.4 **Shock Wave Injuries**

A shock wave can be broadly described as a powerful propagating disturbance caused by a sudden change in pressure, density or temperature, which travels through a medium faster than sound. They carry significant energy but this energy will dissipate with increased distance (62, 63).

There is still some debate as to whether shock waves generated from high velocity rifle bullets cause damage to tissues far removed from the impact site. Sellier and Kneubuehl (27) claim that the remote effects in tissues were the result of shock waves rather than temporary cavitation. They believed that while shock waves may not cause any obvious damage, cellular damage can be caused by the steep increase, followed by a sudden decrease in pressure.

Fackler (11, 28, 64, 65) was one of the most vocal critics of the shock wave theory, as he had seen no physical evidence to support it while performing surgery on battle field injuries. However, supporting opinion had already been provided as early as 1947 by Harvey (12, 13), as well as by more contemporary authors (1, 43, 62, 66-73).

Various experiments using simulant models has also provided increasing evidence to support the theory that shock waves can cause tissue-related damage and damage to the nervous system (43, 51). One of the most interesting is a study by Courtney and Courtney (74) which showed a link between traumatic brain injury and pressure waves originating in the thoracic cavity and extremities.

The difference of opinion between recognised experts in the field on this issue, clearly demonstrates the complexities involved with wound ballistics in general, and highlights the need for further dedicated research.

#### 1.5.5 **Bullet Design**

The design and construction of a bullet are also important elements in determining its wounding capacity and pathological effects. The bullet's mass and striking velocity establish its potential to destroy tissue, while the shape and construction determine how much tissue is actually disrupted (59, 75). Spitzer shaped bullets are designed to have low drag characteristics, which refers to the amount of air resistance in flight. Bullet yawing upon target strike (deviation of the long axis of the bullet from its line of flight) and tumbling (complete loss of gyroscopic stability) will markedly increase this drag effect and therefore substantially increase temporary cavitation (45, 68).

During firing, the helical rifling within a rifle barrel imparts gyroscopic spin to the bullet. This is sufficient to stabilize the bullet during its flight in air, but tissue is denser than air and the increased drag on the bullet overcomes its rotational stability. While it begins its passage through tissue travelling point first, the bullet soon begins to yaw (15, 45, 53). The changes in both density and elasticity within biological tissues such as fascia overlying skeletal muscle, causes a rapid increase in yaw (1). When the yaw angle exceeds approximately 20° there is generally no recovery and the projectile proceeds towards 90° yaw, thereby presenting its maximum frontal area to the direction of travel. As a result, maximum energy is deposited and 'explosive' temporary cavitation is

achieved. This generally occurs at a penetration depth of between 100mm and 200mm, depending on the type of bullet and the nature of any intervening material (55).

The maximum amount of temporary cavitation can also occur with maximum deformation or fragmentation of a bullet (45, 53). Fragmentation in tissue can substantially increase the size of the permanent wound cavity as each of the multiple fragments spreads out radially from the main wound track and cuts its own path through tissue. This occurs at the same time as the temporary cavity is formed. The perforated tissue within that cavity loses its elasticity and tissue can tear or become detached because it is unable to absorb the amount of stretch that it normally would be able to (6, 31, 76). Therefore, it logically follows that a fragmenting bullet will make a larger wound than a non-fragmenting one (1, 75).

#### **1.5.6 Military Rifle Bullet Design**

Military bullet designs are constrained by the Hague Convention of 1899, which prohibits the use of bullets which expand or flatten easily in the human body, such as bullets with a hard envelope (jacket) which does not entirely cover the bullet core, or is pierced with incisions. The Hague Convention IV of 1907, Article 23(e), forbids the use of arms, projectiles or material calculated to cause unnecessary suffering (16, 31, 53, 68, 77). Therefore military bullet design is limited in comparison to the civilian or law enforcement market, where soft lead nose hunting bullets or bullets with polymer tips are common place and are generally capable of greater wound trauma and incapacitation because they are designed to expand. The USA was not a signatory to the Hague Convention of 1907.

#### **1.5.7 Calibre 5.56x45mmNATO**

The 5.56x45mmNATO bullet is often described as a “varmint” cartridge due to its small calibre. Nevertheless, it became NATO’s second standard small arms calibre for military forces in 1979 (54). This second standard was always intended to complement NATO’s first standard small arms ammunition i.e. 7.62x51mmNATO. The current SS109 design contained in NATO’s Standardization Agreement (STANAG) 4172 replaced the former M193 bullet design after 1975. It was developed by the Belgian company Fabrique Nationale and was slightly heavier and longer. It has a nominal weight of 4.018g (62gr), a nominal muzzle velocity (MV) of 944.9m/s (3100fps) and

generates 1799J (1325f-lb) of muzzle energy (ME). By comparison the former M193 bullet weighed 3.565g (55gr), had a nominal MV of 987.6m/s (3240fps) and generated 1743J (1282f-lb) of ME. It also has a solid lead core and a copper jacket (78, 79).

Bullets of this kind are classed as Spitzer shaped. The United States military version of the 5.56x45mmNATO cartridge which incorporates the SS109 designed bullet is designated the M855 and has a mild steel penetrator. The ADF version of this cartridge is designated the ASF1 ball. The term 'ball' refers to it being a FMJ bullet (4). Figure 1 describes the relevant features of the ASF1 ball Spitzer shaped bullet.

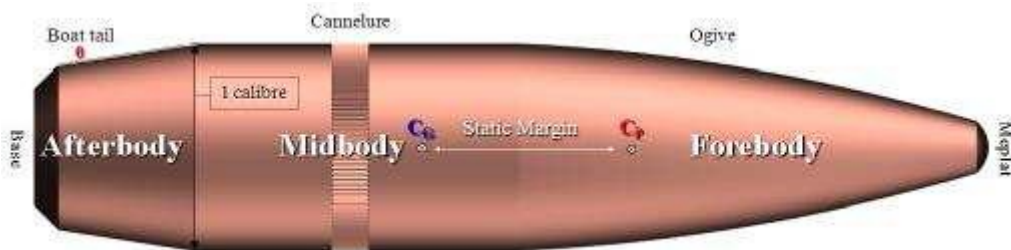


**Figure 1. Main features of the Spitzer shaped ASF1 ball bullet. Figure provided by Krstic 2007.**

At high impact velocities, all of these bullets tend to fragment and the penetrator (located in the nose) may become separated. Another feature of these bullets is that they consistently exhibit curved trajectories during gelatine impact testing because their centre of gravity is located to the rear of the bullet's centre of drag (centre of pressure). The centre of drag is defined as the theoretical point (usually in the forebody) at which all drag forces can be said to be acting, which causes the bullet to turn as it starts to yaw during tissue or gelatine penetration (1, 80, 81). These types of bullets typically have full metal jackets comprised of copper nickel gilding metal, as well as a lead-antimony alloy core. Antimony is added to the lead to increase its stiffness for superior penetration (82).

The 5.56x45mmNATO bullet typically exits the muzzle of a rifle with up to 6° of yaw at launch. As the bullet moves farther from the muzzle the gyroscopic stabilisation dampens the yaw, which gradually decreases to approximately 2° throughout the region of stable flight (pre-transonic – greater than Mach 1.2). This explains why close range

wounds from this calibre are generally more destructive than long range wounds, because the bullet has become more stable over a greater range and has less remaining kinetic energy. Bullet fragmentation also decreases with increased shooting distance, and this explains why these bullets penetrate deeper at 100m range than they do at 3m (75, 83).

Another important feature of certain high velocity bullets like the 5.56x45mmNATO is their tendency to fragment. Fragmentation is the result of rapid yaw growth and is caused by a combination of forces that bend the projectile sufficiently to fracture the jacket (1, 54, 81). All types of STANAG 4172, 5.56x45mmNATO bullets tend to flatten and break at the cannelure. This occurs because the cannelure is the weakest portion of the bullet jacket and stress forces focus on this area during maximum yaw. The bullet point tends to flatten but remains in one piece because of the structural integrity associated with the design (cone shape), but the rear section breaks into many fragments. This feature can cause major tissue disruption (84).

Fackler et al. (85) report that during ordnance gelatine block testing at various ranges involving the M855 bullet used in the model M16 A2 service rifle, the bullet will fragment and the jacket behind the cannelure will break at a range of 50m. At 150m most of the bullet breaks at the cannelure and the jacket behind the cannelure is flattened but unbroken. At 250m the bullet flattens behind the cannelure but does not break and at 350m the bullet remains intact with a slightly flattened appearance. Again this is due to the bullet achieving greater stability as the target distance increases, as well as less residual energy to disassemble itself.

Reducing the barrel length of assault rifles such as the M16 in calibre 5.56x45mm, will also reduce the velocity generated. This can potentially reduce the effectiveness of this calibre depending on the target distance by decreasing the likelihood the bullet will fragment (47).

### 1.5.8 **Calibre 7.62x39mmSoviet**

Calibre 7.62x39mmSoviet is also known by the designation M43 and 7.62 Short to differentiate it from other 7.62mm calibre rounds. It is most commonly used in the AK47 pattern assault rifles which are common throughout the Middle East region, as well as the former Soviet States and many countries within the African continent. It is also



common in Chinese SKS military style assault rifles. This calibre is available in a number of different bullet weights, one of the more common being 7.97g (123gr), which has a nominal MV of 720.9m/s (2,365fps) and generates 2,077J (1528f-lb) ME (78). Ammunition in this calibre comes from a wide variety of manufacturers from many different countries including Russia, China, Germany, Bulgaria and Egypt. The bullet construction varies depending on the manufacturer but is commonly the Russian and Chinese military design consisting of a FMJ boat tail bullet with a copper-plated steel jacket, steel core/penetrator that is sheathed in lead with a small lead tip. However, rounds with copper cartridge cases and FMJ bullets that are constructed with copper bullet jackets and lead cores are also available (2, 75, 82, 86).

The wounding features of this calibre vary dramatically depending on the type of bullet construction as detailed above. The military style FMJ bullets with copper plated steel jackets, steel cores/penetrators display poor wounding capabilities because of low muzzle velocity and the fact that the bullet is not designed to expand or fragment. As a result, they exhibit wounds similar to non-expanding small calibre handgun bullets and often over-penetrate so that much of their energy and momentum is not expended within the body (2, 75, 87, 88).

Fackler (75) conducted a series of ballistics ordnance gelatine tests using this calibre and found that the bullet typically penetrates approximately 260mm with the point forward before beginning to yaw and so wound tracks are very small. Fackler's results in gelatine also reflected his experience in Vietnam with battle field injuries inflicted by this calibre. However he also noted that copper jacketed bullets with lead cores in 7.62x39mm performed quite effectively. This type of bullet construction caused the bullet to yaw soon after penetrating tissue and the bullet tended to flatten as a result of the forces applied to it. This caused a small amount of lead fragments to be expelled out of its open base, but did not significantly add to its wounding potential. However, the yawing effect increases the surface area of the bullet as it penetrates tissue, creating a much larger permanent cavity and significant temporary cavitation.

#### 1.5.9 **Calibre 9mm Luger**

Calibre 9mm Luger is also known by the designation 9mm Parabellum and 9x19mm. The cartridge was designed by Georg Luger and first introduced with the Luger pistol in 1902. The German Navy were the first to adopt the pistol/calibre combination in 1904,

followed by the German Army in 1908 (78, 89). It has remained one of the most popular cartridges ever designed for military, law enforcement and civilian purposes and is commonly used in a variety of semi-automatic pistols and sub-machine guns. It has also been adopted as the standard NATO handgun cartridge under STANAG 4090 and officially called the 9mm NATO (78, 79). There are a wide range of bullet weights used in calibre 9mm Luger. The most popular are 115gr (7.45g) with a nominal MV of 353.6m/s (1160fps) and generating 467J (345f-lb) of ME; 124gr (8.03g) with a nominal MV of 341.4m/s (1120fps) and generating 470J (345f-lb) of ME; 147gr (9.52g) with a nominal MV of 297.2m/s (975fps) and generating 422J (310f-lb) of ME (78, 90).

There are also a wide assortment of bullet configurations including military style FMJ with an exposed lead base or fully encapsulated, as well as specialty jacketed hollow point bullets (JHP). These are designed primarily for law enforcement or defensive anti-personnel purposes.

FMJ 9mm Luger bullets tend to cause less damage than JHP designs because they do not expand and thus increase their surface area which causes greater wounding. FMJ 9mm Luger bullets often over penetrate and exit the body, retaining a significant percentage of their energy and momentum as well. The author has personally witnessed this when attending numerous shooting scenes involving this calibre.

Handgun calibres such as 9mm Luger are known to cause tissue damage through the mechanism of the permanent cavity rather than temporary cavitation as discussed earlier under the heading 1.5.3.

#### 1.5.10 **Conclusion**

As noted, bullet placement is a critical factor in determining the incapacitation potential of a bullet. The only means of achieving immediate incapacitation is by disruption of the CNS (brain and spinal cord). Rapid incapacitation can be achieved by massive tissue destruction, or collapse of the circulatory system from severe haemorrhage.

There are two main mechanisms of trauma. The first is permanent cavitation, which is the path taken by the bullet while crushing and destroying tissue. This is the main method by which handgun bullets operate. The second is temporary cavitation, which is the radial stretching of tissue around the bullet's wound track. This is caused by high

pressures surrounding the projectile which accelerate material away from its path. This is particularly relevant to high velocity rifle bullets. There is still debate as to whether shock waves generated by high velocity bullets are responsible for remote injuries and cellular damage to tissues and the nervous system.

The other main factors affecting the degree of wound trauma are related to the bullet itself; i.e. apart from bullet placement, the shape, construction, mass and terminal velocity, all determine how much tissue is actually disrupted.

## 1.6 **The Use of Tissue Simulants in Wound Ballistics Research**

### 1.6.1 **Introduction**

Key requirements of wound ballistics research are to determine how a particular type of bullet will perform in animal or human tissue, to assess the nature of the resulting wound characteristics. To achieve this, various tissue simulants have been devised. Simulants are preferable to biological tissues for many reasons including the reduced risk of infectious hazards, ethical considerations and the ability to observe, photograph and compare the behaviour of different ballistic projectiles. As human tissue is heterogeneous, the challenge is to capture its bio-mechanical properties in a simulant material. To date no simulant has successfully achieved this. Soap and clay are two common simulants, but both are too dense and inelastic. They are only able to demonstrate temporary cavity effects as permanent cavities are not preserved. Ballistics ordnance gelatine is another popular simulant material that has the advantage of being elastic and transparent, allowing visualisation of a bullet's trajectory and the temporary and permanent cavitation caused. It also allows filming and photographing of these events. More recently, synthetic homogeneous simulants have been developed to address many of the deficiencies of ballistics ordnance gelatine. However, as with ordnance gelatine, these can still only be considered a soft tissue simulant.

Various human surrogate models have been successfully developed for non-penetrating ballistic purposes as well as blast injuries. Their development has been aided largely by computational finite element analysis. The natural progression is to create a heterogeneous human surrogate for penetrating ballistic trauma, but this remains an elusive quest.

In addition to simulants, human cadavers and animals such as pigs have been used. The bio-mechanical properties of tissues change after death and therefore any results achieved with human cadavers may not be reliable. Pigs are anatomically similar to humans and are considered the most suitable animal for wound ballistic experiments. In addition, their tissues and organs can be obtained quickly. However, there are both ethical and bio-hazard considerations.

The following discussion examines the general need for simulants, the most common types that have been, or are being, used today, and their respective advantages and disadvantages.

### 1.6.2 General Benefits and Properties of Tissue Simulants

MacPherson (17) and Sellier and Kneubuehl (27) state that tissue simulants are preferable to actual tissue for wound ballistics testing because:

- Human tissue is heterogeneous and there are often greater penetration variations which require additional tests before a reliable conclusion can be reached.
- Biological hazards and difficulties exist in preparing, handling and disposing of human tissue.
- Ethical considerations occur when using cadavers or animals.
- The ability to observe and photograph the bullet's interaction is improved with transparent simulants such as ordnance gelatine.

Homogeneous simulants such as ballistics ordnance gelatine are able to produce repeatable bullet impact paths, which demonstrate the physical effects of projectile-tissue interaction, including the permanent and temporary cavities. This is critical to the scientific method (17). Any tissue simulant must also be equivalent to human tissue with respect to density and tensile strength, so that it exhibits the same type of penetration depth qualities and deceleration characteristics (11, 27).

There have been a number of different materials used for this purpose such as duct-sealing compound, clay, soap, wet packs and ordnance gelatine. Plastic (inelastic) soft solids such as clay and soap have no mechanism to store strain energy to allow the

temporary cavity to collapse. Therefore, while they are useful for 'freezing' the maximum dimensions of the temporary cavity in time, the permanent cavity is lost. If this information is used in isolation, the potential for wounding can be seriously overstated, which can lead to invalid conclusions (6, 11, 16, 27, 60, 91-95). Wet packs consisting of water soaked books or newspapers are thought to provide a good indication of bullet expansion and penetration, but only for rifle bullets travelling at velocities of at least 500m/s (91).

Bullet penetration is inversely proportional to the density of the material that has been penetrated. Therefore it is important for any viable candidate soft tissue simulant to have a density around that of water, namely 1g/mL at 25°C. Soft tissue density varies by only a few percent and is generally only a few percent less than water. MacPherson (91) argues that from a modelling point of view, these small variations are not a major concern. Materials such as clay are unsuitable because they are too dense.

### 1.6.3 **Cadaver Testing**

Shooting into cadavers does not provide a close comparison with live tissue because after death the soft tissues undergo various changes as rigor mortis sets in and tissues harden. Tissues lose their natural fluids as well as their elasticity and the blood in vessels drains out or solidifies. The loss of fluids does not allow the transmission of shock waves. In addition, the process of freezing and thawing un-embalmed cadavers for preservation purposes further changes their bio-mechanical properties. Therefore, while cadaveric specimens may replicate some of the effects of a ballistic wound in a living person, they cannot exhibit the myriad of localised trauma to tissues and blood vessels caused by the shock from a penetrating bullet (16, 17, 27). The use of modern embalming fluids may further accentuate post mortem tissue changes. In addition, most cadavers in the western world tend to be older people whose physical condition is no longer representative of the larger population that wound ballisticians are generally interested in. The moral and ethical concerns of the general community to the use of cadavers in ballistic testing also often far outweigh the perceived benefits. Despite this, cadavers are still used in some western countries such as the USA and France. However, their use in many others such as Australia and New Zealand would rarely, if ever, be approved.

#### 1.6.4 **Animal Testing**

Various animals have been used for studying ballistic trauma since around 1880 (96). They include horses, cattle, goats, sheep, dogs and pigs (27, 96). Choosing a suitable animal requires addressing a range of issues such as comparable anatomy with that of a human, skin thickness, the size of the animal relative to a human to represent the full length of wound channels, the availability and the ease of handling. Pigs are anatomically similar to humans and are considered the most suitable animal for wound ballistics experiments and they have been used extensively in the past for this purpose (16, 27, 96). However, while their internal organs have similar bio-mechanical properties, pig skin is much thicker than human skin (27).

The use of animal cadavers for wound assessment has the same limitations as detailed earlier for human cadavers. The extensive use of living animals for ballistic testing has been conducted in the past (9, 16, 19, 21, 27, 96). However, in more recent times, this type of experimentation is rarely if ever approved as, once again, the moral and ethical concerns may far outweigh the perceived benefits.

#### 1.6.5 **Ballistics Ordnance Gelatine**

FBI specification ballistics ordnance gelatine is widely accepted as a human soft tissue simulant if it meets an accepted calibration standard. This standard is based on the porcine penetration tests conducted by Fackler and Malinowski (29). This formulation is said to replicate the combined mechanical properties of skin, fat, fascia and muscle tissue of a porcine thigh when penetrated by a ballistic projectile. The anatomical similarities between pigs and humans have led researchers over many years to accept that the tissue penetration characteristics of ballistic projectiles are the same in both species (16, 27, 97).

The current NATO standard for ordnance gelatine testing is 20% at  $10^{\circ}\text{C}\pm 2^{\circ}\text{C}$  with a Bloom number between 250 and 300 (98, 99). There is no calibration method described in this document and to date the author has found no other authoritative reference which details this. However, this gelatine concentration is still widely used, particularly by military researchers in Europe. The FBI 10% formulation at  $4^{\circ}\text{C}$  is considered more representative of the mechanical response of soft tissue at various strain rates than the NATO 20% formulation (100, 101).

Ballistic gelatine has been in common use for over half a century to evaluate the performance of ballistic ordnance. One of its greatest advantages over other simulants is that it is transparent, which allows visualisation of the bullet's path and the ability to film or photograph these events (17, 91, 102). However, although it may simulate the density and viscosity of muscle tissue, it lacks the bio-mechanical properties of many other tissues and organs that exist within the human body. Describing ordnance gelatine as a soft tissue simulant may also be incorrect, as soft tissue is defined as that which connects supports or surrounds other structures and organs of the body. It includes muscles, tendons, ligaments, fibrous tissues, mesentery, blood vessels, skin, but not all organs or bone (103). These differences alone make it difficult to translate tissue simulation results to wound trauma in humans (16, 104).

Ordnance gelatine is a collagen protein derived from animal products such as skin, bone and tendon through hot water acidic extraction. It is available in consistencies between 50 and 300 Bloom (27, 101, 105-107). The 'Bloom Number' is a measure of the strength and stiffness of the gelatine. In other words, a desired gelatine 'stiffness' can be achieved from either a lower concentration (mass of gelatine per unit volume of water) of a higher Bloom Number gelatine, or from a higher concentration of a lower Bloom Number gelatine.

The best consistency for shooting is type 'A' with a Bloom Number between 250 and 300. However, consistency is determined not only by the Bloom Number but also by the concentration and temperature at preparation (27). It was first used in 20% concentrations and has the advantage over other simulants of possessing elasticity similar to human tissue (1).

Fackler was the first researcher to introduce calibration into ordnance gelatine testing. He did this in the mid 1980's after recognising the deficiencies of un-calibrated gelatine and the need for some form of standardisation (8, 17, 31). His calibration technique was based on comparisons between 10% gelatine at 4°C and live 50kg to 70kg porcine thigh, as well as fresh post mortem porcine thigh. To establish the most suitable tissue simulant, Fackler and others conducted a series of penetration tests using BB copper plated steel spherical projectiles, with a diameter of 4.34mm (calibre 177) and weighing 0.340g. He fired these into freshly euthanized pig, different formulations of gelatine and soap at a velocity of 180m/s±4m/s (29, 30). Table 1 summarises these results.

Tissue/Simulant	Penetration depth	Nos .of sho
Leg of freshly killed 40kg pig	80.8±10.6mm	10
10% Ordnance gelatine at 4°C	80.5±4mm	30
20% Ordnance gelatine at 4°C	40.4±2mm	5
20% Ordnance gelatine at 20°C	80.0±2mm	5
Swedish soap at 4°C	40.2±3mm	5
Swedish soap at 20°C	50.8±4mm	5

**Table 1. Results of tissue and simulant penetration tests (1, 30).**

Upon first glance, the data from Table 1 suggest that 10% ordnance gelatine at 4°C is the closest of the simulants tested to penetration of a porcine thigh. However, Crucq (1) points out that there is no significant difference ( $p>0.05$ ) in the penetration depth for either 10% at 4°C, or 20% at 20°C ordnance gelatine. This is also the case when comparing these gelatine concentrations against the penetration depth given for freshly killed pig leg. A 20% concentration at 22°C has since been shown to equal 10% at 4°C (17). However, as pigs are comparable anatomically to humans, the results also indicated that it was an acceptable human soft tissue simulant (17, 29-31). As a result of this, a calibration standard of 85mm±10mm of BB penetration, at 180m/s±4.5m/s was developed (29). However, not all authors agree and Janzon (15) states that 10% gelatine has a lower density than muscle tissue and therefore allows greater penetration. In addition, Fackler's original data are limited and he sometimes refers to unpublished data to support his position (104).

The results detailed in Table 1 further illustrate the limitations with some of the data produced on this subject. Fackler et al. (29, 30) fired 30 shots into the 10% concentration of gelatine, but only 5 shots were fired into the other concentrations to achieve the reported penetration values. In addition, the spread across the 5 shots of 20% ordnance gelatine was half that of the 10% formulation, indicating a more consistent performance. As fewer shots were fired upon the other concentrations of gelatine, this could leave the data open to some criticism, particularly as it forms the



foundation for the assertion that a 10% gelatine model is equivalent to animal soft tissue.

Gelatine can also be difficult to prepare properly and un-calibrated gelatine will give incorrect results. For example, if too much heat is used during its preparation, it will become weak and excessively flexible, producing erratic experimental results (102, 104-106, 108, 109). Therefore, all test data from any source prior to the mid 1980's should be treated with caution as calibration was not then standard practice (31).

Corzine and Roberts (110) conducted a study in order to determine if a conversion factor could be used to correlate the results of different concentrations and temperatures of gelatine. As a result, they established that a correction factor of 1.3 provides reasonable accuracy when comparing the penetration depth achieved using 20% gelatine at 10°C to 10% gelatine at 4°C. Similarly, a correction factor of 0.76 can be used to compare the results from 10% to 20% gelatine.

Even with proper preparation, however, some batches of gelatine will yield excessive penetration results during calibration tests. MacPherson (111) developed a simplified penetration depth correction for this type of non-standard gelatine using mathematical equations.

Finally, when a bullet is fired through gelatine, it often produces radial cracks that emanate from the wound track. High velocity bullets create large temporary cavities, which in turn create cracks throughout the entire volume of the cavity. The presence of these does not necessarily represent the type of trauma that would occur in human tissue and so they should be ignored when quantifying results to avoid inaccuracies (17).

#### 1.6.6 **New Synthetic Simulants**

In more recent times, a new generation of homogenous synthetic simulants has been developed to specifically address the difficulties encountered when preparing and working with ballistics ordnance gelatine as outlined earlier. Examples include Perma-Gel, physical associating gels (PAG) and transparent gel candle, which are discussed briefly below.

Perma-Gel was developed by Amick, who set up a manufacturing company called PERMA-GEL Inc. in the USA in 2006 to market the product. It is a clear synthetic medium that is room temperature stable and was designed to approximate 10% ordnance gelatine at 4°C, as well as to meet the same FBI calibration standard. It is non-toxic, has superior clarity and unlike ordnance gelatine, will not support bacterial growth and deteriorate with age. It can also be re-melted and re-used. It has started to gain acceptance amongst both military and law enforcement agencies, particularly in the USA (112).

The US Army Research Laboratory has developed two physically associating gelatine (PAG) compositions known as PAG15 and PAG30. They are derived from triblock copolymers which are commercially available and consist of both polystyrene (PS) and polyisoprene (PI). Both formulations contain 80% mass fraction triblock (PS-PI-PS) and 20% mass fraction diblock (PS-PI). PAG15 contains 15% by mass PS and PAG30 contains 30% by mass PS. The final product contains 20% polymer by volume and 80% mineral oil, which is used as a solvent to dissolve the polymer. The preparation process involves placing the solution in a nitrogen-purged vacuum oven at approximately 150°C until it is fully dissolved, which takes approximately 6 hours. The melted solution is then poured into aluminium moulds which are pre-heated. Stress-strain measurements show that both PAGs exhibit similar deformation behaviour to ballistics ordnance gelatine when subjected to high strains at high loading rates. While further research is continuing, PAGs appear to be an alternative tissue simulant that do not suffer from the drawbacks of ordnance gelatine (113, 114).

Transparent gel candle is a commercially available product that was developed by Morrison and Heilman in the USA in 1997. It is composed of kraton and white paraffin oil. Kraton is a thermoplastic rubber polymer (elastomer) and the best formulation for ballistics studies is 15% Kraton and 85% white paraffin oil. To prepare it, white paraffin oil is heated to 110°C while the kraton is slowly added. Once completely dissolved, the formulation is cooled to 4°C for 24 hours and is then ready to use. BB pellet calibration tests have shown that the above formulation met the FBI calibration standard and was equivalent to 10% ordnance gelatine at 4°C. It can therefore be regarded as a suitable soft tissue simulant. In addition, transparent gel candle offers superior clarity to

ordnance gelatine, permanent and temporary cavities can be better photographed, and it does not deteriorate or suffer bacterial contamination like ordnance gelatine (115).

However, while these new synthetic simulants are a step forward, they are still homogenous and cannot replicate the variety of heterogeneous tissues and organs within the human body, as well as their mechanical responses.

### 1.6.7 **Computational Models and Physical Surrogates**

Finite element analysis (FEA) is the dominant mathematical computational modelling method used for a wide range of engineering and bio-medical/bio-mechanical functions. It is based on the theory that an approximate solution can be reached to a complex problem by reducing it to a finite number of simple problems (finite elements) using linear and non-linear equations in specialised 2-dimensional and 3-dimensional computer programs, such as that created by ANSYS Inc., an engineering simulation software developer. These programs use a system of nodes (points) which form a mesh (grid). The mesh contains programmed structural and material properties which stipulate how the particular structure will react to various loading conditions. However, the technique is only as accurate as the variables which are used. FEA is particularly suited to designing and evaluating new concepts or materials, predicting their performance as well as existing product refinement (116-119).

Medical research has been advanced by the use of FEA, including understanding how organs behave under various stresses, and respond to trauma. As a result, FEA modelling has allowed the development of a number of physical surrogate models for non-penetrating ballistic impact and blast purposes. Examples include the Human Surrogate Torso Model (HTSM). This was designed as a replacement for ballistics clay to evaluate behind armour blunt trauma associated with ballistic vests in accordance with the National Institute of Justice (NIJ) standard (120-122). Another is the frangible surrogate leg (FSL), which was developed by the Australian Defence Science and Technology Organisation (DSTO) as part of their Human Surrogate Program. It is designed to be as anatomically accurate as possible and is constructed of materials which simulate bone, cartilage, soft tissue and connective tissue. It is able to reproduce loading response to evaluate anti-personnel landmine lower leg injuries. This model has been recognised by NATO and further enhancements have been undertaken by a private defence contractor (Adelaide T&E Systems) (123-125). Similar work has also

been undertaken by Cronin et al. (126). Yet another example is the Human Surrogate Head Model (HSHM) developed by the Johns Hopkins University Applied Physics Laboratory in the USA to investigate the brain's response to blast trauma. This research was commissioned because of the large number of US military troops who have suffered from traumatic brain injury (TBI) over the last 10 years as a result of improvised explosive devices (IED) during the Iraq and Afghanistan wars. The HSHM is fabricated from bio-simulants and consists of a skull, brain, face and skin. Pressure sensors are distributed throughout the model to measure acceleration and pressure. By gaining a better understanding of TBI, it is hoped that improved ballistic helmet protection and medical treatment can be developed to address this type of severe injury (127).

From the examples mentioned it can be seen that human surrogate models are already in wide use for non-penetrating ballistic purposes as well as blast injury evaluation. However, to date no heterogeneous human surrogate model has been developed to assess the dynamics of penetrating wound trauma caused by bullets.

#### 1.6.8 **Conclusion**

Simulants are preferable to cadavers and animals for wound ballistics research for a variety of reasons including moral, ethical and bio-hazard considerations. A number of different homogeneous simulants have been used over time, with ballistics ordnance gelatine being the most widely accepted soft tissue (muscle) simulant.

A number of new homogeneous synthetic simulants have been developed to address the deficiencies of ordnance gelatine, which is known to be difficult to prepare and very temperature dependant. Some of these are gaining wider acceptance amongst military and law enforcement agencies. However, being homogeneous, none of these simulants can replicate the wide variety of heterogeneous tissues and mechanical responses within the human body.

Advances in computational finite element analysis have assisted in creating successful human surrogate models for non-penetrating ballistic purposes as well as blast injuries.

## 1.7 Mechanical Properties of Selected Human Tissue

### 1.7.1 Introduction

An anatomically correct simulant model, which replicates the bio-mechanical properties of the major organs and tissues within the human thorax and abdomen, is an alternative option for conducting wound ballistics research. Tensile strength, strain, elasticity and density are some of the most important bio-mechanical properties to consider in assessing responses to medium and high velocity bullet impacts (124, 128).

The lungs, heart, aorta, liver, kidneys, small and large intestines are among the most common organs to sustain major injury as a result of gunshot wounds. However, their bio-mechanical properties are quite different, resulting in different responses to bullet strike and different types of injuries (50).

An examination of the specific bio-mechanical properties of some of the major tissues and organs within the thorax and abdomen was undertaken to determine how these properties determine their response to bullet strike.

### 1.7.2 Bio-mechanical Properties of Tissue

Bio-mechanics is the science that explains the effects of a variety of forces upon the form and motion of a body (57). The study of the mechanical properties of human tissue requires the use of particular terminology. Some of the more common terms are:

- *Tensile strength* (stress): the ratio between a force and the area upon which it is presumed to act. It includes the intermolecular resistance within a body to the deforming action of an outside force (57).
- *Breaking strength*: the force per unit area required for a tissue to break or fracture under load (57). Silver (129) states the strength of a tissue is determined by stress when a tissue tears.
- *Strain* (deformation): the change in the dimensions of a body as a result of the application of force. It can also be described as 'ultimate percentage elongation' (57). Silver (129) describes it as the changes in tissue dimension (length) when compared to its initial length.

- *Elasticity*: the property of a material enabling it to return to its original shape and dimensions after removal of a force (stress). *Elastic limit* is the greatest stress that can be applied to a material or body without leaving a permanent deformation after removal of the force (57).
- *Mechanically stabilised state*: one in which stable or constant strength values are obtained (57).
- *Viscosity*: a measure of how much resistance a fluid exerts to motion (129).
- *Viscoelasticity*: a combination of time dependence and the ability to bear a load in tension. It is therefore the force associated with elongation (129).
- *Density* of a tissue: determined by its mass compared to volume that this mass occupies (129).

An understanding of the anatomy, physiology and bio-mechanical properties of relevant tissues and organs in the thorax and abdomen provides the foundation for determining appropriate simulant materials that can be used to create an anatomically correct model for ballistic testing purposes.

Figure 2 provides an overview of some of the main organs within the thorax and abdominal regions that lie within an area called the 'centre of mass.'

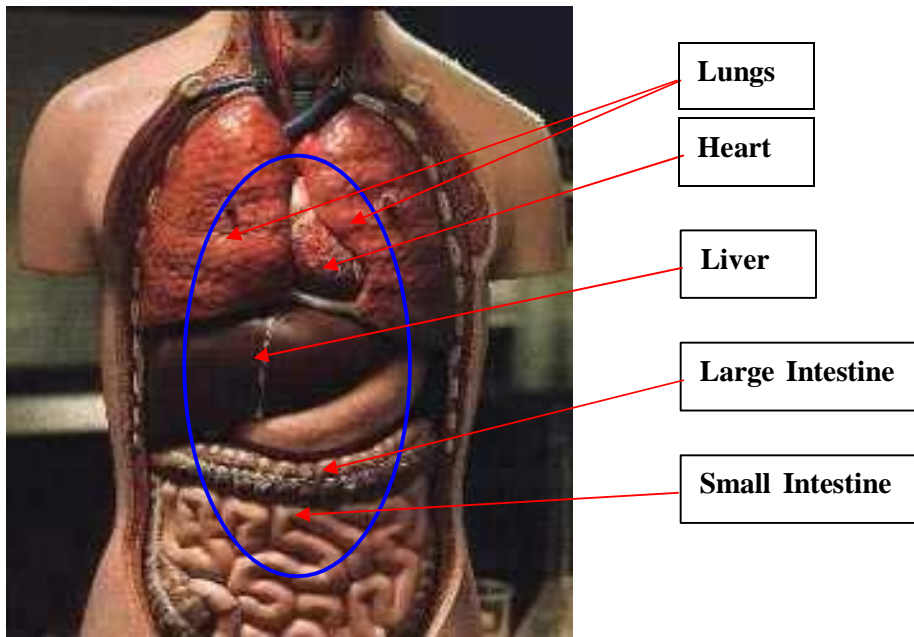


**Figure 2. Anterior view of the thorax and abdomen showing some of the major organs within the 'Centre of Mass' (marked with blue circle) (130).**

The following provides an overview of some of the bio-mechanical properties of organs and tissues within the 'centre of mass.'

Skin is the largest organ in the body and is essentially a thin membrane with several layers. The surface layer is called the epidermis and under this is a connective layer called the dermis. A bed of loose areolar tissue called the subcutis or tela subcutanea, binds the skin to the superficial skeletal muscles and other tissues (99). For impact loadings and wounds, a failure criterion based on the tearing strength of skin is deemed appropriate. This strength varies around the body's surface with values from  $8.3 \times 10^6$  to  $133.9 \times 10^6 \text{N/m}^2$  (103, 131).

The surface area of the lung is very large, approximately  $1 \text{m}^2/\text{kg}$  of body mass, to accommodate gas exchange, and yet the lungs are light and each weighs about 300g (132). They are composed of approximately 300 million small air sacs of different sizes called alveoli, separated by thin viscoelastic tissue walls, and are connected to the trachea by the bronchi. They are bounded by visceral pleura, the outer surface of which is a smooth, moist and slippery membrane made up of a relatively thick layer of collagen and elastin. The pressure in the lungs must be either higher or lower than

atmospheric pressure for air to flow freely between the atmosphere and the alveoli. The expanding force which controls this is known as transpulmonary pressure (133, 134). The mechanical properties of the lungs are designed to minimise energy losses to assist with normal breathing rates. Therefore, the loss of lung elasticity makes deflating the lungs more difficult and greatly increases the energy expended in breathing. Conversely, when a lung is deflated, air is still trapped in the alveoli by the collapsed airways and the lung can withstand very large compressive pressures because it acts like a sealed balloon (103, 132, 133).

Muscles are composed of many parallel fibres and the total stiffness of a muscle is dependent on the number of fibres or muscle volume. Muscles combine the elasticity of soft tissue with the ability to actively contract and produce forces. In determining the force exerted by the muscle, the geometry of its attachment will define its leverage. Peak forces for human skeletal muscle are obtained when the muscle length is held constant i.e. isometric contraction. These forces are between 190N and 255N for each 2.5cm<sup>2</sup> of muscle cross sectional area (103).

The heart is a relatively small organ with dimensions of approximately 120mm in length, 90mm in width at its broadest point and 60mm in thickness. It weighs about 300g in an average adult. It is surrounded and protected by the pericardium, which consists of 3 layers. The outer fibrous pericardium is a layer made of a tough inelastic fibrous connective tissue. This prevents overstretching of the heart and anchors it to the mediastinum, which separates the left and right chest cavities. The inner serous pericardium is constructed of thinner and more delicate membranes with 2 separate layers. The heart wall consists of 3 regions. The outer is the epicardium, the middle the myocardium and the inner layer the endocardium. The myocardium forms the bulk of the heart and is constructed of cardiac muscle. Cardiac muscle is different from striated or smooth muscle found elsewhere in the body. It is a modified form of muscle which contains myocardial cells, which contract to cause the beating of the heart (130, 134-136). Data from Yamada (57) indicate that cardiac muscle has about the same tensile strength as skeletal muscle. Therefore, it should be similar to 10% ordnance gelatine at 4°C (30).

The aorta is the largest artery in the body and the vena cava the largest vein. The aorta is effectively an auxiliary pump that expands when blood pressure increases. Kinetic



energy is created during this process and stored in the form of strain energy (analogous to potential energy). The strain energy is subsequently returned to the blood as blood pressure decreases. The average diameter of an aorta in a human is 25mm and the average vena cava is 30mm. As both are very large vessels, if damaged massive blood loss will be caused and most likely result in death (129).

Arterial and venous blood vessels are comprised of elastin, smooth muscle, collagen and connective tissue (135). The term elastic artery means one where there is more elastic tissue than smooth muscle. The aorta, pulmonary trunk, brachiocephalic trunk, subclavian and common carotid arteries are all regarded as elastic arteries and change their shape because of changes in blood pressure (137). Data from Yamada (57) indicate that the ultimate tensile strength is greatest in the common carotid artery followed by the descending aorta, ascending aorta and pulmonary trunk. The average ultimate percentage elongation (strain) was found to be greatest in the pulmonary trunk, followed by the common carotid artery, ascending aorta and descending aorta. There appears to be no difference between males or females in ultimate strength or strain values. The only factor affecting these is age, which is discussed in more detail later.

Where most arteries carry oxygenated blood from the heart to tissues, most veins carry deoxygenated blood from tissues back to the heart. Veins can be broadly categorised as pulmonary or systemic. Pulmonary veins differ from other veins because they contain oxygenated arterial blood that is returned to the left atrium of the heart from the lungs. Systemic veins return deoxygenated blood to the right atrium of the heart from the majority of the remainder of the body (138). The structure of veins is different from arteries in a number of ways. They are generally closer to the surface of the skin and their relative wall thickness is lower, meaning that they are not as muscular as arteries. This is because the blood pressure within them is much lower. Veins also have valves to keep blood flowing back to the heart. They contain a high concentration of smooth muscle and changes in blood pressure, muscle contraction or tension, will cause the blood volume within them to change and affect cardiac output. Being thin walled, veins are easily collapsible when subjected to external compression. In addition to smooth muscle, they also contain a high quantity of collagen but very little elastic tissue. The elastin - collagen ratio is approximately 1:3 (135).

Veins are the major storage area for blood holding approximately 60% to 70% of the total blood volume. The venous tree includes blood reservoirs such as the spleen, liver and lungs. A change in pressure will cause these vessels to gradually assume a new size to accommodate the change in blood flow. This phenomenon is called stress-relaxation and occurs to a greater extent in veins than arteries. This allows the cardiovascular system to hold extra volume in the case of a transfusion, or adjust to a decreased volume following haemorrhage from a wound of significant size (137).

There have been numerous definitions and methods used for estimating vascular elasticity, which makes it difficult to compare results in the literature. Some authors use the relationship between the change in pressure inside the vessel and the relative change in its diameter. The 'Direct *in vitro* Method' subjects a strip of vessel to known forces or pressures and the associated elongations or volumes are recorded. Either a length-force or volume-pressure curve is obtained for which a coefficient of elasticity can be calculated. This method was used by early pioneers such as Roy and MacWilliam, and is still considered a valuable tool in the study of vascular properties (137).

The liver is an intraperitoneal organ, freely suspended by mesentery, and the largest gland in the body. The falciform ligament, a portion of the ventral mesentery, connects the liver to the anterior abdominal wall and the gastrohepatic mesentery connects it to the stomach and duodenum (134). It weighs about 1.4kg in the average adult and is the largest solid organ in the body. It occupies most of the hypochondrium and part of the epigastrium (136). It is an organ with high density but low elasticity and tensile strength (1, 57, 58, 81). A human can survive with a significantly reduced amount of liver, but the liver is particularly vulnerable to bullet injury due to its mechanical properties.

The average adult kidney is 100mm to 120mm in length, 50mm to 75mm in width, 25mm thick and has a mass of approximately 150g. The outer surface of the kidney is protected by a tough fibrous capsule (57, 134). The inner cortex and medulla have a similar high density but low tensile strength similar to that of liver (57). An individual can function normally with the loss of one kidney, so this provides a safety margin should a person suffer a significant wound to this organ (139).

The intestines are also known as the large and small bowel. The small intestine is divided into three segments, the duodenum, jejunum and the ileum. It is the major site of digestion and absorption of about 90% of nutrients. It averages 25mm in diameter and 6.4m in length. A visceral peritoneum completely surrounds it with the exception of a large portion of the duodenum. The small intestine also contains two layers of smooth muscle. The outer layer is the thinnest with longitudinally arranged fibres, whilst the inner layer has thicker circular fibres (136, 138).

The large intestine completes the process of absorption and expulsion from the body. It averages about 65mm in diameter and 1.5m in length. It is divided into four regions called the cecum, colon, rectum and anal canal. The colon is further divided into the ascending, transverse, descending and sigmoid colons. The outer layer of the large intestine contains longitudinal muscle and the inner layer circular muscle similar to the small intestine, but portions of the outer longitudinal muscle are thickened into bands called taeniae coli (136). These give the large intestine a slightly higher tensile strength than the small intestine, with the ascending colon having the highest value, followed by the transverse colon and then the descending colon. In general terms, both intestines have a similar tensile strength to that of the oesophagus (57). Although the intestines have elastic properties, they contain fluid or semi solids much of the time.

Most research on the mechanical properties of biological tissue has focussed on muscles and connective tissues. Connective tissue is primarily composed of flexible elastic fibres, stiff collagen fibres and a ground substance which is gel-like and protein based. These properties make these tissues viscoelastic (103). Tendons and ligaments are classed as soft tissues, but are constructed of almost pure collagen, which makes them fairly inextensible. Bone and skin also contain significant quantities of collagen. The tensile strength of collagen is due to its tightly packed microscopic structure (133). Elastin is a very extensible fibrous protein and provides tissue with the ability to change shape and size without permanent damage. Much of the tissue within the body is elastic in nature (129).

### 1.7.3 High and Low Velocity Impact Characteristics

As a general rule, impacting objects cause injury to the body by energy transfer and these injuries result from tissue deformation beyond its recoverable limit. Compression of the chest and abdomen at high rates of loading is the primary mechanism

responsible for injuries to these areas, as it results in the stretching of internal organs and vessels. Structures like the rib cage can fracture, and organs such as the heart, liver and stomach can rupture. There are different ways in which organs can be stretched, which results in different types of injuries. Low and high speed impacts will generate different biomechanical responses. For example, in low speed impacts, the organ or vessel is loaded slowly and the kinetic energy is absorbed gradually through the mechanism of compression. The elastic properties of the tissue as well as the pressure which is built up resist this compression. However, in high speed impacts, the process of rapid loading is resisted by a reaction force which is proportional to the speed and deformation of the tissue. There is also an inertial component to the reaction force where the body develops high internal pressure. The ability of an organ or structure within the body to absorb energy without injury is called tolerance. Fluid filled organs such as the heart, stomach or intestines can absorb energy by tissue deformation if compressed slowly, but when loaded rapidly, they cannot deform quickly enough and may rupture. Therefore tolerable compression inversely varies with the velocity of impact (124, 128, 140).

One of the most important properties of tissue regarding high velocity impacts is density; the higher the density, the greater retardation effect on the bullet, as more energy is absorbed by the tissue which reduces bullet velocity. The specific gravity of a tissue is a measure from which tissue density can be calculated. It involves comparing the density of a material to the density of water (1g/ml) (50, 53).

Table 2 provides a comparison between the densities of biological tissues compared to simulant media. From Table 2 we can see that 10% gelatine has a similar density to skeletal muscle and is slightly denser than liver. However, it is quite different from fat, lung and bone.

Medium	Density (kg/m <sup>3</sup> )
Skeletal muscle	1020 - 1040
Liver	1010 - 1020
Fat	800
Skin	1090
Lung	400 - 500
Bone	≥ 1110
Brain	1040
Swedish soap	1060
20% Gelatine at 10°C	1060
10% Gelatine at 4°C	1026

**Table 2. Comparison between the densities of some biological tissues and simulant media (1).**

The density of tissue also determines the amount of drag on a projectile. Lungs have a much lower drag than muscle because of their lower density due to their high air content. Tissues of similar density have similar drag properties, for example liver and muscle (15, 81).

The abdomen is more susceptible to injury than the thorax as there is no rib cage or other surrounding bone structure to protect the internal organs. Haemorrhage is the major cause of death for a person with an abdominal injury (141). Solid organs such as the liver, kidneys or spleen have high densities and low elasticity. Cavitation has the effect of tearing and in some cases fragmenting these organs, resulting in major injuries. Therefore, they are very vulnerable to high energy bullet impacts. The permanent cavity volume can almost equal that of the temporary cavity in the liver because of the low strength of the tissue (51, 53). The effect upon structures such as the stomach or colon is dependent upon their contents and the ballistic dose (energy deposition rate profile) received. Microscopic damage has been found in the small and large intestines up to 200 mm from the wound channel. This is thought to occur because the intestines contain gas pockets and haematomas may develop because of 'complex' (i.e. reflected) pressure waves generated by temporary cavitation (51).

The thorax contains ribs, lungs, and major organs and vessels such as the heart and aorta, and the oesophagus. The effects of high energy transfer and cavitation will vary depending on the structure involved. DeMuth (142) found there is little or no evidence

of temporary cavitation in lung tissue. However, the author considers that this statement needs qualification; while there may be a minimal elastic response, there is unlikely to be 'no' response at all. Bullets with high velocities will transfer only small amounts of energy due to the low specific gravity, low water content and high elasticity of lung tissue, as well as the damping effect of the air content which prevents pressure waves from travelling very far from the wound track. However, if a damaged airway opens into the pleural cavity, a pneumothorax will most likely occur with air escaping into the pleural cavity. If this occurs, the lung may fail to re-expand (53, 59).

Few people survive high energy transfer injury to fluid filled structures such as the heart, aorta, main pulmonary arteries or vena cava because of major haemorrhage (53, 59). Injuries to these organs can be the result of permanent or temporary cavitation with high velocity rifle bullets; i.e. even if the heart is not struck directly by a bullet, it may be affected by temporary cavitation and can be displaced causing cardiac arrest (15). Open wounds caused by laceration of the great veins may cause death in the absence of major haemorrhage by air embolism (53).

While soft tissue yields to pressure effects, bones do not do so because they are dense, have far less elasticity and are therefore prone to fracture. Injuries to bones are almost always accompanied by soft tissue damage surrounding the bone (51). Fractures to bones can occur by a direct bullet strike or due to high energy transfer and the pressure effects of temporary cavitation. Bone fragments can then become secondary projectiles, which may combine with projectile fragments to cause soft tissue damage near the bone, including damage to blood vessels and nerves (53).

#### 1.7.4 **Conclusion**

From these descriptions, it can be seen that the specific characteristics of tissues should be taken into account when designing criteria for simulant materials. This would allow for a higher level of confidence in relation to the results achieved.

## 1.8 **Methods of Injury Assessment in Bullet Wound Trauma – A Military and Police Perspective**

### 1.8.1 **Introduction**

Accurate assessment of injuries to humans from bullet wound trauma is important for many reasons including determination of the nature of the wounds, formulating appropriate medical treatment where indicated, and linking wounds with potential weapons and ammunition. In addition, the study of injuries may assist in evaluating the performance of ammunition in facilitating its future development and in the development of various forms of ballistic protection. Military and law enforcement agencies are particularly interested in this subject to ensure that an aggressor ceases to be a threat as soon as possible, and that soldiers and police officers are appropriately protected from bullet injuries.

The terms 'lethality' and 'incapacitation' are used by military and law enforcement agencies respectively to measure the effectiveness of a particular firearm and ammunition combination. The two terms are however, fundamentally different. The term 'incapacitation' may be the more useful as it identifies the need to immediately or rapidly incapacitate an aggressor, but acknowledges that such injuries may not always be lethal.

Various assessment models have been developed, some based on the measurement of kinetic energy alone. These assume that the amount of energy transferred to tissues is directly proportional to the damage incurred. However, these fail to recognise that other factors involved in energy transfer may not cause any tissue disruption. To date there is no existing wound trauma evaluation model that fully addresses all the physiological complexities involved in bullet and tissue interaction.

An anatomically based model which addresses the physiological response to wound trauma would seem an appropriate alternative to develop in conjunction with the use of the existing internationally recognised Abbreviated Injury Score (AIS) and an appropriate Injury Scoring system such as the Maximum Injury Severity Score (MAXAIS) or the New Injury Severity Score (NISS) to evaluate incapacitation injuries.

The following analysis will examine the differences between the concepts of lethality and incapacitation used by military and law enforcement agencies, as well as the use of

scoring systems to assess and classify the severity of trauma-related tissue injuries. In addition, previous wound trauma models will be examined and the difficulties discussed when relying solely on combat or civilian shooting data to determine the effectiveness of different types of ammunition.

### 1.8.2 **Measures and Indices**

Terms such as ‘stopping power’ (21) and ‘wound trauma incapacitation’ (17) are used to describe a bullet’s ability to inflict a lethal or incapacitating injury. There are two distinct schools of thought regarding the validity of various measures used during the evaluation process. NATO currently uses ‘lethality’ indices to measure the terminal (wound ballistics) performance of ammunition, whereas law enforcement agencies use ‘incapacitation’ indices for the same purpose. The two terms are fundamentally different and can cause confusion if they are not well understood or defined. However, the purpose behind both is simply to provide a quantitative measure of the effect of a single round of ammunition.

### 1.8.3 **Lethality versus Incapacitation**

Incapacitation and its associated terminology are most commonly used in the law enforcement arena to describe the cessation of a life threatening action against a police officer or civilian by an aggressor. As already discussed, ‘immediate’ or ‘instant’ incapacitation is usually only possible if there is significant CNS damage, whereas ‘rapid’ incapacitation is achieved by massive haemorrhage from the heart or major blood vessels, or significant injury to the limbs. Even if the heart has been destroyed, there may be sufficient oxygen within the brain and musculoskeletal system to continue to support voluntary action for 5 to 10 seconds (2, 44). However, incapacitation does not necessarily mean, or require, that a person’s wounds are fatal. If the threat from an adversary has been removed within the specified time frame of the threat, the firearm and ammunition combination can be considered effective.

Lethality is quite different from incapacitation. It refers simply to a weapon systems ability to inflict a fatal wound. It can also be used to describe the accuracy of a weapons system. There are complex mathematical models available that are based on a uniform random number algorithm to determine vulnerability (143, 144). NATO uses



these types of indices, but this information is usually classified and is therefore not readily available.

Indices based on lethality are arguably easier to model as it is more straightforward to rate a wound as potentially lethal or not. However, although a wound may ultimately prove to be fatal, it may take quite some time (minutes, hours or even days) for this to occur. Therefore although mortally wounded, an adversary may not be incapacitated and may still represent a threat.

The military also use the term 'casualty criteria' in an attempt to quantify the amount of kinetic energy a bullet or fragment must have to put an adversary out of action. These criteria characterise the effectiveness of ammunition using injury scoring systems. These systems are based on the premise that a projectile or fragment is deemed to be effective when its kinetic energy is sufficient to penetrate specified material to a required depth, and incapacitation probability tables have been devised for bullets and fragments of known energy. However, there is significant discrepancy among authors as to how much energy is required to put an individual out of action. Thus the effectiveness of a projectile cannot necessarily be judged by one energy value alone and must be judged by the 'probability of incapacitation', where factors such as the anatomical strike site and the type of activity that the aggressor was engaged in (tactical scenario) are also taken into account (27).

#### 1.8.4 **Abbreviated Injury Scale**

The Abbreviated Injury Scale (AIS) was one of the first anatomically based systems devised to assess and classify the severity of trauma related tissue injuries. However, it does not include a scoring mechanism to predict mortality or survivability. It was introduced in 1971 by a committee which included members of the American Medical Association, The Society of Automotive Engineers and the American Association for Automotive Medicine. It was initially designed for motor vehicle accident injury assessment and included only 73 main injuries, but has evolved to include most injury types. It is widely used throughout the world, but particularly in the United States, parts of Europe, Japan, Australia and New Zealand (145-147). It is also used for medical trauma care and training, as well as in a variety of research fields, including the assessment of bullet wound trauma (148, 149).

AIS uses a classification system where each injury is given a six digit code based on its anatomical site, as well as the nature and severity of the injury. The body is divided into nine regions: the head, face, neck, thorax, abdomen, spine, upper extremities, lower extremities and external. There are in excess of 2000 codes which describe different injuries within these regions (146, 150, 151). Table 3 summarises the AIS scale that is used for injury classification.

<b>AIS Severity Score</b>	<b>Injury Severity Description</b>
1	Minor
2	Moderate
3	Serious – not life threatening
4	Severe – life threatening
5	Critical – survival uncertain
6	Maximum – untreatable

**Table 3. Scale of values used for AIS severity code classification (146).**

From Table 3 it can be seen that a score of 1 indicates a minor injury compared to a score of 6 which is regarded as non-survivable. The AIS does not allow for a combination of injuries to be given a single score, which is a function of scoring systems such as the Injury Severity Score (ISS) and New Injury Severity Score (NISS) described below.

The AIS has undergone revisions in 1976, 1980, 1985, 1990, 1998 and 2005, with an update in 2008. Some revisions have been more extensive than others, for example AIS 98 and AIS 2005, which are still in common use (152, 153). AIS 08 is a minor update of AIS 05 with the addition of 15 new codes, 10 code level changes and 3 code format changes. There are also a number of wording and instructional changes (151, 154-156). There have been a number of studies over the years comparing different AIS editions to each other to determine any mapping difficulties, or the effect on the various scoring systems that the AIS forms the basis for. Most have shown some mapping

complications due to the addition of new codes which have no equivalent in earlier versions, which can affect the accuracy of ISS and NISS calculations. In addition, it appears the re-classification of codes or coding rules with successive versions, as well as improvements in management techniques, has resulted in a substantial decrease in patients classified with major trauma, particularly those with injuries to the head, thorax and extremities (151, 153-162). There is, however, no doubt that successive versions have refined and brought about continuous improvement of the AIS despite the difficulties outlined.

Military organisations also use the AIS scale in conjunction with existing wound data obtained from a variety of databases (148, 149). The largest of these databases is called the Wound Data and Munitions Effectiveness Team (WDMET), which collates data from over 3,000 combat incidents from the latter half of the Vietnam War. Another database, called the International Early Conflict Care (IECC) database, documents other American, British and Israeli combat injury data. Champion (148) has been responsible for incorporating these data into the AIS 2005 civilian and military scaling systems, so that they can be used to better understand the nature and severity of combat injuries. Data from the conflicts in Afghanistan and Iraq have been gathered and analysed using these systems.

#### **1.8.5 Other Injury Scoring Systems**

There are a large number of different injury scoring systems that provide a numerical measure of the severity of multiple injuries. It is not intended to discuss all of the available scoring systems as some have been successful while others have not. Therefore, only those in common use and considered viable in the development of an anatomical model will be discussed in detail.

Injury scoring systems can be divided into two classes namely consensus-derived and data-derived. Consensus-derived are the more traditional and are based on the AIS severity score as commonly assigned and agreed upon by clinical experts. They include the Injury Severity Score (ISS), the New Injury Severity Score (NISS) and the Anatomic Profile Score (APS). Data-derived scoring systems are based on survival probabilities which are calculated from large trauma databases. They include the International Classification of Disease Injury Severity Score (ICISS) and the Trauma Registry Abbreviated Injury Scale Score (TRAIS) (163, 164). A comparison study by

Moore et al. (164) found that data-derived scoring systems predicted mortality more accurately than consensus-derived scores when the only consideration is anatomic injury severity. However, when age, physiologic status and anatomic injury severity are jointly considered, data-derived scores offer little advantage over consensus-derived scoring systems. They also found that data-derived scores had the advantage of being objective and the ICISS in particular required no specialised coding. However, because ICISS and TRAIS are based on probabilities, their systems incorporate mortality risk factors other than anatomic injury severity and this is a significant disadvantage. They concluded that overall the best consensus-derived scoring system was APS and the best data-derived was TRAIS.

#### 1.8.6 Injury Severity Score (ISS)

The Injury Severity Score (ISS) was developed in 1974 by Baker et al. (163). It is an anatomical scoring system and was devised because the AIS had no method for classifying multiple injuries into a single score. It is a refinement of the AIS where the body is divided into six anatomical regions instead of nine. Each injury is given an AIS severity code and a single figure is derived by adding together the square of the score for the three most severe injuries within the ISS regions. ISS scores range from 0 to 75 and any AIS injury score of 6 (non-survivable) is automatically assigned an ISS score of 75. An ISS score of 16 or more is classed as major trauma (146, 147, 163, 165, 166).

The ISS has been shown to be far more accurate at predicting mortality rates than the AIS alone. However, there has been considerable criticism of the ISS (166-170). Comparative studies by Meredith (171), Sacco (172) and Stephenson (173), point out the following deficiencies:

It does not take into account multiple injuries to the same anatomical region and therefore may underestimate other severe injuries that have been sustained.

- Many injury patterns to different regions can result in the same ISS score, but these injuries may have inherently different mortality risks.
- Any AIS error is magnified by the ISS scoring system.

Despite the criticisms, the ISS continues to be the most favoured and widely used anatomic scoring system (174).

### 1.8.7 **New Injury Severity Score (NISS)**

The New Injury Severity Score (NISS) is a refinement of the ISS. It was developed in 1997 after recognition that there were deficiencies with the ISS system (147, 166, 175). It uses the sum of the squares of the three highest AIS scores, independent of the region of the body. The advantage of this system is that it is simpler to assess the severity of respective injuries. In addition, it takes into account multiple severe injuries to the same region but does not differentiate between severe injuries in different locations (146, 147). It also excludes physiological data from outcome prediction just as the ISS does (166). One study by Di Bartolomeo et al. (176) shows that the predictive ability of NISS can be improved even further by using an additional variable, namely adjusting for the number of injuries.

NISS is easier to calculate than ISS and while some studies have shown it is equivalent to ISS, the majority have shown that NISS is more accurate than ISS in predicting the outcome of severe and specific trauma, as well as intensive care unit admission and hospital length of stay (172, 174-186).

A common difficulty identified with both ISS and NISS systems is that identical scores can be obtained from different AIS triplets (set of three AIS severities) which carry significantly different inpatient mortality risks. This is contrary to the general assumption that patients with different injuries but the same score have similar survival expectations. This anomaly occurs because both scores are calculated using three AIS scores and so it is possible to obtain the same ISS or NISS score from different combinations of the AIS. This potential flaw has quality control implications for patient assessment and treatment. Therefore caution must be exercised when interpreting the results from both ISS and NISS values generated by different AIS triplets (167, 187-189).

### 1.8.8 **Trauma Injury Severity Score (TRISS)**

The Trauma Injury Severity Score (TRISS) is another system based on the ISS. It uses a person's age, type of injury, Revised Trauma Score (RTS) and ISS to determine the probability of survival. The RTS is a combination of the Glasgow Coma Scale (GCS), systemic blood pressure (SBP) and respiratory rate (RR). The RTS is calculated by adding the coded values of each of these together. A patient's probability of survival

(Ps) is determined by a formula which uses both ISS and RTS, as well as different coefficients for age ranges.

The TRISS method differs from the ISS because it also takes into account physiological injury and physiological response in addition to anatomic injury. However, it has the same type of problems as the ISS and does not evaluate multiple injuries to the same body region. It also does not recognise pre-existing medical conditions which are known to affect mortality rates in serious trauma patients (166, 190-192).

The GCS mentioned earlier and used in TRISS calculations, not only measures brain injury but also brain function. It is determined by the total of three coded values which describe a person's motor, verbal and eye response to pain or speech. The motor response is considered the most important predictor of outcome (193, 194).

#### **1.8.9 International Classification of Disease Injury Severity Score (ICISS)**

The International Classification of Disease Injury Severity Score (ICISS) was introduced in the mid 1990's by Osler et al. (195). It is based on the International Classification of Disease-9 (ICD-9) trauma classification codes and was developed to address problems with the ISS. It uses survival risk ratios (SRRs) which are determined by dividing the number of survivors by the total number of patients within each ICD-9 code. The sum of the SRRs for each injury sustained by the patient becomes the ICISS figure. One of its major benefits is that most trauma centres already classify their patients using the ICD-9 system. It is also easier to score than the ISS as a person's probability of survival is based on prior patient survival rates with comparable injuries classified by the ICD-9. This information is stored in large databases which continue to expand. In addition, all injuries are taken into account and modelled (164, 166, 167, 195-197). However, Chawda et al. (166) point out some limitations with the ICISS system. It does not use physiological data and because of this, some hospitals are reluctant to use it. In addition, different hospitals may use different ICD-9 codes, which make it difficult to compare hospital performance. Nevertheless, various studies have been conducted comparing the ISS and ICISS. Some have shown that the ICISS is a better predictor of survival than the ISS (195, 197-201). Others have shown that it is a better predictor of mortality than the ISS (171, 172, 174, 195, 202, 203). Yet another study found that the ICISS performed as well as the ISS, but did not outperform it. However, being an

evidenced based system with consistent performance and ease of use, it has some advantages over the ISS and may prove to be a successor to it (204).

ICD-10 is now in use in some parts of the world. There are some major changes from ICD-9, including an expanded code set which allows for more information to be conveyed in the code, and consistent modernised terminology. However, there is no clear mapping between the old and new codes, which can create problems when transitioning. It will be interesting to see a more detailed comparison once data has been collected over a greater period of time (205).

#### **1.8.10 Trauma Registry Abbreviated Injury Scale Score (TRAIS)**

The Trauma Registry Abbreviated Injury Scale Score (TRAIS) is based on survival probabilities and uses the same calculation method as ICISS. However, instead of using ICD-9, it uses AIS derived SRRs in relation to a patient's injuries. A study by Moore et al. (164) found that TRAIS was the best data derived system and more accurate than ICISS. However, this opinion was qualified by the additional finding that ICISS performed better than TRAIS with severe injuries sustained to the extremities or thoracic and spinal regions. Kilgo et al. (196) found it was also the best AIS based system for predicting mortality and the simplest to calculate.

#### **1.8.11 Anatomic Profile Score (APS)**

The Anatomic Profile Score (APS), also known by the shorter name Anatomic Profile (AP), is another consensus derived scoring system. It was developed to address the limitations of the ISS by including all serious injuries in a particular body region. Injuries to the torso and head are scored higher than injuries to other body regions. All serious injuries defined as AIS 3 or above, have been placed into four categories namely:

- A head and spinal cord
- B thorax and anterior neck
- C all remaining serious injuries
- D all non-serious injuries

Serious injuries to each region are calculated as the square root of the sum of the squares of the relevant AIS scores. If a region has no injury it receives a zero score. Probability of survival is calculated using a logistically calibrated equation (logistic-regression analysis) that is determined from three modified components from three different body regions.

The APS has been shown to be better than the ISS in determining patient survival and mortality. However, this improvement in performance is modest and its mathematical complexity is a major limitation (166, 188, 196, 206). The study by Moore et al. (164) found that the APS was the best consensus derived scoring system.

#### 1.8.12 **Maximum Abbreviated Injury Score (MAXAIS)**

The Maximum Abbreviated Injury Score is the simplest measure that has been proposed, because it only uses the most severe injury and AIS severity code to predict mortality. This option was introduced because there is no consensus as to how many injuries should be considered in a scoring model and to what degree multiple injuries predict outcome. A comparative study by Kilgo et al. (196) found that the MAXAIS was statistically superior at predicting mortality risk than other systems. It was also much simpler to score and the problem of incomplete cataloguing of injuries was far less of an issue than with scoring systems that rely on multiple injury evaluation. The results of this study are in general agreement with an earlier study by Meredith et al. (171) which found MAXAIS was superior to ISS or NISS, but not quite as good as APS. Its main advantage over the APS was that it is much easier to calculate. However, a later study by Harwood et al. (180), which is arguably more detailed, disagreed with the conclusions of Kilgo et al. (196). They found that the MAXAIS was equivalent to NISS in predicting mortality in blunt trauma patients, but NISS was superior to MAXAIS in predicting mortality in orthopaedic trauma patients, particularly those with multiple injuries. In addition, they found that NISS was superior to MAXAIS for predicting hospital length of stay in blunt trauma patients with non-lethal complications, but MAXAIS was superior to NISS at predicting mortality in patients with penetrating trauma and also those without orthopaedic injuries. The authors point out that one of the reasons for the difference in results is that the study by Kilgo et al. (196) was conducted in North America where there is a much higher incidence of penetrating trauma due to gunshot wounds than in Europe where this later study was conducted. Military research



organisations in various countries prefer to use MAXAIS for purposes such as body armour analysis because of its simplicity and superior performance with penetrating injuries (149).

## 1.9 Previous Wound Trauma Models

There have been a number of models developed to determine the amount of wound trauma a particular firearm and bullet combination may cause. Some of these models have been relatively successful, while others have not. None can claim to address all of the complex issues involved with wound trauma in all organs and tissues. Some of the major models that have been developed are briefly examined below.

### 1.9.1 Kinetic Energy Models

Kinetic energy (KE) is calculated using the formula  $KE = \frac{1}{2} mv^2$ , where  $m$  is mass and  $v$  is velocity. Although KE was once thought to be the principal mechanism behind bullet wound trauma, this concept has caused widespread controversy (53). While the pioneering work of Kocher supported this relationship (5), Hatcher (21) suggested that the amount of energy expended in the body by a projectile is not a measure of its stopping power, although it is important in the context of hydro-dynamic shock. MacPherson (17) states that bullet wound trauma models based solely on KE cannot be validated, as wound damage is caused by stress (force) and not energy, and a large amount of a bullet's KE results in tissue stresses that are not significant enough to cause actual damage. An example of this would be temporary cavitation associated with handgun rounds, which causes no significant injury. Theories associated with KE assume that the amount of energy transmitted to the tissues is directly proportional to the damage inflicted. This fails to recognise that there are other factors involved which dissipate energy, but do not cause parenchymal disruption. These include:

- Sonic pressure waves related to bullets that travel faster than the speed of sound.
- Heating of tissues.
- Heating of the projectile.
- Motion imparted to the tissue.

### 1.9.2 Stopping Power Model

Hatcher (21) was one of the first researchers to assign a numerical figure to the approximate incapacitation potential of a particular handgun bullet. His original formula was based on energy but having realised the flaws with energy based models, he later developed a 'relative stopping power' (RSP) model and formula based on momentum (21, 27, 84, 207). He also found that the momentum formula results were much closer to La Garde's empirical work with Thompson in 1904 when they were commissioned by the US Department of War to find the most effective handgun cartridge for US military use. They conducted a series of experiments using cadavers and live animals. The cadavers were suspended by the neck to act like a ballistic pendulum. When fired at with different calibres of cartridges, the 'shock' or momentum imparted into the cadavers caused them to move like a pendulum and this movement was measured. Therefore, the greater the movement, the greater the momentum and the more effective the cartridge under test was considered to be (27, 207).

Momentum is measured by a bullet's mass multiplied by velocity and can be derived from the bullet's KE divided by the velocity, and multiplied by two. Hatcher (21) stated that the destruction of tissue varies with the square of the diameter of the bullet in question, unless the bullet becomes distorted. He also stated that stopping power is approximately proportional to the square of the total tissue mass disrupted in the permanent wound cavity in relation to handgun bullets. The temporary cavity effect was unknown to Hatcher and so was not factored into his formula (17). Hatcher's formula was  $RSP = \text{bullet cross sectional area} \times \text{momentum} \times \text{shape factor}$ . The shape factor was an empirical figure he assigned (27, 207). This model has since been placed into a mathematical equation form by MacPherson (17):

$$\text{Stopping Power} = KmVAB$$

Where:

K = scaling constant

m = bullet mass (proportional to weight)

V = bullet velocity

A = bullet cross-sectional area

B = bullet shape (form) factor.

Hatcher (21) described his formula as an approximation at best, but it became the standard for handgun bullets for decades. He cautioned however, that the formula was not fully applicable to rifle bullets because yaw and tumbling were also significant factors affecting their stopping power (17, 21).

Some authors, such as Sellier and Kneubuehl (27) claim that Hatcher's momentum formula can no longer be regarded as current with respect to biological effects. This is because it favours projectiles with a high momentum such as calibre 45 Automatic, also known as 45ACP (Automatic Colt Pistol), and discounts those that might be known to perform equally as well or better in actual shooting situations. They cite 9mm Luger as an example, even though this calibre commonly over penetrates and therefore might not deliver all its momentum to a body. They claim that actual shooting scene experience has shown this calibre to be at least equal to or even more effective than, 45ACP. Despite this, the RSP momentum formula rates the 45ACP 50% higher than the 9mm Luger cartridge. In addition they point out that in most cases an advancing aggressor that has been shot will not fall backwards through the mechanisms of recoil and transferred momentum. Instead the injured aggressor will maintain velocity in the direction of the shooter before falling forward, because of their inertia.

Sellier and Kneubuehl's (27) choice of a comparison between calibres 9mm Luger and 45ACP to demonstrate their point is questionable. This is because the Relative Incapacitation Index (RII) discussed further below, rated 9mm Luger highly for law enforcement purposes. However, following poor field performance, the RII model was abandoned and a larger calibre recommended for FBI use, namely the 10mm Automatic. Severe recoil and adverse wear on semi-automatic pistols in this calibre lead to the development of calibre 40 Smith & Wesson, which outperforms 9mm Luger and replaced it as the most common calibre accepted by law enforcement agencies. The 45ACP still remains a highly regarded calibre (6, 10, 26, 208-210).

### 1.9.3 **Relative Incapacitation Index (RII)**

In 1973 the US Department of Justice, National Institute of Justice (NIJ), sponsored research to determine the effectiveness of 142 handgun cartridges for law enforcement purposes. A 'Relative Incapacitation Index' (RII) was devised and published in 1975 (84, 207, 208). It was the first attempt since the Thompson-La Garde tests on cadaver's and live steers in 1904, to scientifically classify the terminal effects of handgun ammunition (208). It was also the next attempt to produce a wound trauma model following the relative stopping power model produced by Hatcher (17).

The RII scale was a numerical value calculated from a combination of target vulnerability, hit distribution and bullet terminal ballistics. It used computer simulation of bullet penetration in a human represented by over 150,000 cells in a three dimensional 'computer man'. To achieve this, the human body was divided into 25mm horizontal slices and each slice was further divided into grid cells measuring 5mm x 5mm. The centre of vulnerability was considered to be in the chest area at the level of the axilla. Each cell was awarded a numerical value relative to its likelihood of instant incapacitation by a team of physicians, who also considered superimposed temporary cavity measurements onto the computer image. These were based on shots into 20% gelatine at 10°C as mandated by the US Army Surgeon General (26, 27, 84, 207). While the temporary cavity was measured, the permanent cavity and penetration depth were not (26). The importance of KE was the principle upon which this model and method rested. The results provided a rated value for almost all commercially available handgun ammunition and were designed to assist law enforcement in their selection of operational ammunition.

The RII scale relied on two assumptions: i) that 20% gelatine is a realistic tissue simulant and ii) that temporary cavity tissue disruption is as incapacitating as that which occurs in a permanent cavity. However, neither of these assumptions is now considered accurate, as calibration of gelatine had not been developed at that time, and the temporary cavity has been shown to contribute very little to wound trauma involving handgun bullets (10, 17, 211). In 1987 the FBI Wound Ballistics Workshop identified failings in the RII scale and by the early 1990's it was no longer in use (6, 10).

#### 1.9.4 **Federal Bureau of Investigation (FBI) Test Program**

Following the failure of the RII model, the FBI defined certain bullet effectiveness parameters and developed an ammunition test program. This program established standards and test protocols to evaluate cartridges against typical barriers encountered by law enforcement officers such as heavy clothing, windshield glass and building materials. It also stressed the need for adequate penetration, which was defined as a minimum of 300mm in tissue to cater for shots from any angle into the torso (17). The program did not seek to develop a wound trauma model, but its test protocols are still used by many ammunition manufacturers and law enforcement agencies in a manner that arguably provides the basis of a 'model' for this type of evaluation.

#### 1.9.5 **The Verwundungsmodell Schütze (VeMo-S)**

In the late 1990's, the German Office of Defence Technology and Procurement sponsored the development of a computer based model for similar reasons as the RII "computer man". The Verwundungsmodell Schütze ("Rifleman Wound Model" VeMo-S) differed as it did not model a particular person. Instead it approximated anatomical structures using geometric shapes. Approximately 400 anatomical structures were modelled and an incapacitation factor based on time dependence was assigned to each structure for energy density or effectiveness. In addition, ballistic data from each bullet was calculated along the length of the geometric wound channel and the amount of damage to a structure was calculated from this. Unlike the computer man model, the VeMo-S data was validated using actual shooting scene cases taken from war surgery and forensic case work. This model is multi-functional and has also been used for shooting scene reconstruction purposes as well as other forensic applications related to projectile and fragmentation injuries (84).

#### 1.9.6 **Knock Down Power**

This is another term used to describe bullet wound trauma incapacitation. It relies upon the momentum values for a given bullet and implies that a bullet has the ability to move a target. However, bullets do not generally knock a target down. Newton's third law of motion states that "for every action there is an equal and opposite reaction", thus if a bullet had the energy to knock down a target, it would also knock down the shooter (26, 27, 212).

### 1.9.7 **Mathematical models**

A number of mathematical models have been developed over time to predict penetration or to measure the incapacitation effect resulting from a particular wound channel in the body. These include the 'the knockout value' developed by Taylor in 1948, the 'power index rating' developed by Matunas in 1984, and the 'bullet penetration model' developed by MacPherson in 1994 (17, 27). Crucq (1) developed an advanced two dimensional computer generated modelling system called WB2D, which simulates and graphically illustrates predicted wound trauma with specific types of ammunition. The computer model has been used by military research organisations.

While these models are very useful and cost efficient, obtaining the required physical data regarding tissues in vitro is difficult as the biomechanical properties of tissue may change when subjected to extremely high forces over a very short time span (84). In addition, practical experience will tell the researcher that no two bullet impacts into tissue are exactly the same and most mathematical models do not recognise this (27). Mathematical models also tend to be complex and difficult to understand for those not familiar with the field.

### 1.9.8 **Combat and Street Shooting Data Modelling**

Marshall and Sanow (209, 210) provide one of the best examples of researchers who have analysed bullet effect based on data from actual street shootings. Their conclusions were based solely on the history of shooting incidents for a given factory manufactured cartridge within the United States; i.e. they compiled the percentage of single shot incidents achieved with each type of ammunition. A shot was registered in their study if the offender immediately collapsed or stopped within three metres of impact. However, the statistics they obtained do not detail which anatomic structures were disrupted or damaged by the bullet, or take into account that many of their single shot events may have been the result of psychological rather than physiological factors. Thus their results have been criticised (27, 213-216). Hatcher (21), Jussila (16) and MacPherson (17) make similar comments when discussing the issue of models based solely on data from combat shootings or civilian street shootings as such data rarely address the complexities involved in wound trauma and are by definition anecdotal. However, data of this type can still be very useful for modelling purposes if analysed in

conjunction with accurate data on the projectile and detailed information on the anatomical structures that have been damaged (84).

#### 1.9.9 **Conclusion**

Accurate evaluation of bullet wound trauma is important for not only the medical and pathological assessment of injuries, but also for military and law enforcement purposes. However, none of the existing models fully address the complexities of bullet-tissue interaction.

An anatomically based model which addresses physiological responses to wound trauma would seem to be the most logical option to pursue. The first step is to establish which organs within the thorax and abdomen are most commonly damaged in fatal shootings and are responsible for death. These 'critical' organs form the basis for the development of simulant materials to model them. In addition, the use of the existing internationally recognised Abbreviated Injury Score (AIS), together with a suitable scoring system to evaluate incapacitation injuries in the model, would seem appropriate. From the analyses conducted, it can be seen that there are many different scoring systems available and each has its own advantages and disadvantages. The MAXAIS is the simplest and was superior to NISS at predicting mortality in patients with penetrating trauma such as gunshot wounds. MAXAIS is already in use by military research organisations for this very reason (149). Therefore it is worthy of serious consideration for an anatomical model. In addition, NISS has been shown to consistently outperform ISS and is also in common use, so it should be considered as an alternative option.

## **2. MATERIALS AND METHODS**



## **2. Materials and Methods**

### **2.1 Human and Animal Ethics**

All data collection outlined in chapter 3 and the experimental work outlined in chapters 4 and 5, were undertaken in accordance with the guidelines determined by the National Health and Medical Research Council and approved by the Ethics Committee of the University of Adelaide (Approval number H-004-2009).

### **2.2 Data Collection and Experimental Procedures**

#### **2.2.1 An Analysis of the Characteristics of Thoracic and Abdominal Injuries and Ballistic Data in Gunshot Homicides in Israel**

Post mortem reports were obtained from all cases of gunshot homicide involving thoracic and/or abdominal trauma where full autopsies were performed at the National Centre of Forensic Medicine in Tel Aviv, Israel. The data collected spans a 7 year period, 2000-2001 and 2004-2008. Israel was chosen as the source for data as it represents a well-defined area where gunshot homicides involve only a limited range of bullet types, and where full autopsies are generally performed on victims. In addition, high quality ballistics assessments are also conducted.

De-identified information on the age, sex, height and weight of the victims was recorded, in addition to the number of bullet injuries, sites of the entrance and exit wounds, bullet path through tissues, and the type and nature of the tissue and organ trauma. The causes of death were predominately due to organ and tissue trauma within the thorax and abdomen, although some victims also suffered fatal head injuries from additional bullet wounds.

The corresponding forensic ballistics data was only available for the cases registered between 2004 and 2008. This was obtained from the Israel National Police Firearms Identification Laboratory and the Toolmarks and Materials Laboratory. Both of these Laboratories are part of the Division of Identification and Forensic Science, located in Jerusalem. This data included calibre, bullet type, bullet damage, type/s of firearm involved and approximate shooting distance.

Shooting distance estimation was performed in several different ways. Traditional chemical analysis methods were employed in those cases where distance estimation

was a critical element of the case. This was achieved using the Modified Griess Test (MGT) for the presence of nitrite compounds, Sodium Rhodizonate Test (SRT) for the presence of lead and Dithiooxamide (DTO), also known as Rubeanic Acid Test, for the presence of copper residues (35, 217). A combination of these three tests, together with a visual examination and infra-red (IR) imaging, was used on victims' garments. The MGT alone was used for adhesive lifters collected from bodies and crime scene objects that could not be transferred to the laboratory for analysis (217, 218). These tests and test firings using the actual firearm or the same type of firearm, combined with the same type of ammunition, provided an accurate minimum and maximum distance within which the shootings could have occurred.

The forensic pathologists conducting the post mortem examination of the deceased also provided an estimation of the shooting distance involved. Generally they would indicate if the distance was contact, close contact, less than 1m or greater than 1m, based on the appearance of the wound and the presence or absence of visible propellant tattooing on bare skin or light coloured clothing. This estimation has been used for the purposes of the present study in those cases where chemical analysis was not conducted.

In a smaller number of cases, a minimum and maximum range could be established if the shooting occurred within a known room size or area, and was combined with the opinion given by the pathologist.

Shots involving contact or close contact ranges were not included to exclude cases of possible suicide. As a result, all shots studied involve ranges in excess of 200mm with most exceeding 1m.

### **2.2.2 Tensile Strength Biomechanics of Thawed Cadavers and the Implications for Wound Ballistics Research**

An un-embalmed cadaver of an elderly female was obtained from the Ray Last Anatomy Laboratory of The University of Adelaide, South Australia. The body had been specifically donated for educational and research purposes to the university by the decedent. The cadaver had been frozen and thawed five times which maximized the effects of repeated freezing and thawing. Samples from tissues and organs were obtained that measured approximately 100mm in length and 25mm in width. The

thickness of each sample varied depending on the type of organ or tissue involved. Samples were taken from: heart; kidney, oesophagus, skeletal muscle, ascending aorta, trachea, spleen, liver, lung, pancreas, pericardium, skin (thorax) and skin (abdomen).

The universal test equipment Hounsfield H50KM (Hounsfield Test Equipment Ltd<sup>®</sup>, Surry, United Kingdom) was used, which operates in the same manner as the model H25KM according to standard methodology (112, 219), to apply uniaxial tension until tissue failure occurred, to determine the maximum tensile strength of each sample of tissue and organ. This hydraulically powered machine has two crossheads, one that is adjusted for specimen length and the other that applies tension to the test sample. Each tissue sample was placed in the stretching test machine longitudinally. One end was secured in the proximal jaws and the other in the distal jaws. The breaking forces (force per unit area) were read digitally and the raw data was recorded on software created for the Hounsfield testing machine using the load cell as Newton (N) value. The settings used produced a maximum load of 200 N, a crosshead speed of 1mm per minute and a maximum extension of between 20mm and 65mm depending on the sample involved. The N values obtained were converted to grams (g) and the cross sectional area (mm<sup>2</sup>) of each sample was established by multiplying the width of each tissue by its thickness. The following formula was applied to compare the ultimate tensile strength (UTS) results (g/mm<sup>2</sup>) to the corresponding reference data in (57).

$$\text{UTS} = \frac{\text{Tensile Breaking Load (g)}}{\text{Cross Sectional Area of Test Material (mm}^2\text{)}}$$

Given that only a relatively small number of tests were performed, statistical analyses were not undertaken.

### **2.2.3 Pig Organ Energy Loss Comparison Experiments Using BB Rifle Pellets**

To measure the energy loss sustained by projectiles in different media, data were obtained using the organs of freshly euthanized pigs, two different concentrations of ballistics ordnance gelatine and a synthetic test simulant. Steel BB rifle pellets were fired through these media and the velocity in metres per second (m/s) before and after perforation was recorded using two chronographs, which are electronic velocity

measuring devices. The energy loss measurements in joules per metre (J/m) were derived from the velocity figures by applying the following formula and dividing the result by the thickness of the test media:  $KE = \frac{1}{2} mv^2$

Pig organs and tissues were obtained from a local certified abattoir. The pigs had an average weight of 80kg. The organs were delivered direct to the laboratory within 2 hours of the animals' deaths. All organs were cut into thin transverse sections approximately 20 to 30mm in thickness to enable full BB perforation with the exception of the aorta, spleen and fat (due to the thinness of their parenchyma). The aorta and spleen were not sectioned as they are such thin organs in a pig and BB pellet perforation was not difficult. Fat sections were also thin enough to allow BB pellet perforation without sectioning.

All organs and tissues were tested at room temperature, which ranged between 16°C and 18°C, as well as at 37°C (human body temperature). To heat the organs and tissues to 37°C, they were placed into sealed plastic bags and immersed into a temperature controlled stainless steel water jacketed bath at a temperature not exceeding 37°C. The temperature was checked using a laboratory grade thermometer. The organs and tissues remained in the bath for a minimum of 1 hour to ensure that the entire organ was heated through before velocity testing was conducted. A small number of organs were also tested at 4°C for comparison purposes against the other temperatures. To achieve this, the organs were placed in a commercial grade climate controlled refrigerator at a temperature of 4°C overnight.

To establish if sample decomposition might affect results, hindquarter muscle at 37°C was tested on two occasions 60 hours apart, having been left at room temperature (16 to 18°C) between the tests.

The pig organs and tissues chosen for the experiments were selected based on the results from the homicide study in Chapter 3, which found that the most common organs and tissues to suffer bullet wound trauma within the thorax and abdomen were (in descending order of occurrence); heart, lungs, liver, aorta, spleen and kidney. Fat was also tested because of its subcutaneous position. In addition, hindquarter muscle was tested, as it forms the basis for the assertion by Fackler and Malinowski (29) that 10% gelatine at 4°C is a suitable soft tissue simulant.

The study from Chapter 3 also showed that ribs were commonly struck by bullets entering the thorax. However, tests involving ribs were not undertaken because of the difficulty involved in accurately shooting through rib, the danger of ricochet and the potential for damage to the chronographs and other test equipment used in this experimental design.

Both FBI formulation 10% ballistics ordnance gelatine at 4°C and the NATO formulation 20% ordnance gelatine at 10°C, were tested and compared to the pig organs. Gelita® Type 'A' gelatine powder with a Bloom number of 250 was used. Propionic acid (mould inhibitor) was added at the accepted ratio of 5ml per 1000g of finished product. The powders were hand mixed with water and the gelatine mixture was hydrated at room temperature for approximately 4-6 hours before being melted in a temperature controlled, stainless steel water jacketed bath at a temperature not exceeding 40°C. The melting process took approximately 10-12 hours. The gelatine solution was then poured into square plastic containers measuring 150mm x 150mm, which had a depth of both 20mm and 30mm. This provided two thicknesses of gelatine to test, which was comparable to the average thicknesses of the various pig organ and tissue samples. The containers were sealed with plastic wrap to prevent dehydration. The containers were placed into a commercial grade climate controlled refrigerator at the required temperatures of 4°C and 10°C to allow the gelatine to cure for a minimum of 72 hours.

A number of the FBI formulation blocks were positioned side by side and calibrated in accordance with the accepted procedure outlined by Fackler and Malinowski (29). This involved using a Daisy® model Powerline 901 BB rifle in calibre 4.5mm, to fire nickel coated circular steel Daisy® BB pellets through the gelatine blocks at a velocity of  $180\text{m/s} \pm 4.5\text{m/s}$  to achieve a penetration depth of  $85\text{mm} \pm 10\text{mm}$ . As there is no separate calibration standard for the NATO formulation, the same calibration methodology for the FBI was applied. The results were comparable with those outlined in chapter 6, which showed an average penetration depth of  $40.4\text{mm} \pm 2.3\text{mm}$  after 100 hours curing time for the NATO formulation.

The solidified gelatine blocks were subsequently removed from the refrigerator and fired upon within two to three minutes. The velocity loss results were measured using two chronographs.

A homogeneous test simulant was also used for comparison against both of the ordnance gelatine formulations and the pig organs/tissues. This simulant was provided by a private company (Adelaide T&E Systems) and is known as Simulant 'A'. The manufacturing formulation is subject to patent but can be broadly described as a temperature-stable proprietary synthetic tissue simulant. It was provided in circular blocks with a diameter of 190mm and a depth of both 20mm and 30mm. Simulant 'A' was fired upon at room temperature only.

The same Daisy® air rifle and 4.5mm BB rifle pellets that were used for the calibration procedure were also used for all experimental tests. BB pellets were fired through the ordnance gelatine formulations, Simulant 'A' and each organ and tissue at the specified temperatures. The muzzle of the rifle was positioned 1m in front of the entry chronograph and a nominal muzzle velocity of 180m/s was achieved for each shot by pumping the air rifle 6 times.

A sample of 30 pellets was weighed. The mean BB pellet weight was 0.349g (range 0.336g-0.355g; SD 0.006g). The mean value was used for all energy calculations, as it was impractical to weigh the individual BB pellet before conducting each test firing due to the number and timing of test firings. In addition, it was considered that minor differences in projectile weights would randomise given the large number of pellets used (N>1200).

Two Competitive Edge Dynamics® model CED Millennium II chronographs with infra-red capability for indoor use, were used to record the velocity of each BB pellet according to standard methodology (220), before and after perforating the test material. The difference (velocity loss in m/s) was calculated by subtracting the exit velocity from the entry velocity.

Each chronograph was calibrated by comparing the measured velocity against a calibrated Infinition® ballistic Doppler radar unit, which included a model BR3502 radar head and model JB-6E computer program suite. The radar unit is located at the Defence Science and Technology Organisation (DSTO) at Edinburgh South Australia, where the comparison tests were conducted. The following results were achieved: - the entry chronograph measured an average velocity of 176.7m/s for 20 shots, with an uncertainty variance range of between 0.1 and 1.6m/s. These variances were slightly

higher and slightly lower than the Doppler radar readings. The average uncertainty variance over the 20 shots was 0.5m/s, which represents an average uncertainty of 0.282%. The exit chronograph measured an average velocity of 172.5m/s for 20 shots, with an uncertainty variance of between 0.0 and 1.2m/s. All variances were slightly lower than the Doppler radar readings. The average uncertainty variance over the 20 shots was 0.5m/s, which represents an average uncertainty of 0.289%. As the velocity variances of both CED® chronographs were not the same, and the entry chronograph readings were both higher and lower than the Doppler radar readings, no standard calibration adjustment figure could be applied to all of the velocities measured for the media tested.

Consultation with two National Association of Testing Authorities (NATA) accredited private calibration companies revealed there is no 'Australian Standard' applicable to the calibration of chronographs and their uncertainty range. However, the accepted NATA accreditation method of conducting velocity testing equipment calibration requires the readings from the chronograph in question to be compared to another calibrated speed measuring device such as Doppler radar or a Fluke® meter [Personal communication with Abstec Calibrations Pty Ltd and Ballistic Edge Research Laboratory Pty Ltd, 2012]. Therefore, the calibration method adopted for the chronographs in this study is in accordance with NATA specifications. The uncertainty values recorded for both chronographs are very small and did not impact on the overall accuracy of the velocity data.

An apparatus was constructed in order to position and secure each test media prior to the testing procedure. It consisted of a wooden base and two PVC plastic plumbing sections fixed to the base. The PVC sections had circular holes measuring 145mm in diameter. The two sections could be pulled apart to allow a large segment of test material to be placed between them and secured. For smaller segments of test media such as tissue, two clear plastic rectangular plates with a rectangular hole in the centre measuring 85mm x 55mm were placed between the PVC plastic plumbing sections, between which the tissue was secured. The apparatus containing the test media was placed midway between the two chronographs at a distance of 500mm from each (Figures 3 and 4).

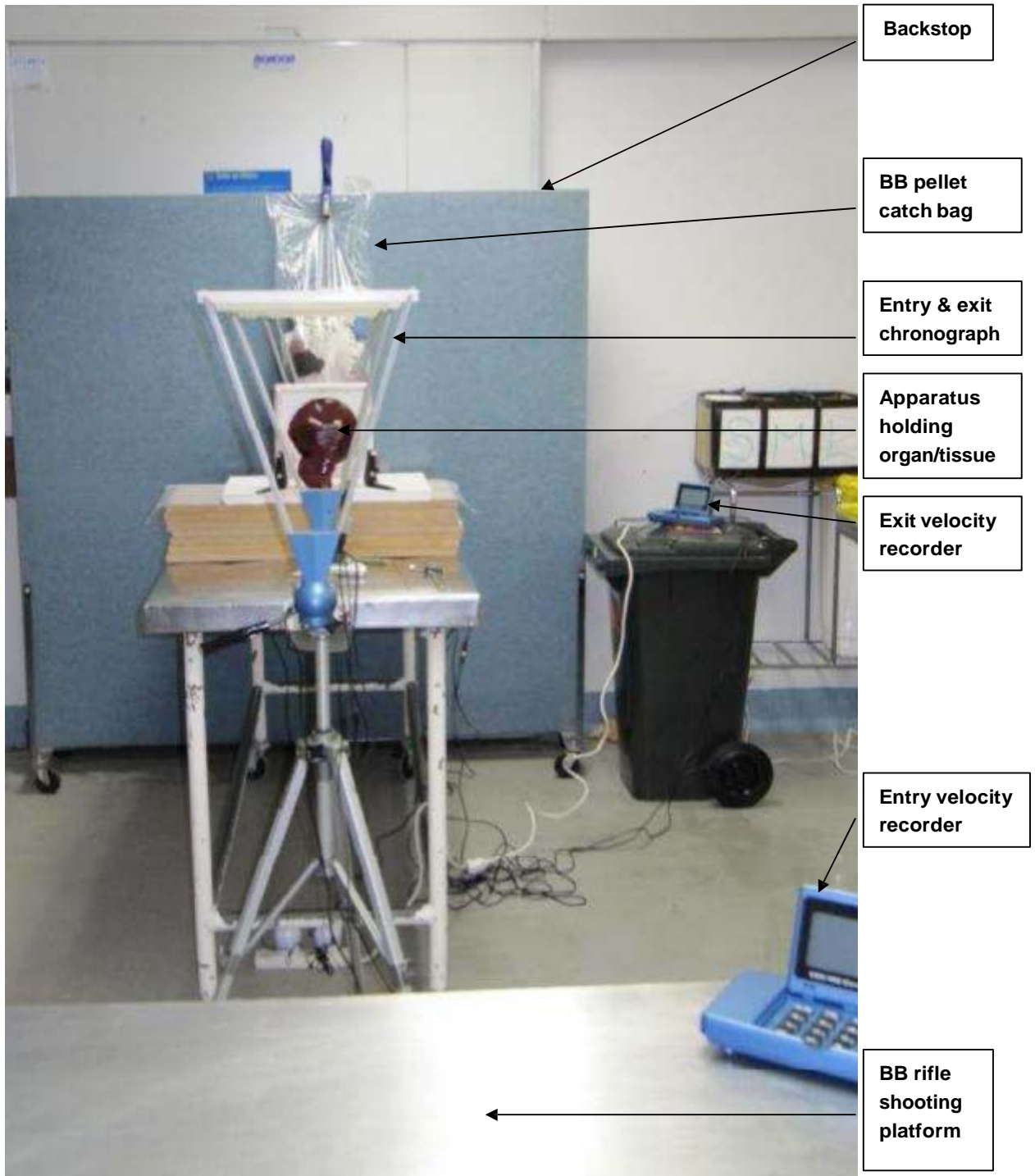


Figure 3. Overall view of pig organ and simulant velocity testing equipment and set up.





**Figure 4. Closer view of velocity testing equipment (chronographs) and tissue/organ/simulant apparatus.**

After each shot was fired, the recorded velocity before and after perforation was obtained from the chronographs. The thickness of the tissue or simulant was measured by inserting a stainless steel probe through the wound channel and marking the depth on the probe. The depth/thickness (mm) of the tissue or simulant was then measured using a Mitutoyo® digital vernier gauge.

#### 2.2.4 Statistical Analysis

Statistical analyses of the energy results were conducted using Graphpad Prism 5.02 for Windows, (Graphpad Software, San Diego California USA). Values are expressed as mean and standard error of the mean. Test results of all organs/tissues and simulants were compared using one way ANOVA with statistical significance set at  $p < 0.05$  and inter-individual comparisons made using Bonneferoni's *post hoc* test.

### 2.2.5 **Ballistics Ordnance Gelatine – How Different Concentrations, Temperatures and Curing Times Affect Calibration Results**

A series of tests with both 10% w/w and 20% w/w concentrations of differing Bloom strength ordnance gelatine were undertaken. The gelatine was prepared in accordance with standard methods (27, 91, 102, 108). As there is no calibration method mentioned in the NATO Standard for 20% ordnance gelatine (98), the same calibration method recommended by Fackler and Malinowski (29) for the 10% gelatine formulation and accepted by the FBI, has been applied to the 20% ordnance gelatine for direct comparison purposes.

Gelita® Type 'A' gelatine powder with a Bloom number of 250 and Croda® Type 'A' gelatine powder with a Bloom number of 285 were used. Propionic acid (mould inhibitor) was added at the usual ratio of 5ml per 1000g of finished product. The powders were hand mixed with three different types of water namely tap water, reverse osmosis (RO) water and de-ionized water. RO water has been filtered to remove a high percentage of minerals, nitrates and phosphates, but not silicates. De-ionized water has had non-ionic gases removed from it and is purer than distilled water. The gelatine mixtures were hydrated at room temperature for approximately 4-6 hours before being melted in a temperature controlled, stainless steel water jacketed bath at a temperature not exceeding 40°C. This melting process took approximately 10-12 hours. The gelatine solution was then poured into plastic containers measuring 210mm in diameter, 150mm in depth, and sealed to prevent dehydration. The containers were placed into a commercial grade climate controlled refrigerator at temperatures of between 3-4°C and the gelatine allowed to cure for varying periods of 21 hours, 100 hours and 3 weeks. These time points were arbitrarily chosen to represent a short, average and extended curing period. The solidified gelatine blocks were subsequently removed from the refrigerator and their temperatures checked with a laboratory grade thermometer. A number of blocks were also conditioned for 72 hours in 10° and 20°C climate-controlled environments until the entire block reached the required temperature. Each block was shot on four occasions from a range of 3m using Crosman® 'Copperhead' steel calibre 4.5mm BB pellets fired from a Daisy® air rifle. The mean penetration distance was established from the combined values of the four shots for each set of tests. An Ohler® model 35P chronograph was used to measure the mean velocity of the pellets from this

air rifle. Six pumps of the air rifle were found to achieve the required velocity of  $180\text{m/s}\pm 4.5\text{m/s}$  (29).

### 2.2.6 Statistical Analysis

Statistical analyses of the energy results were conducted using Graphpad Prism 5.02 for Windows, (Graphpad Software, San Diego California USA). Values were expressed as mean and standard error of the mean. Test results of all ordnance gelatine formulations were compared using one way ANOVA with statistical significance set at  $p < 0.05$  and inter-individual comparisons using Bonneferoni's *post hoc* test.

### 2.2.7 Anatomical Model Pilot Study

Gelita® pork skin based Type 'A' 250 Bloom gelatine was used to manufacture 10% ordnance gelatine at 4°C in accordance with the method and recommendations made by Fackler (102). Each gelatine block measured 305mm x 380mm x 200mm. This size was chosen because of the availability of moulds with these dimensions, which approximate the average Australian male thorax based on available anthropometric data (M. Henneberg personal communication 2007). Gelatine plates with an average thickness of 20mm were used to simulate subcutaneous tissue and fat, as well as to provide a platform for the attachment of skin simulant and to embed bone composite within. All the gelatine blocks and plates were refrigerated for a period of no less than 100 hours at an average temperature of 3°C, in a commercial grade refrigerator. The blocks were transported by refrigerated van to the Defence Science & Technology Organisation (DSTO) ballistic range facility and placed into an onsite refrigerator. One block was removed at a time from the refrigerator and its temperature checked using a thermocouple to ensure that it was at 4°C. The block was then calibrated with a Daisy® air rifle and 4.5mm BB pellets in the manner recommended by Fackler (102). The time delay between removal from the refrigerator and test firing averaged 5 minutes.

An ADF AUSTEYR model F88 ICW (individual combat weapon) in calibre 5.56x45mm NATO was used for all tests. This rifle had a barrel length of 508mm, with a 1 in 7 inch twist rate. The rifle was used with ASF1 ball ammunition manufactured by Australian Defence Industries Ltd (ADI) in 2005. This ammunition is still currently on issue to ADF personnel, and consists of a brass bottleneck style cartridge case with a boxer priming system. The boxer primer is the ignition source for the propellant contained within the

cartridge case. It uses a single flash hole with a separate anvil to detonate the explosive primer compound, which in turn ignites the propellant in the cartridge case (4). This ammunition has a 62gr full metal jacketed bullet, with a lead internal core and steel penetrator inside the forebody (ogive and meplat) of the bullet (Figure 1). The penetrator is designed to assist the bullet to penetrate heavier intervening material such as glass, brick or sheet metal. The ASF1 ball cartridge is based on the FN SS109 pattern in use by NATO forces and conforms essentially to the requirements laid down in STANAG 4172.

The simulant materials were secured to a wooden cradle manufactured for this purpose and gelatine blocks were placed at the rear of the cradle to study the dynamics of the fired bullets and capture them if possible. Figure 5 shows an overall side view of the test rig set up.

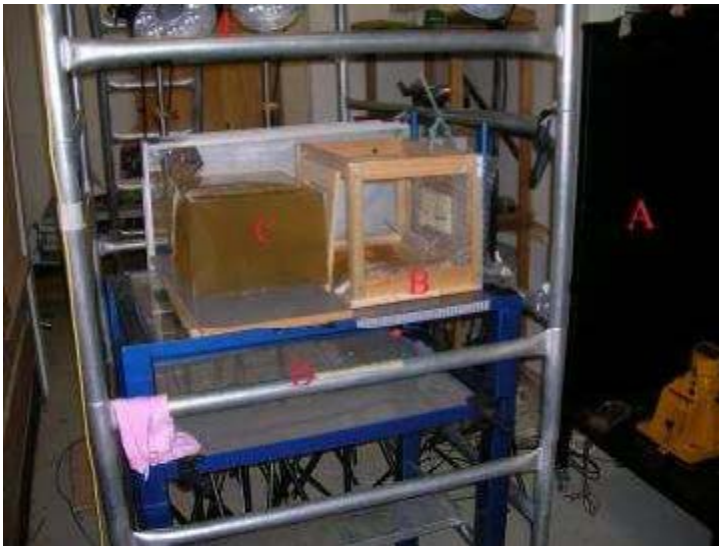


**Figure 5. Side view of the test rig set up within the DSTO ballistic range. The major components of the test rig are marked as follows:**

- A - enclosure which houses an electronic chronograph.**
- B - wooden cradle.**
- C – gelatine witness block.**
- D - scaffold and bench to which the test rig was secured.**
- E – lights for high speed photography.**

The skin simulant and bone composite were designed and patented by Krstic (221-223) during the development of a lower leg physical model for enhanced survivability against landmines. Krstic et al. (224, 225) and Footner et al. (123) detail the development project and calibration methods adopted. The surrogate leg has become part of NATO standard test methodology for landmine countermeasure studies (226).

The skin simulant was manufactured from deer skin chamois and had a thickness range of 1.4 to 1.8mm. It is distributed by the 'Kinch Trading Company' in Hove, South Australia. Figure 6 shows a sample of this product used during the simulant trials.



**Figure 6. A sample of the skin simulant used during the anatomical model pilot study.**

Bone composite material was used to simulate human rib. It was manufactured from a mixture of epoxy resin and hardener, tricalcium phosphate and tungsten powder. The bone composite was formed into a square plate approximately 15mm in thickness and embedded within the gelatine plates. Serrations measuring approximately 2mm in size were made in the composite to provide a gap in order to simulate the flexibility which occurs between individual 'ribs'. The gaps were purposely kept small to ensure that a bullet would strike the composite material. Figure 7 shows bone composite embedded within a gelatine plate.



**Figure 7. A sample of the bone composite embedded within a thin gelatine plate.**

Two methods were used to simulate lung tissue. The first involved providing an air gap of 250mm between the bone composite and the witness (i.e. recording) gelatine block. This 250mm gap is an approximation used to represent the average space occupied by the lungs during inhalation, between the anterior and posterior segments of the thoracic rib cage, arrived at by measuring the distance between the sternum and upper thoracic spine in two standard adults. These data were similar to unpublished data for the same region in relation to the average Australian woman, and an averaged figure was obtained (M. Henneberg personal communication 2007).

The second method of simulating lung tissue involved the use of a single layer of thin plastic bubble wrap attached to the front and rear of the wooden cradle, with the same 250mm air gap between. Bubble wrap was chosen because it contains multiple bubbles of air trapped inside a thin plastic membrane, not unlike the alveoli within lung tissue. No tests have been conducted at this stage to determine the ultimate tensile strength of this material compared to lung tissue. Figure 8 shows the test rig.

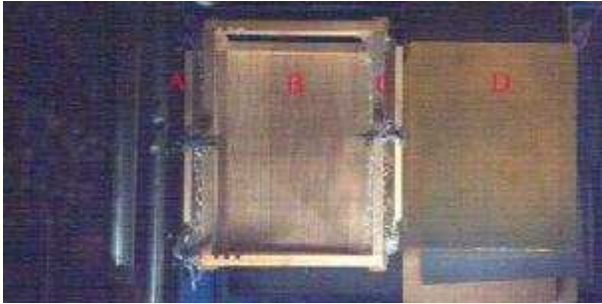


**Figure 8. An overhead view of the simulant test rig. The major components are marked as follows:**

**A – front gelatine plate to which the skin simulant is attached and bone composite embedded. At the rear of the plate is a thin layer of bubble wrap to simulate lung tissue.**

**B – 250mm air gap within wooden cradle to simulate the air gap within inflated lungs.**

**C – rear gelatine plate within which bone composite is embedded and skin simulant attached to the posterior surface. In front of this gelatine plate is another layer of bubble wrap to simulate lung tissue.**

**D – gelatine witness block.**

The F88 ICW was fixed in a remote firing device and all test firings occurred at a distance of 50m. This allowed the bullet to achieve a level of stability in flight (75, 84). In front of the rifle was a set of velocity screens, which were used to measure the bullet velocity at a distance of 3m from the muzzle of the barrel.

One round was fired into each of six simulant models. The bare gelatine block (FBI formulation) was used as a control, because it is commonly used for wound ballistics research. The control test was repeated twice (Test 1 and 1A) to ensure consistency, and those tests provided a baseline for the comparison of the results achieved with the progressive addition of simulant materials to the other gelatine blocks. Test 3 was a repeat of Test 2 for consistency purposes.

The limited availability of the skin and bone simulants, as well as the necessary DSTO resources, did not allow for a repeat of Tests 4 to 7. However, the methodology adopted was designed to achieve consistent results. The control tests (Test 1 and 1A) and the repeated tests (Test 2 and 3) demonstrated this. Therefore there is no reason why confidence in the remaining test results should not be expressed.

The results of all tests were recorded using two high speed Photron Fastcam® digital cameras and software. One camera was mounted to the side and the other above the test apparatus.

Measurements of the maximum permanent cavity dimensions of each gelatine block were obtained using a vernier gauge, after the block had been sliced to reveal the entirety of it. The volume of the permanent cavity (idealized as a cylinder for mathematical purposes) was determined using the following formula:  $\pi r^2 h$

Measurements of the temporary cavity were taken from high-speed video images. The quality of the images produced by the second camera mounted above the test apparatus were poor on occasions, making it difficult to accurately measure the width of the temporary cavity for some tests. This unfortunately did not become apparent until after the tests had been completed and the images were critically analysed. The lack of this measurement for tests 1, 2, 3 and 5 therefore meant that a temporary cavity volume for those tests could not be determined. However, the temporary cavity volume for tests 1A, 4, 6 and 7 (idealized as a sphere for mathematical purposes) were able to be determined using the formula  $\frac{4}{3}\pi r^3$ . This did provide a meaningful comparison between the second control test 1A and the later tests where progressively more simulant materials were added.

The video footage indicated that temporary cavitation occurred further into the block than was later measured. This is purely because the temporary cavity expands dynamically in all directions including back along the shot line. It was decided to measure the commencement of temporary cavitation from the resting position to achieve uniformity.



**3. AN ANALYSIS OF THE CHARACTERISTICS OF THORACIC  
AND ABDOMINAL INJURIES AND BALLISTIC DATA IN  
GUNSHOT HOMICIDES IN ISRAEL**

### **3. An Analysis of the Characteristics of Thoracic and Abdominal Injuries and Ballistic Data in Gunshot Homicides in Israel.**

#### **3.1 Introduction**

Homicidal gunshot wounds and their features are often different to organ and tissue trauma associated with gunshot accidents or suicides. To examine the characteristics of thoracic and abdominal trauma associated with gunshot homicides, a detailed study was undertaken within Israel where approximately 50% of all homicides are firearm related.

The demographics of Israeli society have a direct effect on the work performed by forensic pathologists from the National Center of Forensic Medicine and the subsequent collection of post mortem data. Israel has a diverse ethnic and religious population of approximately 7.8 million people. Approximately 75% of these are Jewish and 20% are Arabs. The remainder are predominately non-Arab Christians, non-Arab Muslims and other residents with no specific religious classification (227). This diversity means that post mortem examinations cannot be conducted on all gunshot homicide victims because of religious beliefs [J. Hiss personal communication 2010]. However, they are still carried out on a large number, approximately 80% of victims. The results can therefore be used to provide clear patterns of the type and nature of the wounds sustained, the most common organs damaged, and the types of firearms involved. This information is essential for the development of anatomical surrogates for assessing wound trauma, as it assists in prioritising which of the major organs will need to be modelled. It also provides additional data to compare the damage sustained from test firings into a simulant model against bullet wound trauma in real organs and tissues.

#### **3.2 Data Collection Study**

The data was collected from post mortem examination reports for a 7 year period over 2000-2001 and 2004-2008. The corresponding forensic ballistics reports were only available for the period between 2004 and 2008. A further description of the 'Materials and Methods' involved is contained in Chapter 2, pages 81 to 82.

#### **3.3 Results**

197 cases of gunshot homicide where death was due to thoracic and/or abdominal trauma were identified. In 61 of those cases taken from 2000 and 2001, no forensic

ballistics data was available. The remaining 136 cases from 2004 to 2008 have forensic ballistics data. The male to female ratio was 179:18. The males were aged from 9 to 75 years (average 32.8 years). Females were aged from 19 to 89 years (average 36.6 years). The average height of males was 176cm, and females 163cm. The average weight of males was 84kg, and females 71kg. This gave an average body mass index (BMI) for males of 27.1 and for females 26.7.

The total number of rounds striking the entire body of males and females was 999, the average number for males was 5.2, and for females 3.7. The total number of rounds striking the thorax and/or abdomen of both males and females was 440, the average for males was 2.3, and for females 2.2.

Entry wounds were significantly higher on the left side of the thorax, abdomen and back (N=253) compared to the right side (N=172). The remainder of the entry wounds were in the mid thorax, mid abdomen and mid back areas (N=15). A more detailed analysis is shown in Figure 9.

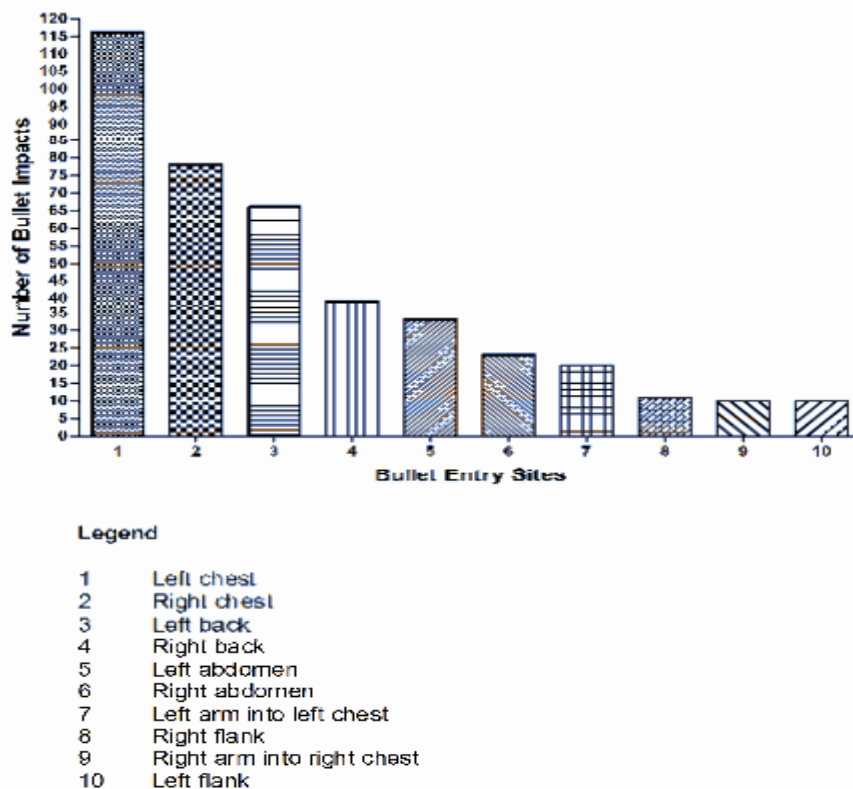


Figure 9. Number of bullet entry impacts into regions of the thorax and abdomen.

No exit wounds were recorded in 52 cases, with a total of 253 exit wounds present in the remaining 145 cases. Two of the cases involved multiple exit wounds as the bullets had fragmented. The calibre of these two rounds could not be confirmed but was suspected to be high velocity and most likely calibre 5.56x45mm or 7.62x39mm Soviet. Given that these wounds represented single bullet strikes, the multiple exit wounds have only been recorded as single exits for statistical purposes in the total number above. The main exit points were the left side of the back (N=56), the right side of the back (N=53), the left side of the chest (N=32), the right side of the chest (N=33), the right side of the abdomen (N=10), the left side of the abdomen (N=8), the left flank (N=6), the right flank (N=6), the mid back (N=5), the right axilla (N=3), the left axilla (N=2) and the mid abdomen (N=1).

Bullets were not recovered in 61 cases. Of the 136 cases where forensic ballistics data were available, 205 individual bullets were recovered and 120 of these were able to be identified. They consisted of calibres 9mm Luger (N=78), 9mm Short, also known as 380 Auto (N=11), either 9mm Luger or 9mm Short (N=3), either 9mm Luger or 5.56x45mm (N=5), 5.56x45mm (N=10), 7.62x39mm Soviet (N=8), 38 Special or 357 Magnum (N=1), 45 ACP (N=1) and 22 Rimfire (N=3). The bullet types involved in the predominant calibre 9mm Luger were full metal jacketed (FMJ) with an exposed lead base (N=52), fully encapsulated FMJ (N=4), jacketed hollow point (JHP) (N=8) and a number of 9mm Luger bullets where the exact type was undetermined (N=14). The bullet types involved in calibre 9mm Short were all FMJ with exposed lead base (N=11). The bullet types involved in calibres 5.56x45mm and 7.62x39mm Soviet were military style commercially manufactured FMJ.

Bullet trajectory through the body, or more correctly termed 'bullet path', was recorded for 423 of the 440 rounds that entered the thorax or abdomen. These bullet paths can broadly be grouped into the following categories, front to back (N=280), back to front (N=117) and to the side (N=26). In most instances a rib or vertebrae was struck during the passage of the bullet and so some deviation of the bullet from its original path occurred. A more detailed breakdown of the main bullet paths is contained in Table 4.

<b>BULLET TRAJECTORY PATH</b>	<b>NUMBER</b>
<b><i>FRONT TO BACK</i></b>	
Front to back, left to right & upwards	40
Front to back, left to right & downwards	74
Front to back, left to right & horizontal	43
Front to back & horizontal	8
Front to back, right to left & upwards	39
Front to back, right to left & downwards	47
Front to back, right to left & horizontal	20
Front to back & upwards	4
Front to back & downwards	5
<b>Sub Total</b>	<b>280</b>
<b><i>BACK TO FRONT</i></b>	
Back to front, left to right & upwards	27
Back to front, left to right & downwards	18
Back to front, left to right & horizontal	2
Back to front & horizontal	6
Back to front, right to left & upwards	27
Back to front, right to left & downwards	16
Back to front, right to left & horizontal	5
Back to front & upwards	7
Back to front & downwards	9
<b>Sub Total</b>	<b>117</b>
<b><i>SIDE</i></b>	
Sideways left to right	20
Sideways right to left & horizontal	6
<b>Sub Total</b>	<b>26</b>
<b>Overall Total</b>	<b>423</b>

**Table 4. Bullet path through homicide victims.**

Shooting distance estimation was undertaken in 151 of the 197 cases. The relevant distance was unknown in the other 46 cases. The estimated distances can be broadly grouped into the following categories, less than 1m (N=16), less than 2m (N=11), approximately 1m (N=7), greater than 1m (N=114) and distant, where the estimated range was not specified (N=3). A more detailed breakdown of the distances involved is contained in Table 5.

<b>ESTIMATED DISTANCE</b>	<b>NUMBER OF CASES</b>
20cm to 75cm	5
25cm to 2m	3
< 1m	11
Approximately 1m	7
> 1m	104
1m to 8m	3
< 2m	8
2m to 3m	1
5m to 6m	1
Several metres (estimated range not specified)	2
10m to 15m	2
20m to 40m	1
Distant (Estimated range not specified)	3
Unknown	46
<b>Total</b>	<b>197</b>

**Table 5. Categories demonstrating the approximate distance of shootings.**

Specific organ and bone damage was recorded in all of the 197 cases. The 440 rounds that entered the thorax or abdomen resulted in a total of 1660 injuries to organs and bones as most cases involved multiple internal injuries. The organs/tissues injured can be broadly categorised as follows: ribs (N=328), heart (N=210), left lung (N=184), right lung (N=162), liver (N=133), diaphragm (N=118), small intestine (N=77), aorta (N=65), vertebrae (N=52), stomach (N=45), spleen (N=42), large intestine (N=40), left kidney (N=33), pelvis (N=24), right kidney (N=20), sternum (N=22), vena cava (N=18), mesentery (N=18), major arteries or veins (N=17), spinal cord (N=11), left scapula (N=10), oesophagus (N=8), right clavicle (N=8), pancreas (N=6), trachea (N=3), left clavicle (N=3), right scapula (N=2) and bladder (N=1). The most common organs involved in lethal injury are shown in Figure 10.

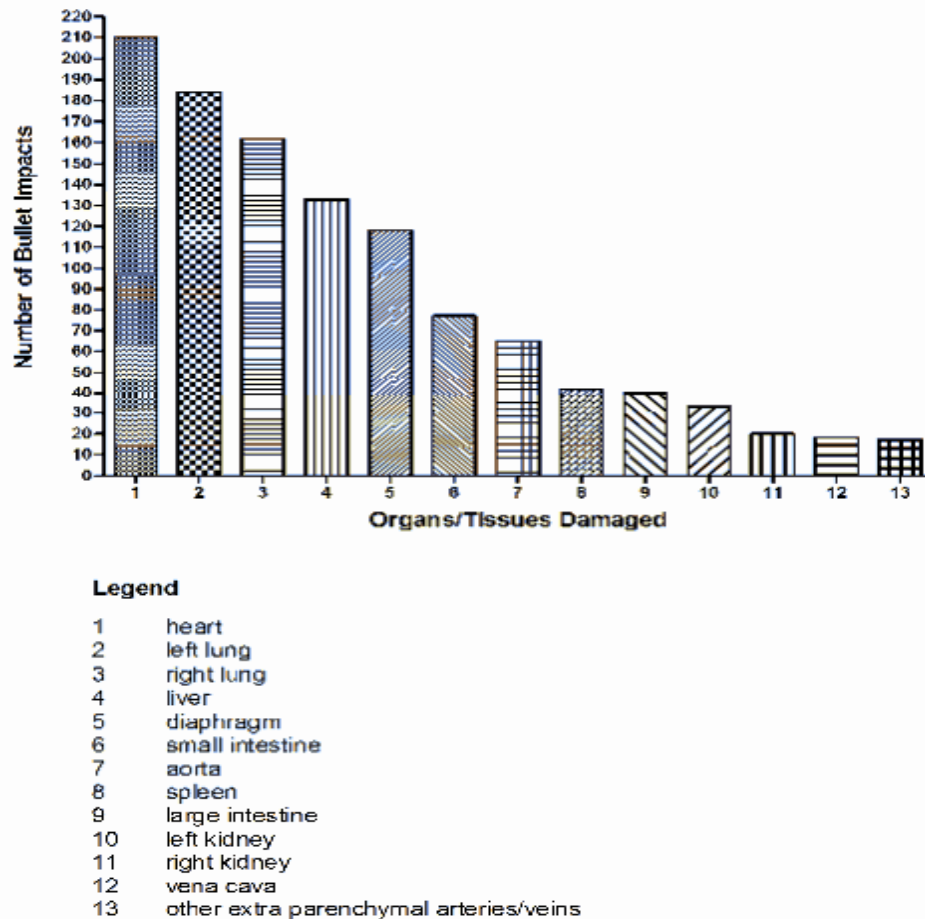


**Figure 10. Number of bullet impacts into major organs/tissues within the thorax and abdomen.**

Of the 440 rounds entering the thorax and abdomen, the ribs were injured on 328 occasions. Every rib on both the left and right side was injured at least once with the most common injuries involving the right 4th rib (N=23), left 3rd rib (N=21), left 6th rib (N=21), left 4th rib (N=20), left 5th rib (N=20), left 2nd rib (N=18) and the right 3rd rib (N=15). Therefore the most concentrated damage occurred between the 2nd and 6th ribs on the left hand side. This area extends from the level of the junction of the 2nd rib and sternum, to the level of the 6th rib in the mid clavicular line. This area covers major organs and vessels such as the left lung, heart, aorta and superior vena cava. A more detailed description of the number of occasions that each rib and the sternum were injured can be found in Table 6.

<b>STERNUM AND RIB INJURY</b>	<b>NUMBER OF BULLET STRIKES</b>
Sternum	22
1 <sup>st</sup> rib (N/S)	1
1 <sup>st</sup> rib left	6
1 <sup>st</sup> rib right	5
2 <sup>nd</sup> rib (N/S)	2
2 <sup>nd</sup> rib left	18
2 <sup>nd</sup> rib right	11
3 <sup>rd</sup> rib (N/S)	2
3 <sup>rd</sup> rib left	21
3 <sup>rd</sup> rib right	15
3 <sup>rd</sup> rib posterior	2
4 <sup>th</sup> rib (N/S)	3
4 <sup>th</sup> rib left	20
4 <sup>th</sup> rib right	23
5 <sup>th</sup> rib (N/S)	7
5 <sup>th</sup> rib left	20
5 <sup>th</sup> rib right	11
5 <sup>th</sup> rib posterior	3
6 <sup>th</sup> rib (N/S)	11
6 <sup>th</sup> rib left	21
6 <sup>th</sup> rib right	7
7 <sup>th</sup> rib (N/S)	12
7 <sup>th</sup> rib left	12
7 <sup>th</sup> rib right	12
7 <sup>th</sup> rib posterior	1
8 <sup>th</sup> rib (N/S)	5
8 <sup>th</sup> rib left	9
8 <sup>th</sup> rib right	12
8 <sup>th</sup> rib posterior	1
9 <sup>th</sup> rib (N/S)	2
9 <sup>th</sup> rib left	12
9 <sup>th</sup> rib right	11
10 <sup>th</sup> rib (N/S)	1
10 <sup>th</sup> rib left	7
10 <sup>th</sup> rib right	3
11 <sup>th</sup> rib (N/S)	2
11 <sup>th</sup> rib left	9
11 <sup>th</sup> rib right	1
12 <sup>th</sup> rib (N/S)	1
12 <sup>th</sup> rib left	3
12 <sup>th</sup> rib right	1
Fractured left rib (N/S)	1
Fractured right rib (N/S)	1
	<b>Total bullet strikes 350</b>

**Table 6. Number of bullet impacts to sternum and each rib.**

**Legend:** N/S = Left or right rib not specified



A specific cause of death (COD) was given by the attending pathologist in all but 5 of the 197 cases. In those 5 cases the COD was simply listed as gunshot injuries. In the remaining 192 cases the COD was primarily the result of combined injury to the lungs (N=128), heart (N=81), liver (N=55), aorta (N=33), major extra parenchymal arteries or veins (N=31), kidney (N=26), spleen (N=15), vena cava (N=6) and internal organ trauma where the specific injury was not documented (N=4). In addition the COD was listed as “blood loss or internal bleeding” in 37 cases.

The most common combinations of organ injury causing death were the heart and lungs (N=24), heart, lungs and liver (N=14), heart, lungs and brain (N=6), lungs and aorta (N=4), lungs and pulmonary artery (N=4), lungs and liver (N=4), lungs, heart, liver and brain (N=4), heart, lungs and kidney (N=3), heart, lungs, aorta and brain (N=3), heart and aorta (N=2), heart and liver (N=2), lungs, aorta and spleen (N=2), lungs, liver and kidney (N=2). In a further 75 cases, the COD was due to a combination of injuries to two to six different organs.

### 3.4 Discussion

As noted above, Israel was chosen for this study as approximately 50% of all homicides result from gunshot wounds and the firearm types involved are generally restricted to semi-automatic pistols in calibre 9mm Luger or 9mm Short (32 Auto), or assault rifles in calibres 5.56x45mmNATO and 7.62x39mmSoviet. In addition, the types of ammunition involved are primarily military or commercial FMJ bullets. These factors limit the variables which must be considered in other countries with high gunshot homicide rates such as South Africa and the United States, where there is a much wider range of commercial ammunition including bullet types such as ballistic tips, soft nose and JHP ammunition. These ‘specialty’ bullet types perform quite differently in tissues compared to FMJ bullets, as many are designed as anti-personnel rounds for law enforcement purposes.

The most common calibre identified in the study was 9mm Luger (N = 78). It is used in Israel in both semi-automatic pistols and sub-machine guns. The most common bullet weight in this calibre was 115gr (7.45g), and the most common bullet construction was FMJ with an exposed lead base. The majority of the FMJ bullets recovered at autopsy were found to have largely retained their original weight with some distortion of the

bullet jacket, and on occasion some extrusion of the lead core from the exposed bullet base.

As discussed in Chapter 1, FMJ 9mm Luger bullets tend to over penetrate and exit the body, retaining a significant percentage of their energy and momentum. This was again demonstrated in the present study where bullets were not recovered in 61 of the 197 cases. Although the calibre of the bullets in those 61 cases is unknown, they were quite likely to be 9mm Luger, as this was the predominant calibre involved in all shootings where forensic ballistics data was available.

Calibre 5.56x45mmNATO was used in at least 10 of the 136 shootings where forensic ballistic evidence was available. This calibre is common in Israel in M16 pattern assault rifles, and the Israel Defence Force (IDF) uses both the M855 and M193 rounds in its M16 A1, M4, Galil and Tavor assault rifles. The M193 was the original round developed for use in the M16 A1 rifle.

Military bullets such as the 5.56x45mmNATO have copper nickel gilding metal jackets and a lead-antimony alloy core. As discussed in Chapter 1, these bullets typically exit the muzzle of a rifle with up to 6 degrees of yaw at launch and only stabilise as the range increases. Therefore close range shots are generally more destructive than long range (75, 85). They also tend to fragment at high impact velocities and the penetrator may become separated (1, 75, 81). All of the 5.56x45mm rounds recovered at autopsy were military M193 construction and had fragmented to some degree, which is consistent with the close engagement ranges involved. Each of the victims sustained significant organ and tissue damage, which can be attributed to the high velocity, high energy and momentum of the bullets, together with their unstable nature and the fragmentation effects at these close ranges. Therefore the wound/s sustained by the homicide victims shot with this calibre were consistent with the published literature (75).

Calibre 7.62x39mmSoviet was involved in at least 8 of the 136 homicide cases where forensic ballistics data was available. AK47 pattern assault rifles were used throughout Israel and the Middle East region. The most common bullet weight involved in Israeli homicides was 7.97g (123gr), which comes from a wide variety of manufacturers. As discussed in Chapter 1, there are two common bullet configurations in this calibre and their wounding features vary quite dramatically. The first is the Russian and Chinese

military design, which consists of a FMJ boat tail bullet with a copper-plated steel jacket, steel core/penetrator and sheathed in lead with a small lead tip. The others are FMJ bullets that have copper bullet jackets and lead cores (2, 75, 86).

Both types of bullet configurations were recovered from homicide victims involving calibre 7.62x39mm. In each case multiple rounds were fired and multiple bullets struck the decedents. The bullets with copper plated steel jackets, steel cores/penetrator were generally recovered in good condition with little distortion. The organ and tissue injuries caused by such bullets were not particularly severe and were consistent with the published literature (75). The 7.62x39mm bullets with copper jackets and lead cores tended to fragment, separating the core from the jacket and leaving most of the fragmented material within the body. These caused more severe wounds, but the damage to the bullets was overall greater than that reported in the published literature (75).

In turning to the characteristics of the victims, this study found that males represented approximately 91% of gunshot homicide victims in Israel with an average age of 32.8 years. Females represent the remaining 9% with an average age of 36.8 years. Comment on possible motives and sociological data behind these homicides was beyond the scope of this study.

Multiple bullet wounds were common to most victims with an average of 5.2 bullets striking males and 3.7 bullets striking females. However, the number of bullets striking only the thorax and/or abdomen of males was 2.3 and females 2.2. A contributing factor to the frequency of multiple bullet wounds was the type of firearms involved in these homicides, namely semi-automatic pistols and assault rifles, both of which have high magazine capacities and the ability for rapid fire, depending on the dexterity of the shooter. As these weapons are also used in suicide attempts in Israel a similar finding occurs, with often more than one bullet wound (H. Gipps personal communication 2010).

Entry wounds were found significantly more often on the left side of the thorax, abdomen and back (N=253) compared to the right (N=172). This may indicate that the offenders were intending to strike the most vital organ in the body, namely the heart, based on commonly held anatomical knowledge. Military training was also considered,

as Israel has a period of compulsory military service for most of its citizens. However, many of the perpetrators were known not to have any formal military training. Gunshot homicides in this study were more likely to be representative of the types of injuries that might be expected in close range military confrontations because of the type of firearms and ammunition involved.

The most common organs and blood vessels damaged in descending order were the heart, left lung, right lung, liver, diaphragm, small intestine, aorta, spleen, large intestine, left kidney, right kidney, vena cava and other extra parenchymal arteries and veins. A comparison of the number of bullet injuries to each is outlined in Figure 9. However, injuries to the diaphragm, small intestine and large intestine would not necessarily be considered immediately life threatening and so these organs were not classified as 'critical organs' for the purpose of this study.

The most common areas within the major organs that were traumatized were: heart - both ventricles, both atria and the inter-ventricular septum, left lung - upper lobe followed by the lower lobe, right lung - upper lobe followed by the middle lobe, liver - left lobe, aorta – the ascending aorta was damaged on slightly more occasions (N=33) than the descending aorta (N=30), vena cava – the inferior vena cava was damaged on more occasions (N=15) than the superior vena cava (N=3). Injuries to the other 'critical' organs such as the spleen and kidney were recorded in less specific detail at autopsy.

It is significant that most of the bullets involved in this study had struck a rib or other bone and that every rib on both the left and right side had been struck at least once as detailed in Table 6. The most concentrated rib damage was between the 2nd and 6th ribs on the left hand side. Impacting a rib would have resulted in some bullet deviation through tissue.

The approximate bullet path through the body was determined by the pathologist at autopsy, based on the wound track/s seen through the organs and tissues. The most common bullet path was front to back, which represented just over 66% of the recorded bullet trajectories in the thorax and abdomen. Back to front bullet trajectories represented just over 27%. The victim and offender interaction at the time of the shooting is not within the scope of this study, but it is reasonable to assume that two thirds of the victims were facing their attacker at the time of the shooting.

The distance over which the shootings occurred was estimated in 151 of the 197 cases. It was found that chemical analysis methods were undertaken in a relatively high percentage of cases. A detailed breakdown of the distances is shown in Table 5. The majority (N=124) were estimated at 1m or greater.

Multiple organ injury was listed in 146 of the 192 cases where a specific COD was determined by the pathologist. This reflects the fact that in most cases multiple rounds were fired. In the remaining 46 cases, the COD was the result of injury to a single organ, or attributable to a single cause. For example, in 8 of these cases, the COD resulted from central nervous system or brain injury despite additional gunshot wounds to the thorax and/or abdomen. While central nervous system and spinal joint injuries were noted, they are not within the scope of this study.

### 3.5 Conclusion

Information collated from this study shows the type and range of injuries that may be sustained in gunshot homicides involving the torso. In addition the type of ammunition that was used was analysed. Although much of the data are specific to cases that were autopsied in Tel Aviv, Israel, generalisations can be made allowing extrapolation of the results to assist in comparing and developing simulants that may be used to further study and evaluate mechanisms and effects of ballistic injuries. Simulants for individual organs or tissues may be developed, or alternatively, more complex models may evolve where a range of different materials are used to more accurately simulate the human body. Before this will be possible, the most common trajectories and involved organs and tissues will need to be determined. This can be derived from the presented data. Specifically, an anatomical model of the thorax and abdomen must include a suitable simulant material for the ribs, heart, lungs, liver, aorta, spleen, kidneys and vena cava, in decreasing order of importance. The simulant materials must also have comparable biomechanical properties. To establish those, two primary sources will need to be investigated, thawed cadavers and fresh porcine organs.

**4. TENSILE STRENGTH BIOMECHANICS OF THAWED  
CADAVERS AND THE IMPLICATIONS FOR WOUND  
BALLISTICS RESEARCH**

## 4. Tensile Strength Biomechanics of Thawed Cadavers and the Implications for Wound Ballistics Research.

### 4.1 Introduction

Human cadavers have been a source of bio-mechanical data used in the study of soft tissue and organ injuries (57). In wound ballistics research, tensile strength is one of the most important bio-mechanical properties used to evaluate medium and high velocity bullet impacts (124, 128). In many countries fresh cadavers are not available for such studies, and so stored bodies (and body parts) may be used that have been frozen and thawed a number of times. A series of tensile strength experiments were conducted using an un-embalmed frozen and thawed elderly cadaver to compare the results with published data for elderly (aged 60 to 79 years) adult tissues (57). It was hypothesised that freezing and thawing human material may result in physical changes that render such tissues and organs less suitable for injury interpretation.

### 4.2 Experimental Design

Tissue samples were obtained from an elderly un-embalmed cadaver that had been frozen at  $-18.5^{\circ}\text{C}$  and thawed on five occasions (W. Fisk personal communication 2013). Tensile strength experiments were conducted and the results were compared with those published in Yamada (57). A full description of the 'Materials and Methods' is contained in Chapter 2, pages 82 to 83.

### 4.3 Results

The following tensile strength results were achieved: heart  $3.56\text{g/mm}^2$ , kidney  $10.27\text{g/mm}^2$ , oesophagus  $22.08\text{g/mm}^2$ , skeletal muscle  $29.46\text{g/mm}^2$ , ascending aorta  $59.98\text{g/mm}^2$ , trachea  $155.40\text{g/mm}^2$ , spleen  $4.65\text{g/mm}^2$ , liver  $10.83\text{g/mm}^2$ , pancreas  $15.18\text{g/mm}^2$ , lung  $29.94\text{g/mm}^2$ , pericardium  $136.84\text{g/mm}^2$ , skin (abdomen)  $355.26\text{g/mm}^2$  and skin (thorax)  $407.88\text{g/mm}^2$ .

These data were compared to published results obtained from non-frozen tissues from elderly persons (Yamada 1970), recognising that tensile strength values were only available for the following organs and tissues at the 95% degree of confidence: heart  $9.2\pm 0.95\text{g/mm}^2$ ; kidney  $4\pm 0.20\text{g/mm}^2$ , oesophagus  $51\pm 1.1\text{g/mm}^2$ , skeletal muscle  $9\pm 0.30\text{g/mm}^2$ , ascending aorta  $68\pm 2.4\text{g/mm}^2$ , trachea  $150\pm 6.5\text{g/mm}^2$ .

A comparison between the results achieved from this study and Yamada's results (57) are contained in Figure 11. Tensile strength values for the other organs and tissues with no published values are contained in Figure 12.

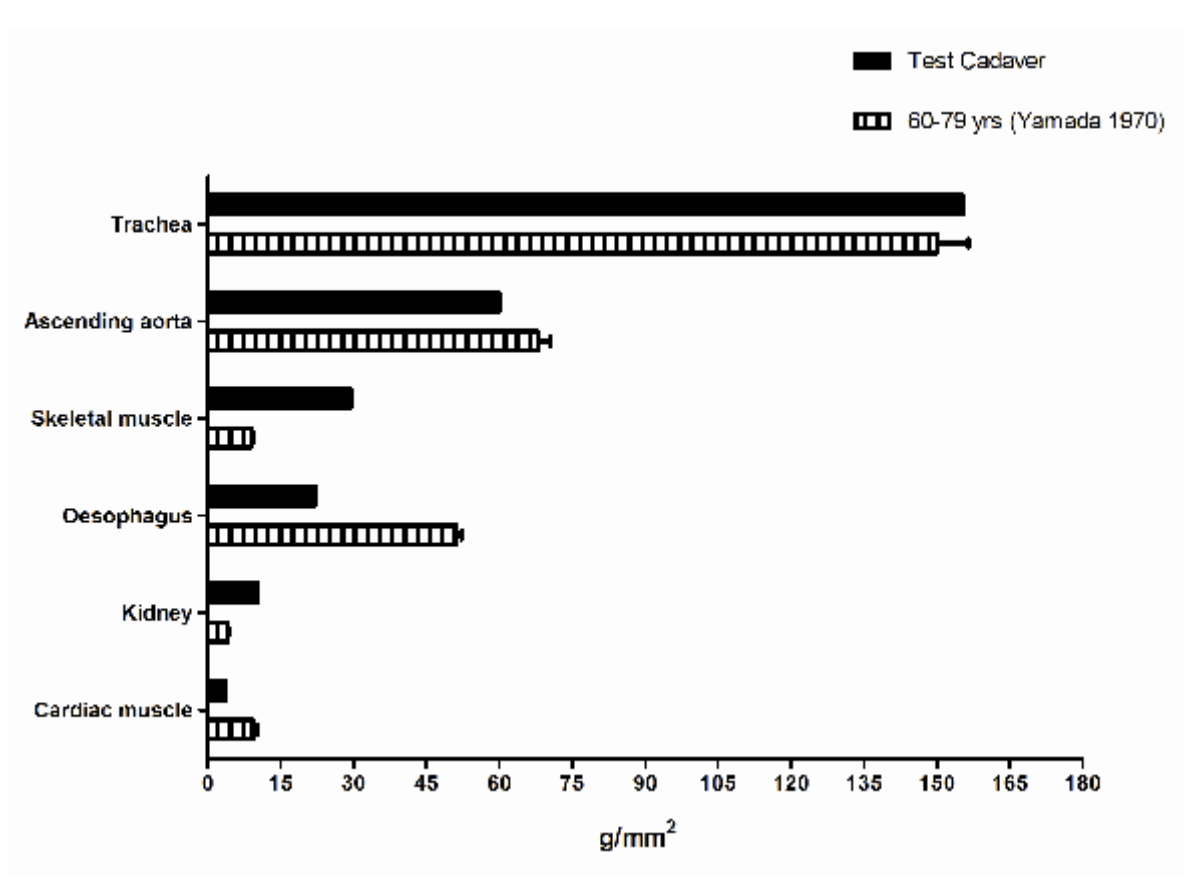


Figure 11. Comparison of tissue and organ tensile strength values (g/mm<sup>2</sup>) from the frozen and thawed elderly test cadaver, to published standards for non-frozen elderly cadavers (57).



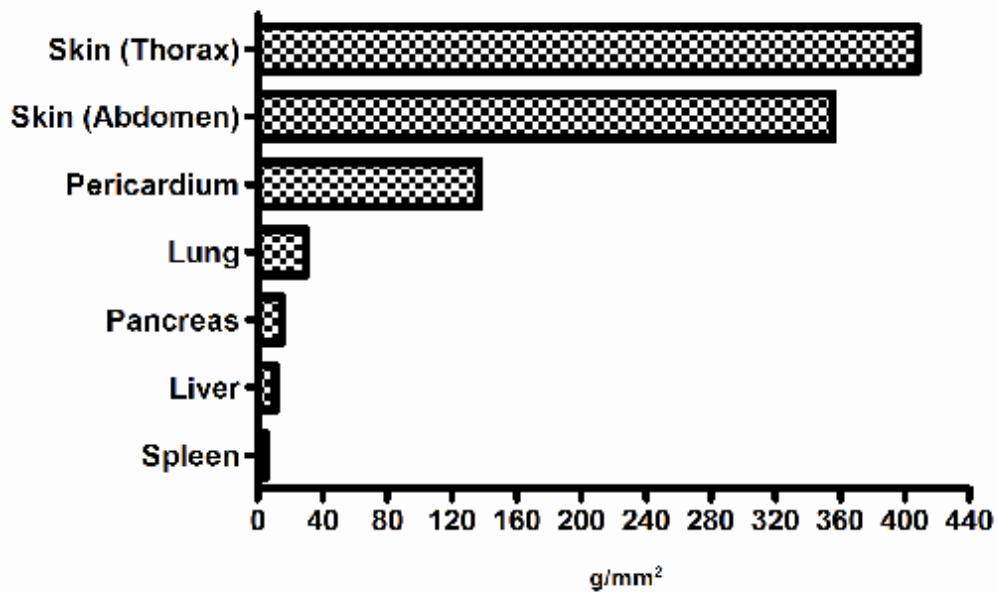


Figure 12. Tensile strength values (g/mm<sup>2</sup>) from other tissues and organs obtained from the frozen and thawed test cadaver that are not mentioned in (57).

#### 4.4 Discussion

It has been asserted that biological materials must be in a mechanically stabilised state for tensile strength tests to be conducted (57). This is achieved by placing whole organs from which samples will be taken in a saline solution and refrigerating them. This method saturates the tissue with water and removes rigor mortis from muscle tissues. The duration of refrigeration is dependent upon the type of tissue or organ. For muscle, two days is recommended, three days for fascia, heart, trachea, oesophagus, stomach, intestines and four days for blood vessels. Although fresh cadaveric tissues and organs are recommended for use, these may not always be available.

A variety of factors may alter the physical properties of tested tissues. For example, tensile strength may vary between the time of death and the testing procedure, as the effects of putrefactive and autolytic processes manifest. Testing in the early post-mortem period will minimise these effects. Another issue involves differences in the mechanical properties of certain tissues in different locations. For example, the percentage of elastin and collagen in the ascending aorta is quite different from that in the descending aorta (129).

Age also has an effect on physical properties of tissues, with elastic tissue degrading with increasing years (57, 129). Yamada (57) has shown that the biological strength values for tissues and organs are generally highest in the 20 to 29 year age group and this has been the age group used as a standard. He determined the average aging rate for the composite strength of the whole body could be ascertained at various ages by using the following formula:

$$\text{Average aging rate (\%)} = \frac{\text{Age} - 20}{2}$$

This simple formula uses the age of 20 years as a standard value, as the aging rate for whole body composite strength values begins to decrease after 20 years of age at a rate of 0.5% per year. The implications of this are clear for strength tests conducted in countries where cadavers used for scientific research are predominately from elderly donors. It can be expected that their tissue strengths will be significantly lower than younger age groups and the data obtained cannot therefore be interpreted as average values or be considered representative of the general population.

Figure 13 shows the progressive decrease in strength properties that occurs for some tissues and organs as age increases beyond the maximum values seen in the 20 to 29 year age group.

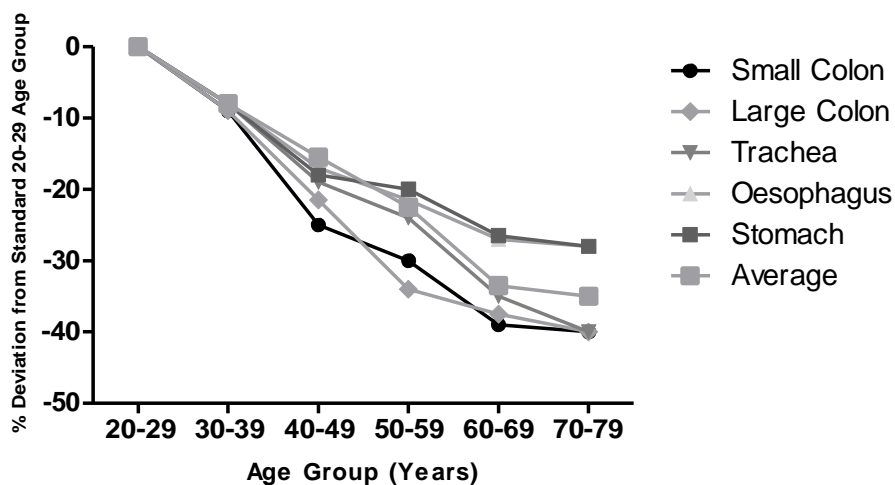


Figure 13. Aging rates for adult human respiratory and digestive organs and tissues (57).

In the current study a series of organs and tissues from a frozen and thawed elderly cadaver were compared to published standards (57). Significantly there was considerable variability, with some organs and tissues having tensile strengths that fell well below the normal range (heart, oesophagus and ascending aorta) compared to others where the tensile strengths were well above the normal range (kidney and skeletal muscle). Only one tissue, trachea, fell within the normal range. The remainder of the study was of use in demonstrating relative tensile strengths of other organs and tissues (Figure 12), with spleen being the least, and skin being the most elastic tissue.

Most published biomechanical data on the effects of freezing and thawing relate to orthopaedic and cryobiology research. The freezing of tissue is known to cause histological changes such as a loss of cellular fluid, cell shrinkage, extracellular fractures and haemolysis. The effects are magnified when intracellular freezing occurs (228-230). The freezing process leads to the redistribution of water and a dramatic reduction in tissue weight. This suggests that water movement and dehydration may play a significant role in changing mechanical properties (231).

Collagen fibres normally exhibit high tensile strength as they prevent premature mechanical failure by limiting the expansion of tissue (232). Baraibar & Schoning (230) showed that when tissue is frozen, however, collagen fibres in the pleura and some connective tissues will become more prominent because they appear to resist deterioration better than the surrounding tissues. Ng et al. (233) showed that freezing tendons for an extended period of time in saline soaked gauze, which is designed to keep the tissue moist, significantly increased their tensile strength by strengthening the collagen fibres and/or the cross-linkage between the fibres. Multiple freeze-thaw cycles (> 5) have been shown to have a significantly greater detrimental effect on the visco-elastic, structural and mechanical properties of human tendons, whereas fewer freezing cycles (<3) have produced results similar to fresh tissue (234).

While some studies have shown little or no effect on the biomechanical properties of tendons or ligamentous soft tissues that have been frozen and thawed (235, 236), others have shown a decrease in tensile strength or strain (237-239). Still others have demonstrated an increase in strength and elastic modulus through collagen fibre cross-linkage due to dehydration (232, 240). Thus, the increases and decreases in tissue tensile strength in the present study, compared to published standards (57), may be a

reflection of the variable and essentially unpredictable contributions of tissue breakdown and collagen cross-linkage during the process of continued freezing and thawing that the test cadaveric tissues were subjected to.

#### 4.5 **Conclusion**

This study has shown that freezing and thawing cadaveric organs and tissues may alter their physical properties in ways that are not predictable, with both increases and decreases in tensile strength. The study has also enabled the relative tensile strengths of such tissues to be compared. While further studies using materials from a greater number of cadavers with different numbers of freeze/re-thaw cycles may enable a more accurate determination of the effects of freezing and thawing on tensile strength, alteration of tissue properties by this process suggests that such material may not provide a reliable simulant for the analysis of ballistic effects on normal human tissues. Therefore, using thawed cadaver tissue is not realistic.

Fresh porcine organs are an alternative source of biomechanical data for the development of simulants. However, an appropriate method of obtaining data that is relevant to ballistic impact must be determined. Those data can also be used to determine what existing simulants, such as FBI and NATO specification ordnance gelatine, are actually comparable to.

**5. Pig Organ Energy Loss Comparison Experiments Using  
BB Rifle Pellets**

## 5. Pig Organ Energy Loss Comparison Experiments Using BB Rifle Pellets

### 5.1 Introduction

To develop suitable simulant materials for ballistics testing, the mechanical properties of surrogates must be matched to the heterogeneous nature of tissues and organs. To assist with this, a series of energy loss experiments were conducted using pig organs and tissues. The determination of which organs/tissues were suitable for modelling purposes was based on information gathered from the homicide study detailed in Chapter 3, which showed that the most common organs/tissues damaged in the thorax and abdomen during shootings in descending order of occurrence were the heart, lungs, liver, aorta, spleen and kidney.

There were three specific aims of this study, namely:

1. To establish which pig organs and tissues at room temperature and 37°C have similar projectile retardation properties.
2. To determine if the FBI and NATO ordnance gelatine formulations, as well as test Simulant 'A', are suitable surrogates to model any of the chosen organs and tissues.
3. To conduct a limited number of tests using pig liver, kidney and fat at 4°C, to determine what effect such a major temperature change might have on the results when compared to those at room temperature and 37°C.

### 5.2 Experimental Design

Selected organs and tissues were obtained from freshly euthanized pigs, and tested at room temperature (16° to 18°C), 37°C (body temperature) and a limited number at 4°C. Their energy loss measurements were compared to two different concentrations of ballistics ordnance gelatine and a synthetic test simulant by firing steel BB rifle pellets through these media and recording the velocity (m/s) before and after perforation using two chronographs. The energy loss measurements (J/m) were derived from the velocity figures by applying the formula  $KE = \frac{1}{2} mv^2$ , and dividing the result by the thickness of the test media. A full description is contained in Chapter 2 'Materials and Methods', pages 83 to 89.

### 5.3 Results

The energy loss results for both of the ordnance gelatine formulations, Simulant 'A' and the pig organs/tissues at the specified temperatures, were compared to each other.

#### 5.3.1 Energy Loss – Ordnance Gelatine Formulations and Simulant 'A'

The mean energy loss for 10% ordnance gelatine at 4°C (20mm thickness) (N=28) was  $98.8 \pm 4.5$  J/m.

The mean energy loss for 10% ordnance gelatine at 4°C (30mm thickness) (N=25) was  $89.6 \pm 3.9$  J/m.

The mean energy loss for 20% ordnance gelatine at 10°C (20mm thickness) (N=24) was  $147.6 \pm 3.1$  J/m.

The mean energy loss for 20% ordnance gelatine at 10°C (30mm thickness) (N=20) was  $132.0 \pm 2.1$  J/m.

The mean energy loss for Simulant 'A' (20mm thickness) (N=21) was  $122.8 \pm 7.3$  J/m.

The mean energy loss for Simulant 'A' (30mm thickness) (N=22) was  $112.7 \pm 8.9$  J/m.

#### 5.3.2 Energy Loss – Organs/Tissues at Room Temperature

At room temperature the mean energy loss for the organs and tissues (in descending order) were: - aorta (N=20)  $316.6 \pm 34.3$  J/m, fat (N=19)  $155.7 \pm 24.4$  J/m, spleen (N=18)  $140.6 \pm 35.4$  J/m, hindquarter muscle (N=20)  $129.6 \pm 16.7$  J/m, kidney (N=19)  $115.5 \pm 26.9$  J/m, lung (N=18)  $109.5 \pm 18.9$  J/m, heart (N=16)  $105.7 \pm 10.0$  J/m, and liver (N=24)  $78.8 \pm 12.2$  J/m.

#### 5.3.3 Energy Loss – Organs/Tissues at 37°C

At 37°C the mean energy loss for the organs and tissues (in descending order) were: - aorta (N=16)  $316.4 \pm 43.0$  J/m, fat (N=17)  $183.6 \pm 21.4$  J/m, spleen (N=18)  $141.3 \pm 27.3$  J/m, hindquarter muscle (N=17)  $120.9 \pm 18.0$  J/m, kidney (N=20)  $126.7 \pm 17.8$  J/m, liver (N=20)  $115.9 \pm 28.1$  J/m, lung (N=20)  $97.4 \pm 21.0$  J/m, and heart (N=22)  $90.1 \pm 8.3$  J/m.

#### 5.3.4 Energy Loss – Organs/Tissues at 4°C

At 4°C the mean energy loss for the organs and tissues (in descending order) were: - fat (N=17) 125.4±19.1J/m, liver (N=20) 115.6±23.3J/m and kidney (N=18) 110.4±12.0J/m.

#### 5.4 Sample Decomposition

Hindquarter muscle at 37°C was tested on two occasions 60 hours apart to determine if energy loss results were adversely affected. Mean average energy loss for hindquarter muscle at 37°C (N=17) was 120.9±18.0J/m. The second series of tests 60 hours later (N=18) showed a mean average energy loss of 116.2±10.3J/m ( $p>0.05$ ).

#### 5.5 Energy Grouping Results Summary

Tables 7 to 10 provide a summary and comparison of the energy grouping results for each separate ordnance gelatine formulation, Simulant 'A' and the pig organs and tissues at room temperature, 37°C and 4°C.



Media Tested	Thickness	Compared to	Temp	Statistical Significance
10% gelatine at 4°C	20mm & 30mm	20% gelatine (20mm & 30mm)	10°C	***
10% gelatine at 4°C	20mm	Simulant 'A' (20mm) Simulant 'A' (30mm) heart lung liver kidney hindquarter muscle spleen fat aorta	Room	*** ns ns ** ns *** *** *** ***
10% gelatine at 4°C	20mm	heart lung liver kidney hindquarter muscle spleen fat aorta	37°C	ns ns ns *** ** *** *** ***
10% gelatine at 4°C	20mm	liver kidney fat	4°C	*** *** ***
10% gelatine at 4°C	30mm	heart lung liver kidney hindquarter muscle spleen fat aorta	Room	ns * ns *** *** *** *** ***
10% gelatine at 4°C	30mm	heart lung liver kidney hindquarter muscle spleen fat aorta	37°C	ns ns *** *** *** *** *** ***
10% gelatine at 4°C	30mm	liver kidney fat	4°C	*** *** ***

**Table 7. Statistical significance (p<0.05)\* of the FBI gelatine formulation compared to the NATO gelatine formulation, Simulant 'A' and pig organs/tissues at room temperature, 37°C and 4°C. \*\*\*=p<0.001, \*\*=p<0.01, \*=p<0.05, ns=not significant.**

Media Tested	Thickness	Compared to	Temp	Statistical Significance
20% gelatine at 10°C	20mm	Simulant 'A' (20mm) Simulant 'A' (30mm) heart lung liver kidney hindquarter muscle spleen fat aorta	Room	*** *** *** *** *** *** ns ns ns ***
20% gelatine at 10°C	20mm	heart lung liver kidney hindquarter muscle spleen fat aorta	37°C	*** *** *** * *** ns *** ***
20% gelatine at 10°C	20mm	liver kidney fat	4°C	*** *** ***
20% gelatine at 10°C	30mm	Simulant 'A' (20mm) Simulant 'A' (30mm) heart lung liver kidney hindquarter muscle spleen fat aorta	Room	ns * ** * *** ns ns ns ** ***
20% gelatine at 10°C	30mm	heart lung liver kidney hindquarter muscle spleen fat aorta	37°C	*** *** ns ns ns ns *** ***
20% gelatine at 10°C	30mm	liver kidney fat	4°C	*** *** ns

**Table 8. Statistical significance ( $p < 0.05$ )\* of the NATO gelatine formulation compared to Simulant 'A' and the pig organs/tissues at room temperature, 37°C and 4°C. \*\*\*= $p < 0.001$ , \*\*= $p < 0.01$ , \*= $p < 0.05$ , ns=not significant.**

Media Tested	Thickness	Compared to	Temp	Statistical Significance
Simulant 'A'	20mm	heart lung liver kidney hindquarter muscle spleen fat aorta	Room	ns ns *** ns ns ns *** ***
Simulant 'A'	20mm	heart lung liver kidney hindquarter muscle spleen fat aorta	37°C	*** *** ns ns ns ns *** ***
Simulant 'A'	20mm	liver kidney fat	4°C	ns * ns
Simulant 'A'	30mm	heart lung liver kidney hindquarter muscle spleen fat aorta	Room	ns ns *** ns ns *** *** ***
Simulant 'A'	30mm	heart lung liver kidney hindquarter muscle spleen fat aorta	37°C	** ns ns ns ns *** *** ***
Simulant 'A'	30mm	liver kidney fat	4°C	ns ns *

**Table 9. Statistical significance ( $p < 0.05$ )\* of Simulant 'A' compared to the pig organs/tissues at room temperature, 37°C and 4°C. \*\*\*= $p < 0.001$ , \*\*= $p < 0.01$ , \*= $p < 0.05$ , ns=not significant.**

Media Tested	Compared To	Temp	Statistical Significance
heart	lung kidney liver hindquarter muscle spleen fat aorta	Room	ns ns *** ** *** *** ***
lung	kidney liver hindquarter muscle spleen fat aorta	Room	ns *** * *** *** ***
kidney	hindquarter muscle spleen fat aorta	Room	ns ** *** ***
hindquarter muscle	spleen fat aorta	Room	ns *** ***
spleen	fat aorta	Room	ns ***
heart	lung kidney liver hindquarter muscle spleen fat aorta	37°C	ns *** *** *** *** *** ***
lung	kidney liver hindquarter muscle spleen fat aorta	37°C	*** ns ** *** *** ***
liver	kidney hindquarter muscle spleen fat aorta	37°C	ns ns ** *** ***
kidney	hindquarter muscle spleen fat aorta	37°C	ns ns *** ***

Media Tested <i>Continued</i>	Compared To	Temp	Statistical Significance
hindquarter muscle	spleen fat aorta	37°C	ns *** ***
liver	kidney fat	4°C	ns ns
kidney	fat	4°C	**

Table 10. Statistical significance ( $p < 0.05$ )\* for pig organs/tissues compared to each other at room temperature, 37°C and 4°C. \*\*\*= $p < 0.001$ , \*\*= $p < 0.01$ , \*= $p < 0.05$ , ns=not significant.

Figure 14 shows an energy loss comparison between FBI and NATO ordnance gelatine formulations, Simulant 'A' and organs/tissues at room temperature.

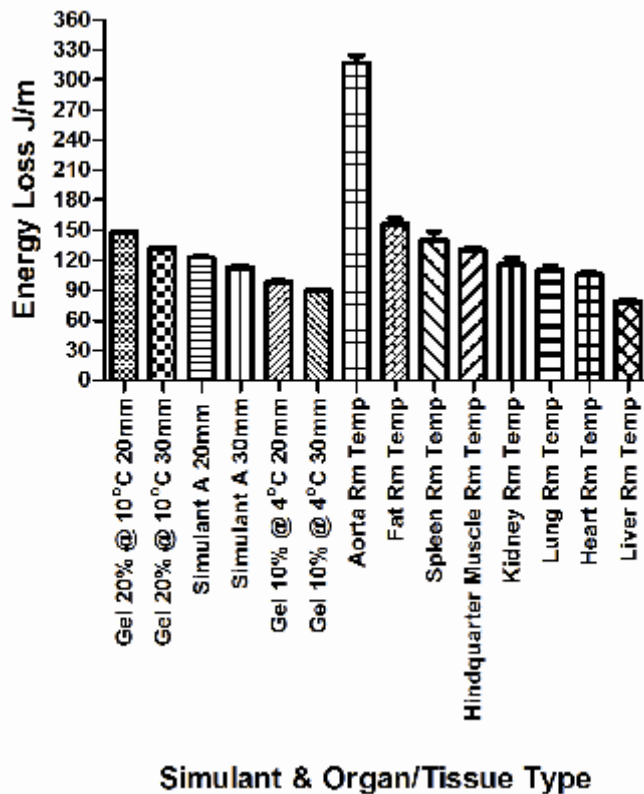


Figure 14. Energy loss comparison between FBI and NATO gelatine formulations, Simulant 'A' and organs/tissues at room temperature.

Figure 15 shows an energy loss comparison between FBI and NATO ordnance gelatine formulations, Simulant 'A' and pig organs/tissues at 37°C.

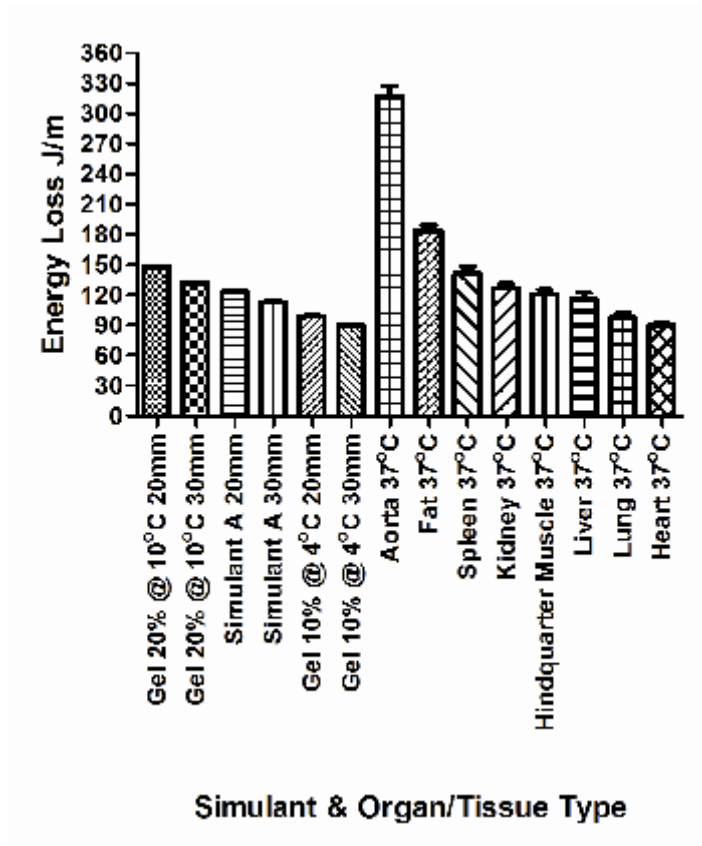


Figure 15. Energy loss comparison between FBI and NATO gelatine formulations, Simulant 'A' and pig organs/tissues at 37°C.

Figure 16 shows an energy loss comparison between FBI and NATO ordnance gelatine formulations, Simulant 'A' and pig organs/tissues at 4°C.

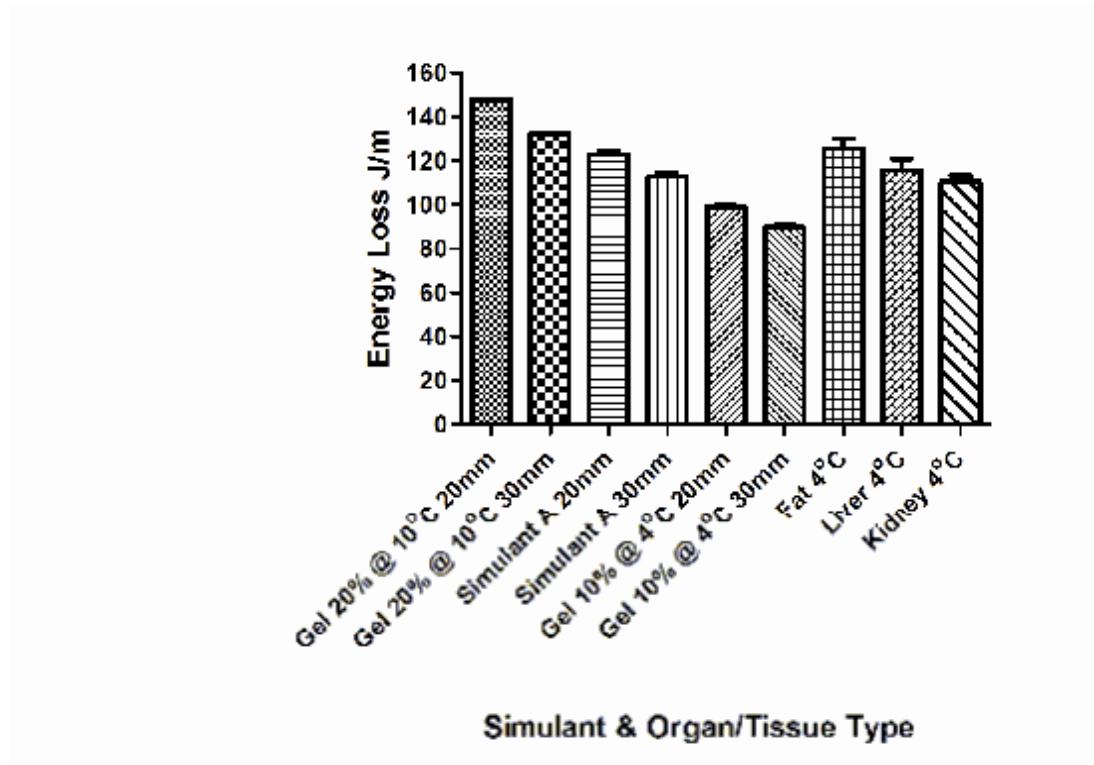


Figure 16. Energy loss comparison between FBI and NATO gelatine formulations, Simulant 'A' and pig organs/tissues at 4°C.

Figure 17 shows an energy loss comparison between FBI and NATO ordnance gelatine formulations, Simulant 'A' and all pig organs/tissues at room temperature, 37°C and 4°C.

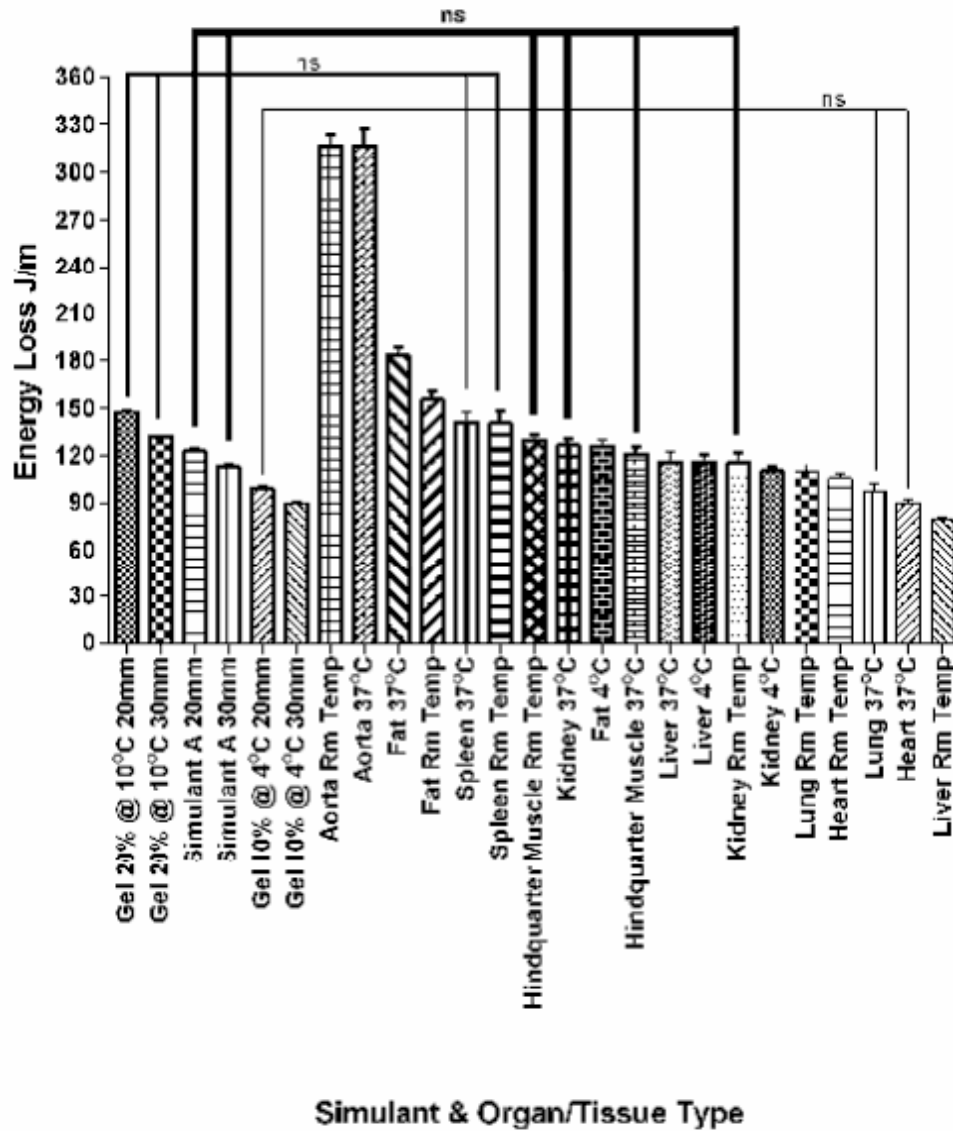


Figure 17. Energy loss comparison between FBI and NATO gelatine concentrations, Simulant 'A' and pig organs/tissues at room temperature, 37°C and 4°C. ns = not significant.



Figure 18 shows an energy loss comparison for pig fat at different temperatures.

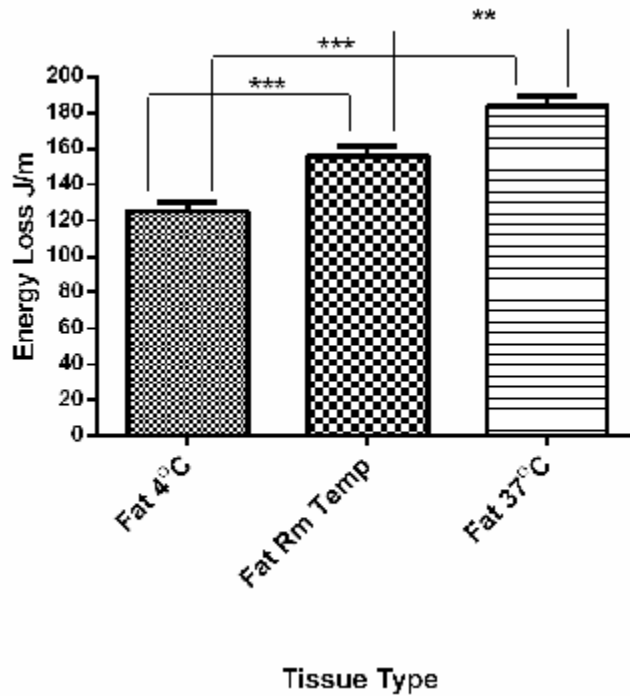


Figure 18. Energy loss comparison for pig fat at 4°C, room temperature and 37°C, showing its anti-thixotropic nature. \*\*\*= $p < 0.001$ , \*\*= $p < 0.01$ .

## 5.6 Discussion

Each material under test was statistically compared using energy loss data (J/m) derived from the original velocity loss data, BB pellet mass and thickness of the test media. It was not possible to weigh each steel BB pellet prior to testing for reasons explained in the 'Materials and Methods' in Chapter 2. As a result, the average weight from a sample of 30 BB pellets was used to establish the required half mass figure for all energy calculations. As mass now became a constant value, velocity became the only variable in the energy equation.

Organs and tissues from pigs were chosen as pigs are the most suitable animal for wound ballistics research (16, 27). For a more detailed discussion see Chapter 1.

Ten percent ordnance gelatine at 4°C and the NATO formulation of 20% ordnance gelatine at 10°C are standards used as soft tissue simulants for ballistics research. Facker and Malowski (29) determined that the 10% formulation was a suitable soft tissue simulant based on porcine penetration tests. These authors showed that it replicated the combined mechanical properties of skin, fat, fascia and muscle tissue of a porcine thigh when penetrated by a ballistic projectile. As a result, it has been accepted as the FBI standard.

In this study, porcine hindquarter muscle was tested without the skin attached. This provides a more valid result during comparisons with the other test media, as skin presents an intermediate barrier which will affect BB pellet velocity and energy loss. The original BB pellet penetration tests conducted by Fackler and Malinowski (29) indicate that skin was attached to the pig thigh. Therefore, it is not surprising that the results achieved from this series of energy loss tests on bare hindquarter muscle show that it is statistically different ( $p < 0.001$ ) to 10% ordnance gelatine at 4°C (Table 7), whereas Facker and Malinowski (29) indicate that it was comparable.

Whilst McPherson (17) indicates that retardation caused by skin is negligible compared to muscle tissue, there will nevertheless be some energy consumed. McPherson quotes a figure of  $11.8\text{J}/\text{cm}^2$  to achieve penetration using a steel 4.5mm (nominal) sphere BB pellet. Haag (131) and Rathman (241) quote figures of 13 and  $18\text{J}/\text{cm}^2$  respectively to achieve this. These values do not appear to include penetration of the subcutaneous tissue and fat which exists between the skin and muscle, so additional energy would be required to penetrate these barriers. Therefore, the difference between Fackler and Malinowski's (29) results compared to the current study can most likely be attributed to a greater amount of energy required to perforate the combination of pig skin, subcutaneous tissue, fat and hindquarter muscle. Additional tests are required to confirm this.

Room temperature and 37°C were the two most important temperature ranges tested. These temperatures were chosen as room temperature is the simplest test environment, and 37°C is human body temperature. Therefore statistically similar results for organs and tissues at both temperatures ensures that any additional simulant/s developed are representative of human body temperature, but are capable of being used at room temperature.

This study showed that 10% gelatine at 4°C (20mm thickness) was comparable to heart and lung at both room temperature and 37°C (Table 7) (Figure 17). A 30mm thickness of the same formulation was comparable at 37°C but not at room temperature ( $p < 0.05$ ) (Table 7). Considering that heart and lung are comparable to each other at both room temperature and 37°C ( $p > 0.05$ ), overall the 10% gelatine formulation was similar to both heart and lung.

The 10% gelatine formulation was significantly different to all other organs and tissues tested at the specified temperatures with the exception of liver (Table 7). However, because liver was significantly different in two of the four tests, overall it can be considered different to 10% gelatine at 4°C.

Twenty percent gelatine at 10°C is the accepted NATO standard. It was significantly different ( $p < 0.001$ ) to the FBI 10% gelatine formulation (Table 7). However, the NATO formulation (20mm thickness) was comparable ( $p > 0.05$ ) to hindquarter muscle, spleen and fat at room temperature, but comparable only to spleen at 37°C. A 30mm thickness of the same NATO formulation was comparable to kidney, hindquarter muscle and spleen at room temperature and to liver, kidney, hindquarter muscle and spleen at 37°C. Thus, the NATO gelatine formulation (20mm and 30mm thicknesses) was similar to spleen only at room temperature and 37°C (Table 8) (Figure 17). However, the NATO formulation (20mm and 30mm thicknesses) was comparable to hindquarter muscle in three of the four tests and significantly different ( $p < 0.01$ ) in the other test (Table 8). From a practical perspective, the NATO gelatine formulation might be considered comparable to hindquarter muscle at both room temperature and 37°C.

The NATO gelatine formulation was significantly different ( $p < 0.001$ ) to heart, lung, fat and aorta at room temperature and 37°C. There was a variable result with both liver and kidney (Table 8). However, as liver was significantly different in three of the four tests, and kidney was different in two out of the four tests, overall they can be considered different to 20% gelatine at 10°C.

Simulant 'A' (20mm and 30mm thicknesses) was found to be comparable ( $p > 0.05$ ) to kidney and hindquarter muscle at room temperature and 37°C. There was a variable result with heart, lung, liver and spleen (Table 9). Both thicknesses of Simulant 'A' were similar to heart, liver and spleen in only two of the four tests. Therefore Simulant 'A' can

be considered significantly different to these organs at both temperatures. However, Simulant 'A' was comparable to lung in three out of the four tests, but significantly different ( $p < 0.001$ ) at 37°C compared to a 20mm thickness. As lung has been shown to be comparable to heart at room temperature and 37°C (Table 10) (Figures 14, 15), and both thicknesses of Simulant 'A' were comparable to heart at room temperature, from a practical perspective Simulant 'A' can be considered comparable to heart and lung at room temperature only.

Simulant 'A' was significantly different ( $p < 0.001$ ) to fat and aorta at room temperature and 37°C.

At both room temperature and 37°C heart was comparable to lung, kidney was comparable to hindquarter muscle and hindquarter muscle was comparable to spleen (Table 10). Therefore one simulant may be suitable for both heart and lung and one simulant for kidney and hindquarter muscle. Although spleen was comparable to hindquarter muscle at both temperatures and comparable to kidney at 37°C, it was significantly different ( $p < 0.01$ ) to kidney at room temperature (Table 10). Therefore a separate simulant would be required for spleen. Similarly, a separate simulant would be required for liver, fat and aorta, as they cannot be grouped with any other organs or tissues tested at the respective temperatures.

For modelling purposes, the FBI 10% gelatine formulation is a suitable simulant for both heart and lung, NATO 20% gelatine formulation is a suitable simulant for spleen, and Simulant 'A' is a suitable simulant for both hindquarter muscle and kidney.

At 4°C liver, kidney and fat were comparable ( $p > 0.05$ ) to each other, while at room temperature kidney and fat were significantly different ( $p < 0.001$ ) to liver and each other. At 37°C kidney was comparable to liver, but fat was significantly different to both (Table 10).

The variations in temperature appear to have had an effect upon most of the organs and tissues tested with the exception of spleen and aorta, where the energy loss values did not change significantly. Heart, lung and hindquarter muscle recorded a decrease in energy loss as the temperature rose from room temperature to 37°C, indicating that their mechanical properties change and they become more permeable. Liver, kidney

and fat exhibited the opposite effect, where energy loss increased as the temperature increased from room temperature to 37°C (Figures 14, 15, 17).

Only liver, kidney and fat were tested at 4°C. Reducing the temperature of these organs and tissues from room temperature to 4°C reduced the energy required to perforate kidney and fat. However, the opposite occurred with liver, where more energy was required to perforate it at 4°C than at room temperature (Figure 17). The most likely explanation for this is that tensile strength increases at this temperature making liver less permeable.

The data for fat (Figure 18) appears the most surprising. Fat can affect the ability of the body to tolerate injuries, particularly from low velocity impacts as it acts as an energy absorbing material (242). Adipose tissue is considered to be anti-thixotropic in nature. Thixotropy is a term used to describe time dependant decreases in the viscosity of a material caused by deformation, but this effect is reversible when the deformation ceases. However, when the deformation causes time dependent reversible increases in viscosity, the term anti-thixotropic is used (243-245). Abdominal fat has a connective tissue lattice that is anti-thixotropic causing an increase in the viscosity and elasticity of the fat and connective tissue, resulting in it acting like a curtain and absorbing energy when struck by the low velocity BB projectile. Increasing the temperature from room temperature to 37°C appears to magnify this property resulting in a greater energy loss to achieve perforation.

Both liver and kidney are known to be dense inelastic organs. An increase in temperature from room temperature to 37°C has made these organs less permeable. One reason for this may be that they also contain quantities of anti-thixotropic tissue. However, further work will be required to clarify this issue.

Organ or tissue decomposition can be expected to influence energy dispersion, but to what extent and how long after death is dependent on storage conditions. To establish whether sample decomposition might be a factor affecting energy loss, hindquarter muscle at 37°C was tested on two occasions 60 hours apart. The original mean energy loss for hindquarter muscle at 37°C (N=17) was  $120.9 \pm 18.0$  J/m. The second set of tests 60 hours later (N=18) showed a mean energy loss of  $116.2 \pm 10.3$  J/m. These two sets of figures were not statistically different ( $p > 0.05$ ), indicating that the 60 hour time

lapse did not have any significant effect on energy loss results for hindquarter muscle at 37°C. Further study would be required to establish the maximum time frame within which energy loss values would be adversely affected by decomposition/putrefaction.

### 5.7 Limitations of Study

The following limitations apply to this study and its results.

Anatomical variation between and among pigs will affect results to some degree because of the heterogeneity of the organs and tissues (246). This factor can be expected to account for higher standard deviation values.

This study was conducted using low velocity BB pellets only. It is not known if a high velocity projectile will record similar results and groupings. To ascertain this, the same tests would need to be repeated at high velocity. Non-deforming steel ball bearings in calibre 5.56mm would be the preferred option at a velocity comparable with the standard issue ADF AUSTEYR model F88 ICW in calibre 5.56x45mm NATO, which was the focus of the experimental study in Chapter 7.

Non-deforming circular steel BB pellets (ball bearings) have been used in the current study to limit the variables involved with using projectiles of different shape. To determine if geometrically different bullets will affect the results, a starting point would be to repeat the same tests using ASF1 ball ammunition fired from a standard issue ADF AUSTEYR model F88 ICW.

There are many other commercially designed deforming bullets in both handgun and rifle calibres that could be further tested to determine how significant a factor projectile geometry is in energy loss.

### 5.8 Conclusion

The primary aims of this study were to establish which of the selected pig organs and tissues are similar to each other at both room temperature and 37°C (human body temperature), as well as to determine if the FBI/NATO gelatine formulations and test Simulant 'A' are suitable surrogates to model specific organs and tissues.

Energy loss data established that heart and lung, hindquarter muscle and kidney, and hindquarter muscle and spleen are comparable paired organs/tissues.

Energy loss data has also shown that FBI 10% gelatine at 4°C is a suitable simulant for both heart and lung, NATO 20% gelatine at 10°C is a suitable simulant for spleen and Simulant 'A' is a suitable simulant for both hindquarter muscle and kidney. A separate simulant would be required for liver, fat and aorta as they cannot be grouped together with any of the other organs or tissues tested at the respective temperatures.

While the two gelatine formulations have been shown to be suitable simulants for a limited number of organs, ballistics ordnance gelatine has its limitations and can be difficult to prepare. These limitations will be explored further.

Simulant 'A' was shown to be a promising alternative option to ordnance gelatine. The main benefit of it is that it is temperature stable and therefore easier to manufacture and handle. The formulation that was used can potentially be modified to simulate additional organs for ballistic modelling purposes.

**6. BALLISTICS ORDNANCE GELATINE – HOW DIFFERENT  
CONCENTRATIONS, TEMPERATURES AND CURING TIMES  
AFFECT CALIBRATION RESULTS**



## 6. **Ballistics Ordnance Gelatine – How Different Concentrations, Temperatures and Curing Times Affect Calibration Results**

### 6.1 **Introduction**

Ballistics ordnance gelatine is the most widely accepted simulant for wound ballistics research. However, it is homogeneous and cannot replicate the heterogeneous nature of human tissue. It is currently accepted as a soft tissue simulant (16, 103, 104), but the Chapter 5 study showed that the standard formulations are comparable to a very limited number of porcine organs.

A series of experiments were conducted using different ordnance gelatine concentrations, water types, temperatures and curing times to see how BB pellet penetration results might be affected in both FBI and NATO specified ordnance gelatine.

### 6.2 **Experimental Design**

Two gelatine Bloom number concentrations, three different water types, three different curing times and different temperature ranges were used with the NATO and FBI ordnance gelatine formulations, to determine what effect this may have on BB pellet calibration results. A full description of the 'Materials and Methods' is contained in Chapter 2 pages 90 to 91.

### 6.3 **Results**

#### 6.3.1 **10% Ordnance Gelatine at 4°C 250 Bloom (FBI Standard)**

##### (a) **21 Hours Curing Time**

The mean penetration depth of 10% gelatine at 4°C 250 Bloom using RO water (N=4) was  $106.9 \pm 1.9$ mm. The mean penetration depth for the same formulation using tap water (N=4) was  $113.7 \pm 2.6$ mm ( $p > 0.05$ ), and for de-ionized water was  $112.0 \pm 2.8$ mm ( $p > 0.05$ ).

The overall mean penetration depth for the three water types was  $110.9 \pm 3.5$ mm.

**(b) 100 Hours Curing Time**

The mean penetration depth of 10% gelatine at 4°C 250 Bloom using tap water (N=4) was 104.8±2.0mm. The mean penetration depth for the same formulation using de-ionized water (N=4) was 107.3±3.0mm (p>0.05).

The overall mean penetration depth for the two water types was 106.1±1.8mm.

**(c) 3 Weeks Curing Time**

The mean penetration depth of 10% gelatine at 4°C 250 Bloom using de-ionized water (N=3) was 98.2±6.6mm. The mean penetration depth for the same formulation at 3°C using de-ionized water (N=3) was 94.6±1.4mm (p>0.05).

The BB penetration results for all 10% gelatine at 4°C and 3°C 250 Bloom formulations after their respective curing times are shown in Figure 19.

**6.3.2 20% Ordnance Gelatine at 10°C 250 Bloom (NATO Standard)**

**(a) 21 Hours Curing Time**

The mean penetration depth of 20% gelatine at 10°C 250 Bloom using RO water (N=4) was 48.6±6.3mm.

**(b) 100 Hours Curing Time**

The mean penetration depth of 20% gelatine at 10°C 250 Bloom using tap water (N=4) was 45.7±1.6mm. The mean penetration depth for the same formulation using de-ionized water (N=4) was 41.7±3.0mm (p>0.05).

The overall mean penetration depth for the three water types tested above after 21 hours and 100 hours curing time was 45.3±3.6mm.

The BB penetration results for all 20% gelatine at 10°C 250 Bloom formulations after their respective curing times are shown in Figure 20.

**6.3.3 20% Ordnance Gelatine at 10°C using 285 Bloom**

**(a) 21 Hours Curing Time**

The mean penetration depth for 20% gelatine at 10°C 285 Bloom using tap water (N=4) was 51.4±0.7mm. The mean penetration depth for the same formulation using de-

ionized water (N=4) was  $48.7\pm 1.5\text{mm}$  ( $p>0.05$ ). An additional test with the same formulation using de-ionized water (N=4) produced a mean penetration depth of  $49.0\pm 0.9\text{mm}$  ( $p>0.05$ ).

The overall mean penetration depth for the two water types was  $49.7\pm 1.0\text{mm}$ .

The BB penetration results for all 20% gelatine at 10°C 285 Bloom formulations after 21 hours curing time are shown in Figure 21.

#### 6.3.4 20% Ordnance Gelatine at 20°C using 285 Bloom

##### (a) 100 Hours Curing Time

The mean penetration depth of 20% gelatine at 20°C 285 Bloom using tap water (N=4) was  $80.6\pm 1.9\text{mm}$ . The mean penetration depth for the same formulation using de-ionized water (N=4) was  $77.7\pm 4.1\text{mm}$  ( $p>0.05$ ).

The overall mean penetration depth for the two water types was  $79.2\pm 3.0\text{mm}$ .

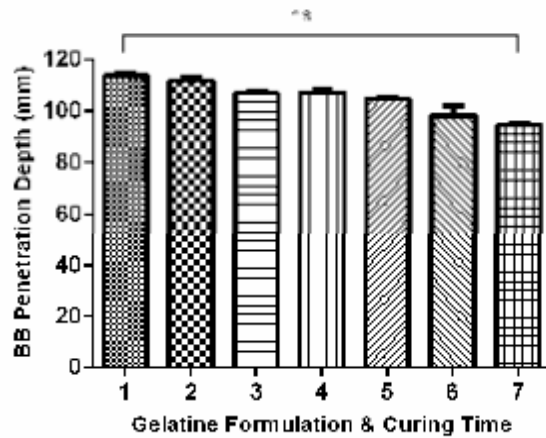
The BB penetration results for both 20% gelatine at 20°C 285 Bloom formulations after 100 hours curing time are shown in Figure 21.

A comparison of all gelatine formulations tested is shown in Figure 22.

There was a significant difference in mean penetration depth between the FBI formulation, NATO formulation and 20% at 20°C 285 Bloom formulation ( $p<0.001$ ), using the respective water types and curing times, with no significant difference ( $p>0.05$ ) between the NATO formulation and the 20% at 10°C 285 Bloom formulation (Figure 22).

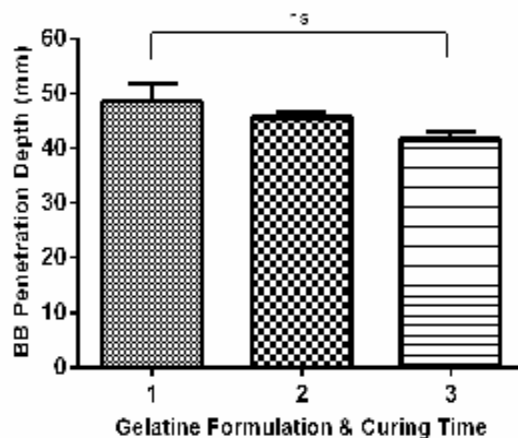
Temperature changes and curing times did affect penetration depth and this was best illustrated with the 20% gelatine formulations using 285 Bloom. At 10°C the mean penetration depth for the two water types tested was  $49.7\pm 1.5\text{mm}$  after 21 hours curing time, whereas the same formulation at 20°C recorded a mean penetration depth of  $79.1\pm 2.1\text{mm}$  after 100 hours curing time ( $p<0.001$ ).

Figures 19 to 22 provide a summary of the BB pellet penetration depths achieved with different formulations of ordnance gelatine at different temperatures over different curing times.



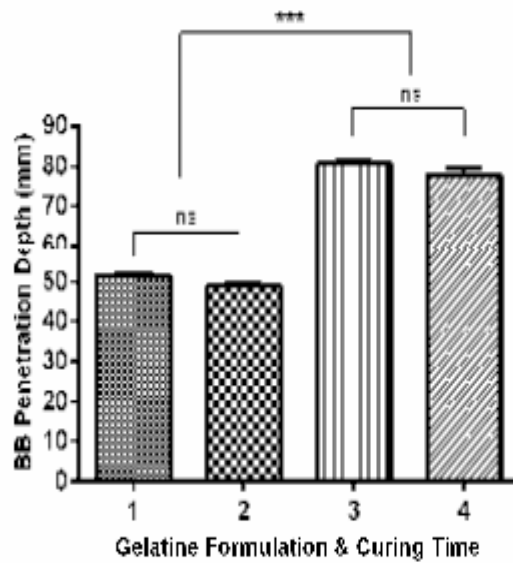
1. 10% gelatine at 4°C 250 Bloom using tap water after 21 hours curing time
2. 10% gelatine at 4°C 250 Bloom using de-ionized water after 21 hours curing time
3. 10% gelatine at 4°C 250 Bloom using RO water after 21 hours curing time
4. 10% gelatine at 4°C 250 Bloom using de-ionized water after 100 hours curing time
5. 10% gelatine at 4°C 250 Bloom using tap water after 100 hours curing time
6. 10% gelatine at 4°C 250 Bloom using de-ionized water after 3 weeks curing time
7. 10% gelatine at 3°C 250 Bloom using de-ionized water after 3 weeks curing time

**Figure 19. Mean BB pellet penetration depth for 10% ordnance gelatine at 4°C 250 Bloom using three different water types and curing times. In addition, the same formulation at 3°C was tested to compare results. ns=not significant.**



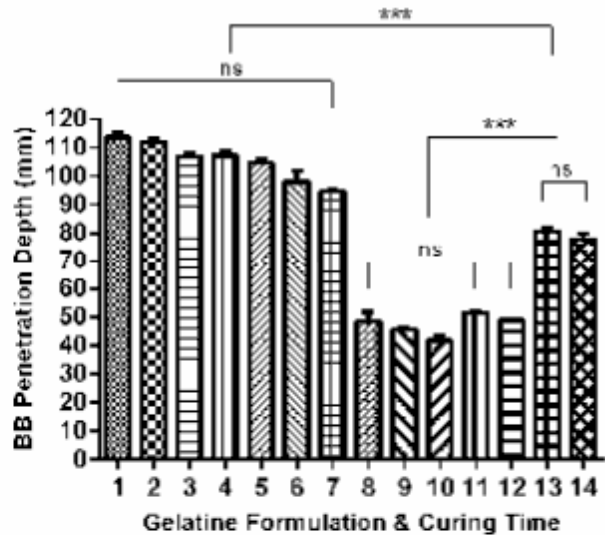
1. 20% gelatine at 10°C 250 Bloom using RO water after 21 hours curing time
2. 20% gelatine at 10°C 250 Bloom using de-ionized water after 100 hours curing time
3. 20% gelatine at 10°C 250 Bloom using tap water after 100 hours curing time

**Figure 20. Mean BB pellet penetration depth for 20% ordnance gelatine at 10°C 250 Bloom using three different water types and two different curing times. ns=not significant.**



1. 20% gelatine at 10°C 285 Bloom using tap water after 21 hours curing time
2. 20% gelatine at 10°C 285 Bloom using de-ionized water after 21 hours curing time
3. 20% gelatine at 20°C 285 Bloom using tap water after 100 hours curing time
4. 20% gelatine at 20°C 285 Bloom using de-ionized water after 100 hours curing time

**Figure 21. Comparison of mean BB pellet penetration depth for 20% ordnance gelatine at 10°C 285 Bloom and 20% ordnance gelatine at 20°C 285 Bloom, using two different water types and a different curing time. \*\*\*= $p < 0.001$ , ns=not significant.**



1. 10% gelatine at 4°C 250 Bloom using tap water after 21 hours curing time
2. 10% gelatine at 4°C 250 Bloom using de-ionized water after 21 hours curing time
3. 10% gelatine at 4°C 250 Bloom using RO water after 21 hours curing time
4. 10% gelatine at 4°C 250 Bloom using de-ionized water after 100 hours curing time
5. 10% gelatine at 4°C 250 Bloom using tap water after 100 hours curing time
6. 10% gelatine at 4°C 250 Bloom using de-ionized water after 3 weeks curing time
7. 10% gelatine at 3°C 250 Bloom using de-ionized water after 3 weeks curing time
8. 20% gelatine at 10°C 250 Bloom using RO water after 21 hours curing time
9. 20% gelatine at 10°C 250 Bloom using de-ionized water after 100 hours curing time
10. 20% gelatine at 10°C 250 Bloom using tap water after 100 hours curing time
11. 20% gelatine at 10°C 285 Bloom using tap water after 21 hours curing time
12. 20% gelatine at 10°C 285 Bloom using de-ionized water after 21 hours curing time
13. 20% gelatine at 20°C 285 Bloom using tap water after 100 hours curing time
14. 20% gelatine at 20°C 285 Bloom using de-ionized water after 100 hours curing time

**Figure 22. Overall comparison of mean BB pellet penetration depths for 10% ordnance gelatine at 3°C and 4°C 250 Bloom, 20% ordnance gelatine at 10°C 250 Bloom, 20% ordnance gelatine at 10°C 285 Bloom and 20% ordnance gelatine at 20°C 285 Bloom, using a combination of three different water types and three different curing times. \*\*\*=p<0.001, ns=not significant.**

#### 6.4 Discussion

The FBI 10% ordnance gelatine formulation is considered to be more representative than the NATO 20% formulation for simulating soft tissue mechanical response at various strain rates (100, 101).

Despite the FBI adopting the 10% formulation for which a calibration standard applies (29), the NATO 20% formulation is still widely used, particularly in Europe. However, there are no published data or separate calibration standards for the NATO formulation, which leads to the inevitable questions, what does the NATO formulation represent as a simulant, and what is the basis for this assumption? The energy loss study in Chapter 5 may have answered this question.

The current study found no significant differences ( $p>0.05$ ) in mean penetration depth for the FBI formulation after 21 hours, 100 hours and three weeks curing time using tap water, RO water or de-ionized water (Figure 19). Similarly, no significant difference ( $p>0.05$ ) in mean penetration depth was found for the NATO formulation after 21 hours curing time using RO water, or 100 hours curing time using both de-ionized water and tap water (Figure 20). In addition, no significant difference ( $p>0.05$ ) in mean penetration depth was found for the 20% gelatine formulation at 10°C 285 Bloom after 21 hours curing time using tap water and de-ionized water, or for the 20% gelatine formulation at 20°C 285 Bloom after 100 hours curing time using tap water and de-ionized water (Figure 21).

There was a significant difference ( $p<0.001$ ) in mean penetration depth between the FBI formulation, NATO formulation and the 20% at 20°C 285 Bloom formulation, using the respective water types and curing times (Figure 22). However, there was no significant difference ( $p>0.05$ ) between the NATO formulation and the 20% at 10°C 285 Bloom formulation using the respective water types and same curing time (21 hours) (Figure 22).

The study has also shown that temperature changes and curing times did affect penetration depth and this was best illustrated with the 20% gelatine formulations using 285 Bloom. At 10°C the mean penetration depth for the two water types tested was  $49.7\pm 1.5$ mm after 21 hours curing time, whereas the same formulation at 20°C recorded a mean penetration depth of  $79.1\pm 2.1$ mm after 100 hours curing time ( $p<0.001$ ) (Figure 21).

It was noted that slight over-penetration, of between 5 to 10mm, was not uncommon during the gelatine tests compared to the accepted calibration standard for the FBI formulation. However, as chronograph readings were not recorded for each individual

shot, and velocity was based on the preliminary velocity testing of the number of pumps of the BB gun required to attain the required velocity of  $180\pm 4.5\text{m/s}$  (29), other factors such as variability in shot to shot velocities from the BB gun must be considered, in addition to the temperatures of the blocks.

McPherson (17) indicates that over penetration is not uncommon due to batch differences and suggests that the following can be undertaken to reduce penetration to within the accepted depth:

- Lower gelatine temperature from  $4^{\circ}$  to  $3^{\circ}\text{C}$ .
- Prepare the gelatine concentration at 11% instead of 10%. This will reduce penetration by approximately 10mm.

The option of lowering the temperature to  $3^{\circ}\text{C}$  was tested with the FBI formulation after three weeks curing time. At  $4^{\circ}\text{C}$  the mean penetration depth was  $98.2\pm 6.6\text{mm}$ , and at  $3^{\circ}\text{C}$  it was  $94.6\pm 1.4\text{mm}$ . This reduction resulted in the mean penetration depth being within the acceptable range although towards the upper limit. However, this result is not statistically significant ( $p>0.05$ ) (Figure 19). Due to time constraints, an 11% concentration was not tested.

Generally, the mean penetration depth appeared to decrease as curing times increased. This was demonstrated with the FBI formulation where the overall mean penetration depth for the three water types tested after 21 hours curing time was  $110.9\pm 3.5\text{mm}$ , compared to  $106.1\pm 1.8\text{mm}$  for the two water types tested after 100 hours curing time and  $98.2\pm 6.6\text{mm}$  for the single water type tested after three weeks curing time. Therefore, the mean penetration depth for the FBI formulation was closest to the recommended standard after three weeks curing time. However, the overall mean penetration differences were not statistically significant ( $p>0.05$ ) (Figure 19).

The NATO standard is a 20% w/w concentration of 250 to 300 Bloom Type A gelatine at  $10^{\circ}\pm 2^{\circ}\text{C}$  (98). A 20% concentration of 250 Bloom gelatine at  $10^{\circ}\text{C}$  achieved an overall mean penetration depth of  $45.3\pm 3.6\text{mm}$  using the three different water types and two different curing times (Figure 20). A 20% concentration of 285 Bloom gelatine at  $10^{\circ}\text{C}$  achieved an overall mean penetration depth of  $49.7\pm 1.0\text{mm}$  using two different water types after 21 hours curing time (Figure 21). In the absence of published data and a



separate calibration standard, neither NATO concentration at 10°C matches the calibration standard for a soft tissue simulant recommended by Fackler and Malinowski (29) and adopted by the FBI.

A 20% concentration of 285 Bloom gelatine at 20°C did meet the calibration standard (Figures 21 and 22), providing results which were on the lower side of the accepted range, with an overall mean penetration depth of  $79.2 \pm 3.0$ mm using two different water types after 100 hours curing time (Figure 21). This formulation can be accepted as matching the FBI calibration standard for a soft tissue simulant (29). Similarly, a 20% concentration of 250 Bloom gelatine at 22°C has since been shown to equal the performance of 10% FBI specified gelatine at 4°C (17).

Cronin and Falzon (247) recently conducted tests on 10% FBI specification gelatine to evaluate the effects of temperature, aging (curing) and strain rates up to a maximum of 170 hours (7 days). They found that BB pellet penetration results, as well as stress (force per unit area) and strain to failure (ratio of the change in length to the original length until failure) figures, were consistent after 72 hours of aging. However, after this time the strain to failure properties decreased while gelatine stiffness (resistance offered to elastic deformation) increased significantly. Despite this, BB pellet penetration results up to 170 hours remained relatively consistent, suggesting that although the mechanical properties changed, they appeared to offset one another, so that the gelatine still responded in the same manner to BB pellet impact. They cautioned however, that these mechanical property changes may have a greater effect on larger calibre, high energy projectiles. Thus, further experimental studies to quantify those affects with handgun and high velocity rifle rounds would be useful.

The current study did not evaluate stress and strain rate properties of ordnance gelatine, but it did evaluate different water types, curing times and temperatures over a wider range of concentrations. While slight over penetration of between 5 to 10mm was experienced with the FBI 10% formulation, this is quite common (111). It was found that increased curing time (up to a maximum of 3 weeks) provided penetration results closest to the required standard. A 20% concentration of 285 Bloom at 20°C was found to meet the penetration and calibration standard after 100 hours of curing time.

## 6.5 Conclusion

Ballistics ordnance gelatine is currently considered an acceptable soft tissue simulant if it meets the required FBI calibration standard. However, the current study has shown that temperature and curing times may have a direct effect on projectile penetration. The study also found that using different water types, namely tap water, RO water and de-ionized water in the manufacturing process, had no significant effect on BB penetration results.

Neither of the NATO 20% concentrations of gelatine at 10°C, or a 20% concentration of 285 Bloom gelatine at 10°C, met the same calibration standard as the FBI recommended 10% formulation at 4°C. Despite this, the Chapter 5 study has shown that the NATO formulation is comparable to porcine spleen. Therefore, it is clear that a separate calibration standard is required when using this formulation.

The penetration depths achieved for 10% concentrations of 250 Bloom at both 3° and 4°C were closest to the recommended calibration standard after 3 weeks of curing time. However, increasing curing time beyond the accepted 3 to 4 day period is not recommended in light of the study by Cronin and Falzon (247).

A 20% concentration of 285 Bloom at 20°C met the same calibration/penetration criteria as a 10% concentration of 250 Bloom at 4°C after 100 hours of curing. Therefore, it can be classed as matching the FBI calibration standard for a soft tissue simulant for wound ballistics research.

The results of this study clearly demonstrate that there may be significant variability in the properties of ordnance gelatine simulants depending on temperature and curing times. If the manufacture of these simulants is not precisely standardised, interpretation and comparison of ballistics results may not be possible. These limitations combined with the small number of porcine organs these gelatine formulations are comparable to (refer Chapter 5), lead to the question of how representative they are of actual bullet wound trauma. To assist in answering this, the behaviour of a selected military rifle round in bare FBI specification gelatine was compared to a series of basic anatomical models of the thorax.

## **7. ANATOMICAL MODEL PILOT STUDY**

## **7. Anatomical Model Pilot Study**

### **7.1 Introduction**

With the assistance of Defence Science and Technology Organisation (DSTO) personnel, a series of eight simulant model test firings were conducted at the DSTO indoor ballistic range facility at Edinburgh, South Australia. The purpose of these experiments was to test the hypothesis that anatomical simulant models, which replicate the heterogeneous nature of human organs and tissues, will provide a more reliable and accurate method to evaluate the characteristics of ammunition than FBI specification bare ordnance gelatine.

The tests compared the performance of bare gelatine blocks with that of basic composite models of a thorax. A simulant human skin and bone composite were included in some of the models to replicate the rib cage within the thorax, as ribs are commonly struck by ballistic projectiles as evidenced from the homicide study. Progressively more skin, bone and lung simulants were added to approximate the average dimensions of a thorax with a lung, as detailed in Chapter 2 'Methods and Materials.'

### **7.2 Experimental Design**

An ADF AUSTEYR model F88 ICW in calibre 5.56x45mmNATO was used for all tests, together with currently issued ASF1 ball ammunition. The bare gelatine and basic anatomical composite models were fixed to a platform positioned 50m from the firing point. High speed video equipment was used to record the results. One round was fired into each of six simulant models. The bare gelatine block (FBI specification) was used as a control. It provided a baseline for the comparison of the results achieved with the progressive addition of simulant materials to basic anatomical models with behind target gelatine witness blocks. Permanent cavity volume measurements are provided for all tests. Temporary cavity volume measurements are only provided for tests 1A, 4, 6 and 7 due to a technical fault with the high speed photographic equipment. Further details regarding this issue and the overall experimental design, are provided in the 'Materials and Methods' section in Chapter 2, pages 91 to 96.

### 7.3 Results

#### 7.3.1 Test 1 (Bare gelatine control block)

The muzzle velocity of the bullet was 877.2m/s. The ASF1 ball bullet fully penetrated the length of the bare gelatine block (305mm). It commenced its passage travelling in a straight line before veering to the left and following a curved path along the same plane until it exited the left rear portion of the block. The bullet was not recovered, but lead fragments from the core were extruded out of the hollow base of the bullet and were found within the largest portion of the permanent cavity. Temporary cavitation resulting from bullet yaw (approximately 20° - point of no recovery) was not visible until the bullet had penetrated 94mm into the block. The largest three dimensional portion of the permanent cavity measured 84mm in width and 78mm in height, over a distance of 146mm. The volume of this permanent cavity was 0.432L.

#### 7.3.2 Test 1A (Repeat - bare gelatine control block)

This test was a repeat of Test 1 to verify the results. The muzzle velocity of bullet was higher than Test 1 at 896.2m/s. Again the ASF1 ball bullet fully penetrated the length of the block. It commenced its passage travelling in a straight line for a short distance before curving upwards and exiting the top of the block at the rear. The bullet was not recovered, but lead fragments from the lead core were extruded out of the hollow base of the bullet and were found within the largest portion of the permanent cavity. The permanent cavity measured 300mm (including the curved path), but temporary cavitation resulting from bullet yaw was not visible until the bullet had penetrated 71mm into the block. The largest three dimensional portion of the permanent cavity measured 74mm in width and 125mm in height over a distance of 223mm. The volume of this permanent cavity was 0.538L. The maximum dimensions of the temporary cavity measured 258mm in length, 254mm in height and 197mm in width. The volume of the temporary cavity was 6.006L.

Figures 23 to 26 show the progression of the ASF1 ball bullet from its stable position in flight, penetrating gelatine and creating the maximum temporary cavity.



**Figure 23. Test 1A. The ASF1 ball bullet (marked A) in flight and about to penetrate the bare gelatine block. In this position the bullet has no significant yaw angle.**

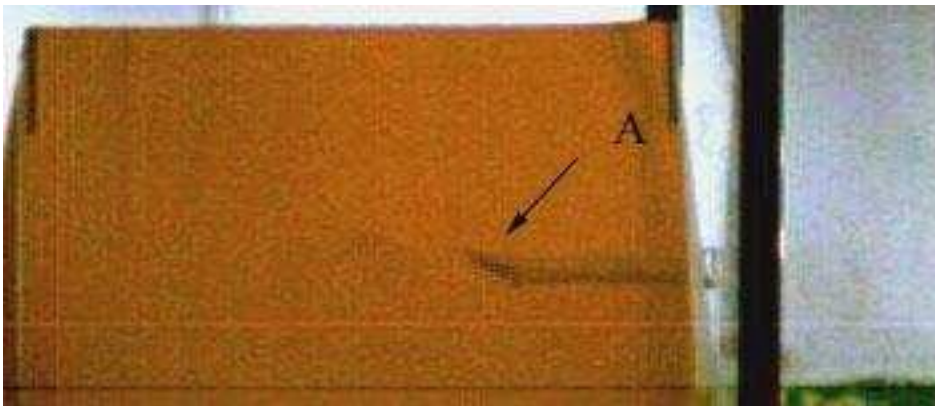


**Figure 24. Test 1A. The ASF1 ball bullet penetrated 70mm into the bare gelatine block. Point A indicates the position at which the bullet has a significant upward yaw angle, indicating loss of stability just prior to the visual commencement of the temporary cavity.**

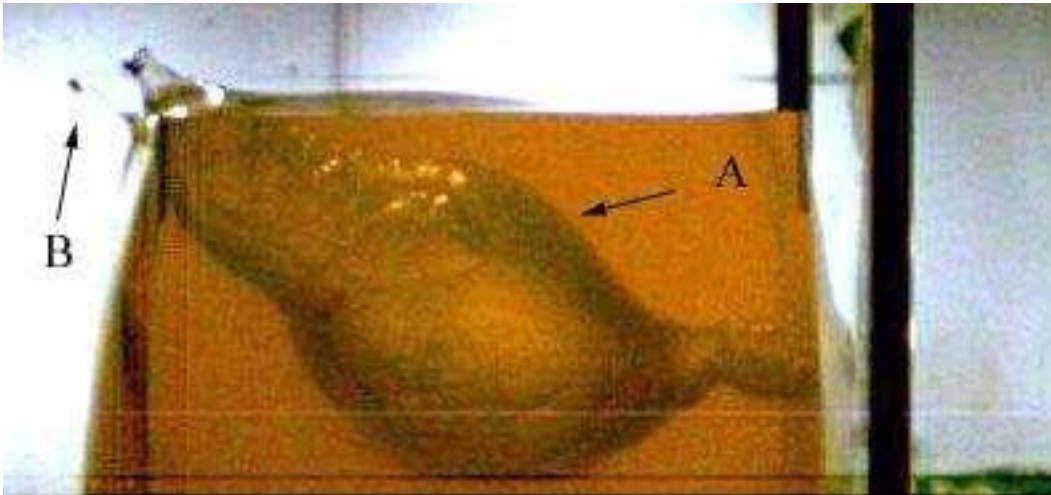


**Figure 25. Test 1A. Point A indicates the temporary cavity forming, including backwards along the shot line. Point B indicates the position of the ASF1 ball bullet having exited the bare gelatine block. Note the high upward departure angle from the block.**



**Figure 26. Test 1A. Point at which maximum temporary cavitation has occurred within the bare gelatine block.**

### 7.3.3 Test 2 (Bare gelatine plate with air gap and gelatine block)

This test involved the use of a 20mm bare gelatine plate, with a 250mm air gap behind it. A bare gelatine block was positioned at the rear of the air gap. The test was designed to simulate a bullet passing through subcutaneous tissue and fat, before traversing an air gap of similar dimensions to an expanded lung filled with air. The muzzle velocity of the bullet was 875.3m/s. The ASF1 ball bullet did not fully penetrate the gelatine block and was recovered from the rear left corner with its afterbody (boat tail and base section) (Figure 1) in a forward position. The copper jacket on the forebody (ogive and meplat section) (Figure 1) of the bullet was damaged and the steel penetrator was visible through this damage. The spent bullet was recovered and marked exhibit 2.1 (Figure 46). The bullet followed a curved path to the left after entering the gelatine block. Lead fragments from the base core were extruded from the exposed bullet base and were scattered within the permanent cavity. The permanent cavity measured 260mm in length, but temporary cavitation commenced 8mm into the block. The largest three dimensional portion of the permanent cavity was 225mm in length, 114mm in width and 76mm in height. The volume of this permanent cavity was 0.776L. The maximum dimensions of the temporary cavity were 251mm in length and 225mm in height. The width could not be measured, and so the volume of the temporary cavity could not be determined.

Figure 27 and 28 shows the progression of the ASF1 ball bullet having passed through the bare gelatine plate before penetrating the bare gelatine block and creating the maximum temporary cavity within it.



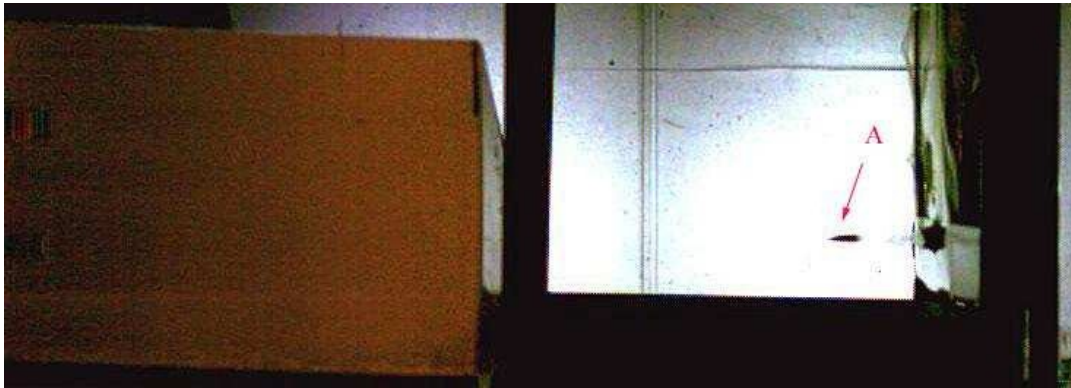


**Figure 27. Test 2. Point A indicates the ASF1 ball bullet having exited the rear of the bare gelatine plate and now in flight within the 250mm air gap. Note that it has no significant yaw angle at this time.**



**Figure 28. Test 2. Point at which maximum temporary cavitation has occurred within the bare gelatine block.**

### **7.3.4 Test 3 (Repeat - bare gelatine plate with air gap and gelatine witness block)**

This was a repeat of test 2 to verify the results. The muzzle velocity of the bullet was similar at 871.1m/s. The ASF1 ball bullet fully penetrated the gelatine block and was not recovered. The bullet followed a curved path to the left and slightly upwards in the block. Lead fragments from the base core were extruded from the exposed bullet base and were largely confined to the permanent cavity. The permanent cavity length

measured 305mm (including the curved path), with temporary cavitation visually commencing later in the block, namely at 50mm. The largest three dimensional portion of the permanent cavity was 88mm in height and 127mm in width over a distance of 192mm. The volume of this permanent cavity was 1.115L. The maximum dimensions of the temporary cavity were 305mm in length and 210mm in height. The width could not be measured, and so the volume of the temporary cavity could not be determined.

#### 7.3.5 **Test 4 (Skin simulant attached to gelatine witness block)**

This test involved the use of a skin simulant attached to the front of a bare ordnance gelatine block. It was designed to determine what effect skin would have on the dynamics of bullet penetration compared to firing through a bare gelatine block. The muzzle velocity of the bullet was 871.6m/s. The ASF1 ball bullet fully penetrated the block and followed a straight path to its exit point. Temporary cavitation visually commenced immediately upon impact, but the bullet did not fragment or extrude lead fragments within the block. However, the exit point at the rear of the block was large measuring 56mm x 26mm, and the bullet was not recovered. The largest three dimensional portion of the permanent cavity was 64mm in height and 119mm in width over the total permanent cavity length of 210mm. The volume of this permanent cavity was 0.712L. The maximum dimensions of the temporary cavity measured 210mm in length, 179mm in height and 191mm in width. The volume of the temporary cavity was 3.317L.

Figure 29 shows the ASF1 ball bullet entry point through the skin simulant that was attached to the anterior surface of the bare gelatine block.

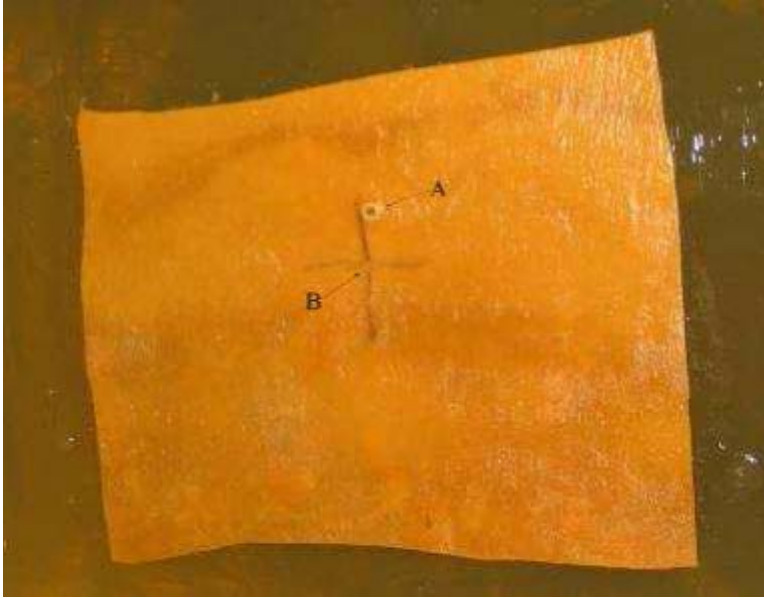


**Figure 29. Test 4. Skin simulant attached to the anterior surface of the bare gelatine block. Point A indicates the ASF1 ball bullet entry hole and Point B the aim point drawn in black.**

### **7.3.6 Test 5 (Gelatine plate with skin and bone composite, air gap and gelatine block)**

This test involved the use of a 23mm gelatine plate with skin simulant attached to the anterior surface and bone composite embedded within. Behind this was a 250mm air gap, followed by a bare ordnance gelatine block.

The test was designed to simulate a bullet passing through skin, subcutaneous tissue, fat and rib material, before traversing an air gap of similar dimensions to an expanded lung filled with air.

The muzzle velocity of the bullet was 871.1m/s. Temporary cavitation commenced immediately after the ASF1 ball bullet had penetrated the skin. Two of the six 'ribbed' areas of the bone composite were shattered and this area of damage measured 54mm x 31mm. The bullet then deviated from its original line of flight and followed an angled trajectory upwards, striking the block 45mm below the superior edge. This shattering and 'ricochet' effect was consistent with that seen in the homicide study (refer Chapter 3). The entry hole into the block was quite large, but the bullet exited the top of the

block after only travelling 175mm (Figure 31). This meant that the true horizontal penetration distance could not be determined, as the bullet exited the block prematurely due to the ricochet effect. However, it can be expected to have been a greater distance than that recorded. The ASF1 ball bullet was not recovered, but small fragments of lead were extruded from the bullets base and were found along the length of the permanent cavity. In addition, small fragments of the bone composite that had acted as secondary projectiles were found within the permanent cavity. This was consistent with the wounding features of shattered bone noted in the homicide study (refer Chapter 3). The maximum three dimensional portion of the permanent cavity measured 175mm in length, 85mm in height and 91mm in width (fissures not included). The volume of this permanent cavity was 0.553L. The maximum dimensions of the temporary cavity were 225mm in length and 212mm in height. The width could not be measured, and so the volume of the temporary cavity could not be determined.

Figures 30 to 33 show the ASF1 ball bullet in flight, the resulting permanent and temporary cavities, and the damage sustained to the bone composite embedded within the gelatine plate.

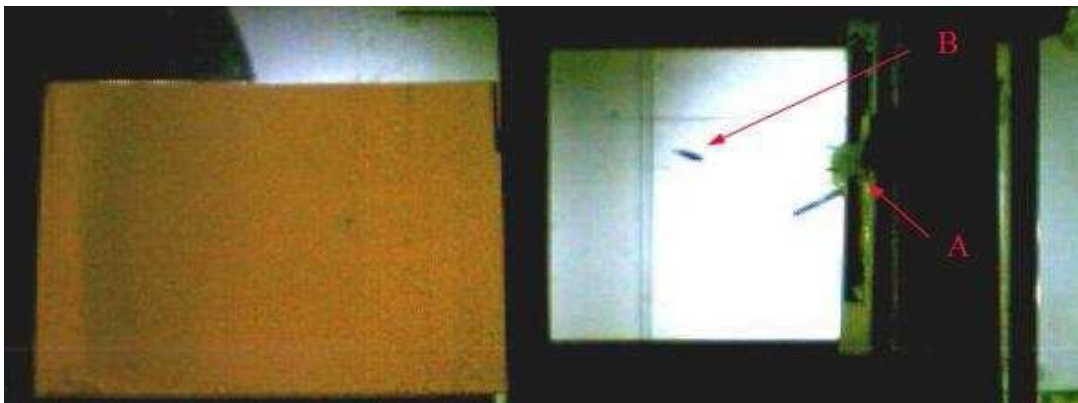


**Figure 30. Test 5. Point A indicates damage to the back of the gelatine plate containing skin simulant and embedded bone composite. Point B indicates the ASF1 ball bullet in flight within the 250mm air gap. Note the angled upward trajectory.**

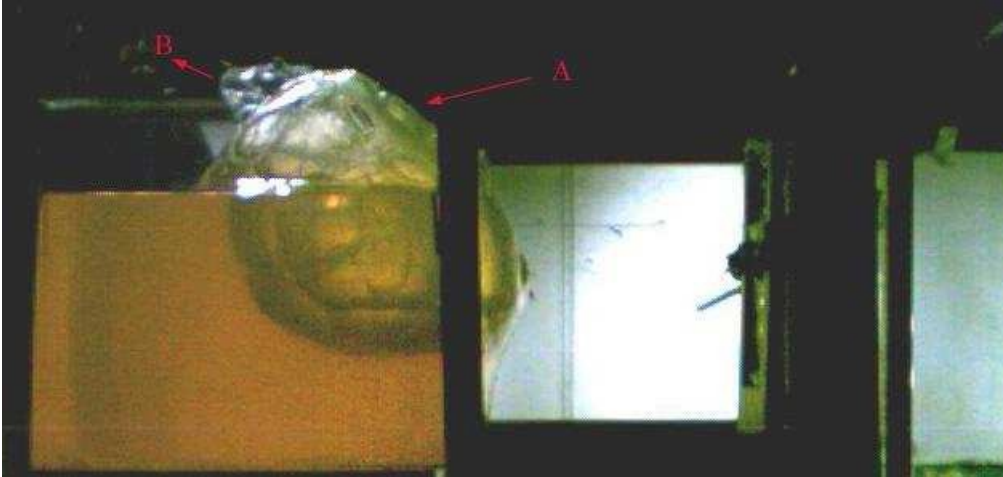


**Figure 31. Test 5. Point A indicates maximum temporary cavitation. Point B indicates the departure angle of the ASF1 ball bullet, still following an upward trajectory.**

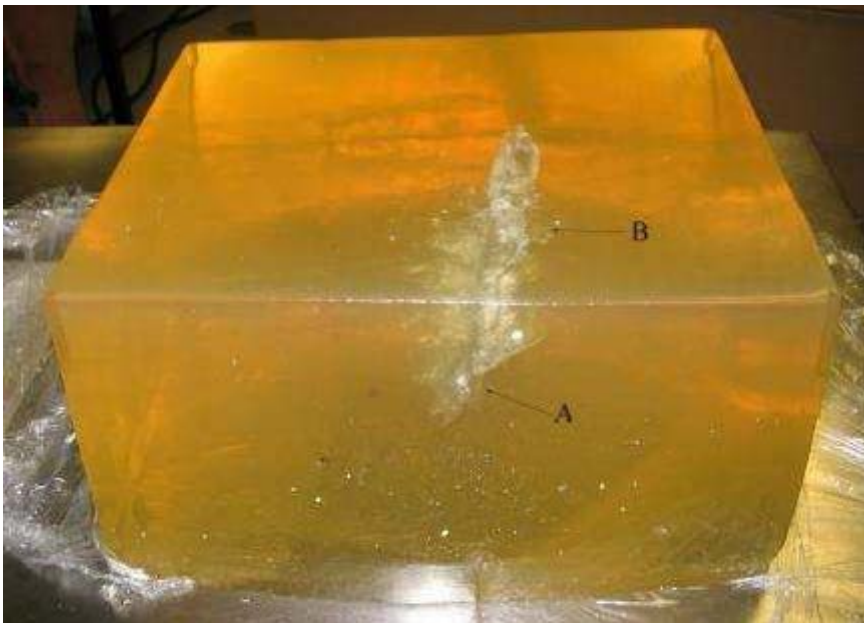


**Figure 32. Test 5. Point A indicates where the ASF1 ball bullet entered the gelatine block and Point B indicates the permanent cavity that was formed. Note: The fissures do not form part of the actual permanent cavity.**



**Figure 33. Test 5. Bone composite that was embedded within the gelatine plate showing a large area of damage.**

#### **7.3.7 Test 6 (Gelatine plate with skin and bone composite, bubble wrap, air gap, bubble wrap and a gelatine block)**

This test involved the use of a 19mm gelatine plate, with skin simulant attached to the anterior surface and bone composite embedded within. Behind this was a thin layer of bubble wrap, followed by a 250mm air gap, another layer of bubble wrap and a bare ordnance gelatine block.

The test was designed to simulate a bullet passing through skin, subcutaneous tissue and fat, rib and the parietal and visceral pleura surrounding the lung, before traversing an air gap of similar dimensions to an expanded lung filled with air.

The muzzle velocity of the bullet was 886.3m/s. Temporary cavitation commenced immediately after the ASF1 ball bullet had penetrated the skin simulant, and the superior 'rib' of the bone composite was shattered leaving an area of damage measuring 27mm x 17mm. Bone composite fragments were propelled away from the gelatine plate but did not enter the block, due to its behind target position. However, these fragments did enter the thorax of the model and the effects were consistent with those seen in the homicide study (refer Chapter 3). The bullet caused a large 13mm oblique angled entry hole in the gelatine block, as it had yawed approximately 30° upwards from its original

flight path, measured in the horizontal plane. In this yawed position, the bullet caused immediate temporary cavitation within the bare gelatine block and followed a curved path to the left and slightly downwards. It came to rest in the left rear corner of the block, with its forebody in a forward position but still angled upwards at approximately 30°. The jacket around the forebody had fractured exposing the steel penetrator. The mid body (bearing surface) and afterbody were also flattened. The spent ASF1 ball bullet was recovered and marked exhibit 6.1 for identification purposes (Figure 47). Small lead core fragments were extruded from the bullet base and were found within the permanent cavity. The damage to the bullet was consistent with the type of flattening and fragmentation damage seen in 5.56x45mm bullets recovered and examined during the homicide study (refer Chapter 3).

The permanent cavity measured 315mm in total length (which included the curved bullet path). However, if measured in a straight line from the anterior surface of the block, the penetration depth was 245mm, with the largest three dimensional portion of the permanent cavity measuring 122mm in height and 88mm in width over a distance of 146mm. The volume of this permanent cavity was 0.742L. The maximum dimensions of the temporary cavity were 273mm in length, 154mm in height and 207mm in width. The volume of the temporary cavity was 3.080L.

Figures 34 to 36 show the progression of the ASF1 ball bullet after it had passed through the gelatine plate and entered the gelatine block, as well as the damage caused by it to the bone composite.

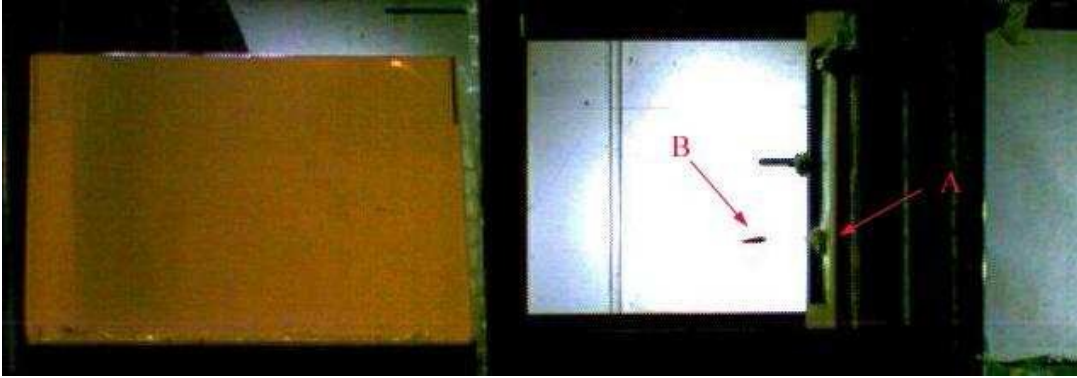


**Figure 34. Test 6. The ASF1 ball bullet in flight after exiting the gelatine plate, which has skin simulant attached to the anterior surface and bone composite embedded within it. Point A indicates the exit hole and Point B indicates the bullet with a slight downward trajectory and yaw angle.**



**Figure 35. Test 6. The maximum temporary cavity is shown. Point A indicates the dynamic nature of this cavitation extending backwards along the shot line into the air gap. Point B indicates the resting position of the ASF1 ball bullet.**





**Figure 36. Test 6. Point A indicates the damage sustained to the bone composite embedded within the gelatine plate.**

**7.3.8 Test 7 (Gelatine plate with skin and bone composite, bubble wrap, air gap, bubble wrap, followed by a second gelatine plate with skin and bone composite, and a gelatine block)**

This test involved the use of a 20mm gelatine plate with skin simulant attached to the anterior surface and bone composite embedded within. Behind this was a thin layer of bubble wrap, followed by a 250mm air gap and another thin layer of bubble wrap. Behind this was another 20mm gelatine plate with embedded bone composite and skin simulant attached to the posterior surface. At the rear of this gelatine plate was a bare ordnance gelatine block.

This test was designed to simulate a bullet passing through skin, subcutaneous tissue and fat, rib bone, anterior parietal and visceral pleura surrounding the lung, before traversing an air gap of similar dimensions to an expanded lung filled with air. The bullet then exited the visceral pleura surrounding the posterior lung and passed through the bone of the posterior ribs, subcutaneous tissues and fat before exiting the posterior skin.

The muzzle velocity of the bullet was 889.2m/s. Temporary cavitation commenced immediately after the ASF1 ball bullet had penetrated the anterior skin simulant. It struck the centre of the bone composite and fractured the third 'rib' leaving an area of damage measuring 16mm x 13mm. A second fracture in the bone composite plate was noted in the top left corner and measured 23mm x 39mm. This was not directly struck by the bullet, but appears to have been caused by temporary cavitation and the transfer of energy by a shock wave within the bone composite, an effect discussed in Chapter 1 and most recently examined in a detailed study by Kieser et al. (248).

After travelling through the bubble wrap and air gap, the bullet struck the posterior bone composite plate and almost shattered it completely. It then exited the posterior skin simulant leaving a very large and irregular shaped exit hole, which measured 44mm x 51mm at its widest point. The bullet deviated slightly to the right and entered the gelatine block sideways at an oblique angle (maximum yaw), creating a large entry hole measuring 24mm in length. This resulted in immediate temporary cavitation within the gelatine block, with the bullet following an upward path slightly to the right. It penetrated 180mm into the gelatine block before coming to rest with its forebody in a forward position, but pointed upwards at an angle of approximately 45° measured from the horizontal plane. The jacket around the forebody had fractured, exposing the steel penetrator. The mid body and afterbody were also flattened. The spent ASF1 Ball bullet was recovered and marked exhibit 7.1 for identification purposes (Figure 48). A small quantity of lead core fragments were extruded from the base of the bullet and deposited within the permanent cavity. The damage to the bullet was consistent with that seen in bullets recovered and examined during the homicide study (refer Chapter 3). The largest three dimensional portion of the permanent cavity measured 113mm in height and 73mm in width over a distance of 139mm. The volume of this permanent cavity was 0.473L. The maximum dimensions of the temporary cavity were 189mm in length, 185mm in height and 175mm in width. The volume of the temporary cavity was 3.055L.

Figures 37 to 44 show the progression of the ASF1 ball bullet as it exited the anterior gelatine plate and passed through the air gap, before negotiating the posterior gelatine plate and entering the gelatine block. Some of the figures show the damage caused to the bone composite and skin simulant.

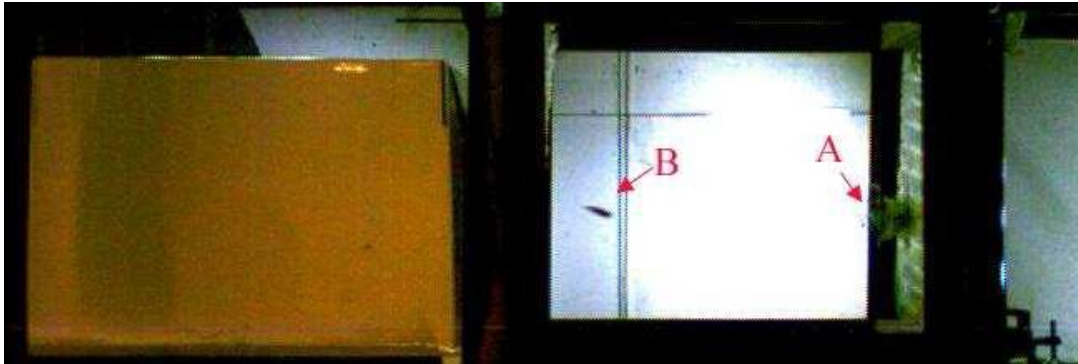


**Figure 37. Test 7. The ASF1 ball bullet in flight within the air gap having exited the anterior gelatine plate, which has skin simulant attached to the anterior surface and bone composite embedded within it.**

**Point A - exit point through the gelatine plate**

**Point B - ASF1 ball bullet at a high yaw angle just prior to entering the posterior gelatine plate.**

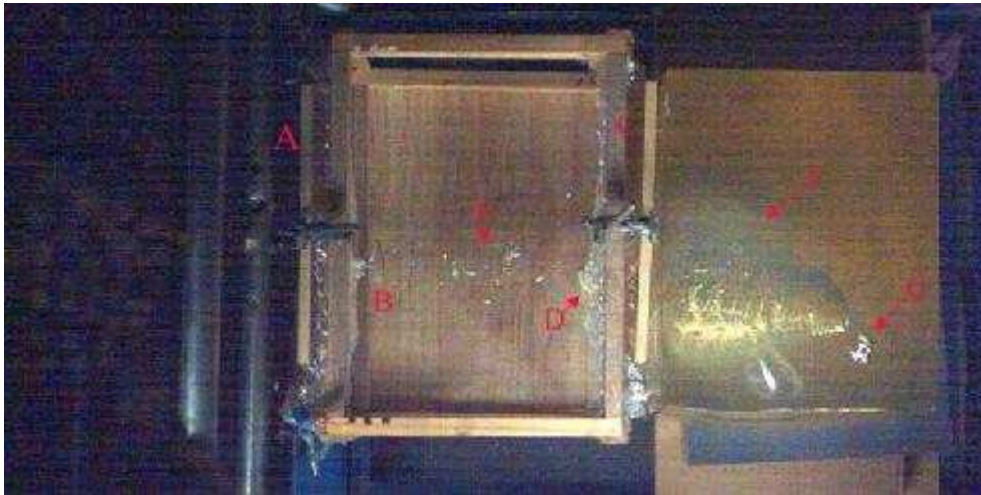


**Figure 38. Test 7. An overhead view of the immediate temporary cavitation which occurred in the gelatine block.**

**Point A – anterior gelatine plate.**

**Point B – exit point of the ASF1 Ball through the anterior gelatine plate.**

**Point C – posterior gelatine plate.**

**Point D – entry point of the ASF1 Ball into the posterior gelatine plate.**

**Point E – bone composite material forced rearward into the air gap.**

**Point F – temporary cavitation commences immediately within the gelatine block.**

**Point G – position where the spent ASF1 ball bullet has come to rest within the gelatine block.**

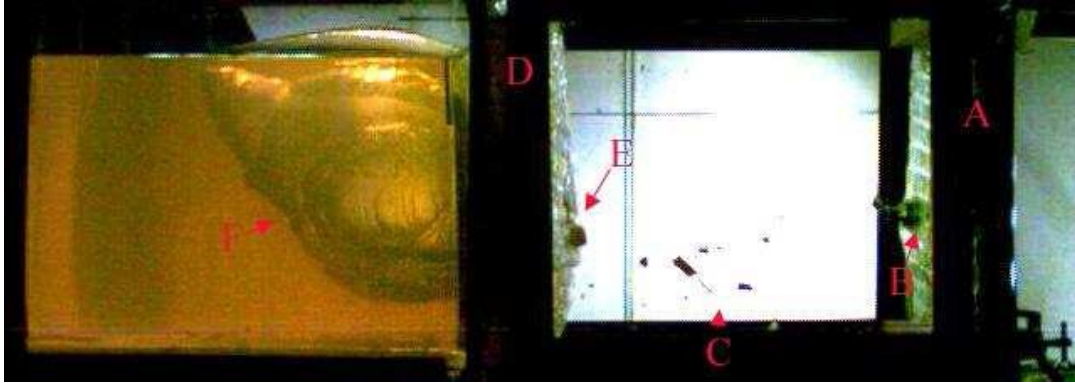


**Figure 39. Test 7. A side view of the dynamic nature of the damage caused by the ASF1 ball bullet.**

**Point A – anterior gelatine plate.**

**Point B – exit point through anterior gelatine plate.**

**Point C – bone composite from posterior gelatine plate forced into the air gap.**

**Point D – posterior gelatine plate.**

**Point E – entry point in posterior gelatine plate.**

**Point F – maximum temporary cavitation within the gelatine block.**

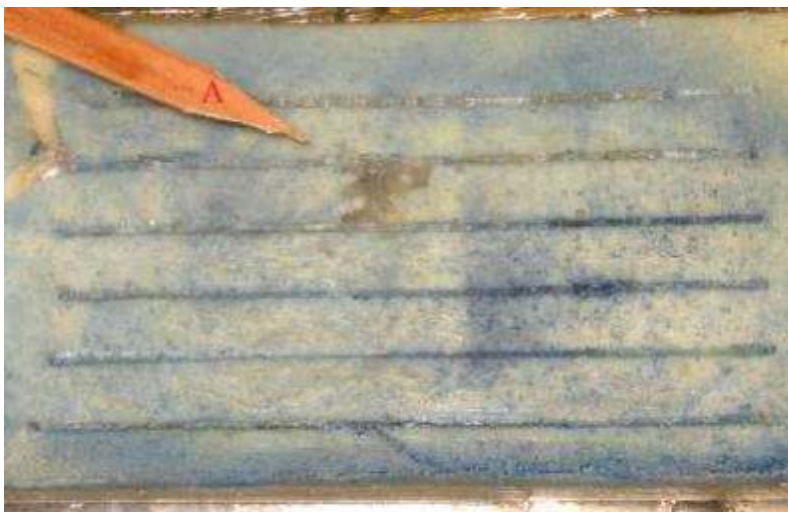


**Figure 40. Test 7. Point A indicates the entry point of the ASF1 ball bullet through the bone composite embedded within the anterior gelatine plate.**



**Figure 41. Test 7. Point A indicates the exit point of the ASF1 ball bullet through the bone composite which was embedded within the anterior gelatine plate. Point B indicates the remote damage caused to the bone composite through the transfer of energy from the shock wave associated with temporary cavitation.**



**Figure 42. Test 7. The extensive damage caused by the ASF1 ball bullet to the bone composite embedded within the posterior gelatine plate.**



**Figure 43. Test 7. The extensive damage caused by the ASF1 ball bullet at maximum yaw as it exited the skin simulant attached to the back of the posterior gelatine plate.**

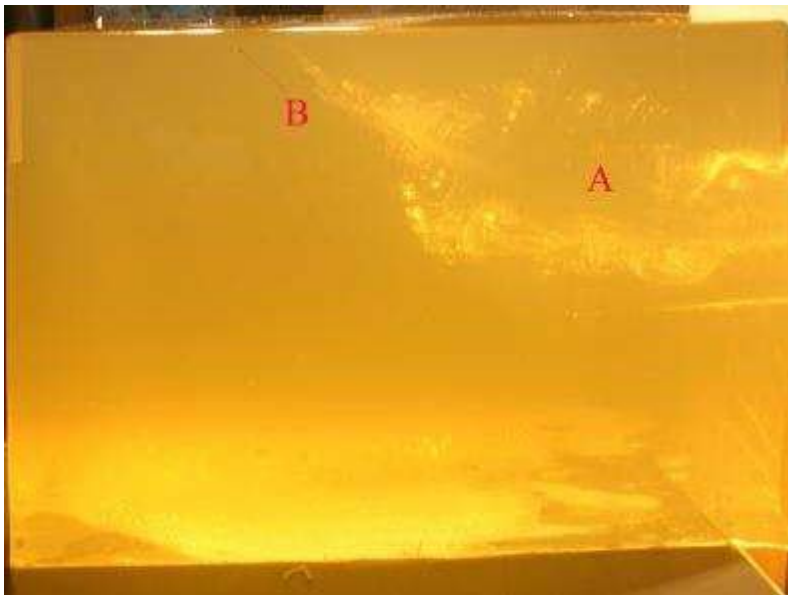


**Figure 44. Test 7. Point A indicates the permanent cavity. Point B indicates the upward trajectory of the ASF1 ball bullet through the gelatine block.**

Figures 45 to 48 show an un-fired ASF1 ball bullet, for comparison purposes, and the damage sustained to the three ASF1 ball bullets recovered from Tests 2, 6 and 7 respectively.

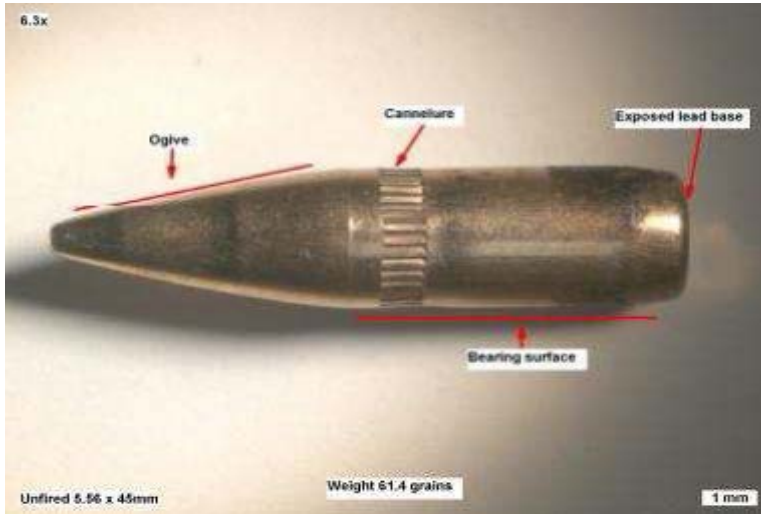


**Figure 45. Unfired ASF1 ball bullet with its features described.**



**Figure 46. Test 2. Recovered ASF1 ball bullet. The bullet is deformed and the jacket around the forebody has torn to reveal the steel penetrator. Lead from the internal base core has been extruded from the base of the bullet and was found within the permanent cavity. Total retained bullet weight = 87% of the original weight.**





**Figure 47. Test 6. Recovered ASF1 ball bullet. The bullet is deformed and the jacket material around the forebody has torn to reveal the steel penetrator. Lead from the internal base core has been extruded from the base of the bullet and was found within the permanent cavity. Total retained bullet weight = 85% of the original weight.**

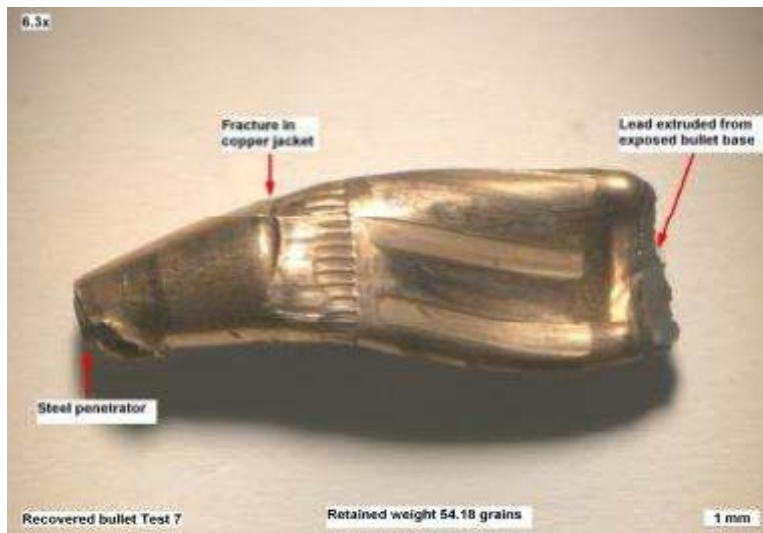


**Figure 48. Test 7. Recovered ASF1 ball bullet. The bullet is deformed and the jacket material around the forebody has torn to reveal the steel penetrator. Lead from the internal base core has been extruded from the base of the bullet and was found within the permanent cavity. The forebody jacket has also fractured near the cannelure. Total retained bullet weight = 87% of the original weight.**

Figures 49 to 52 provide a direct comparison of temporary cavitation commencement, bullet penetration depth and the volumes of the maximum permanent and temporary cavities created in each test.

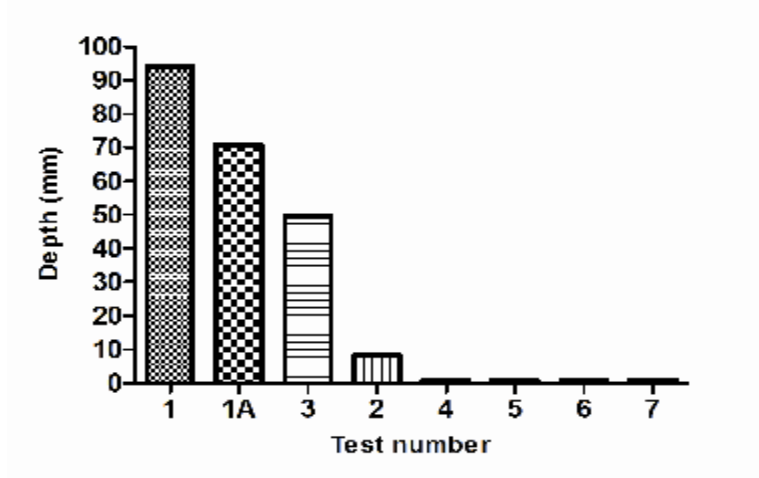


Figure 49. Temporary cavitation commencement depths for each anatomical stimulant model compared to the two gelatine control blocks (Numbers 1 and 1A).

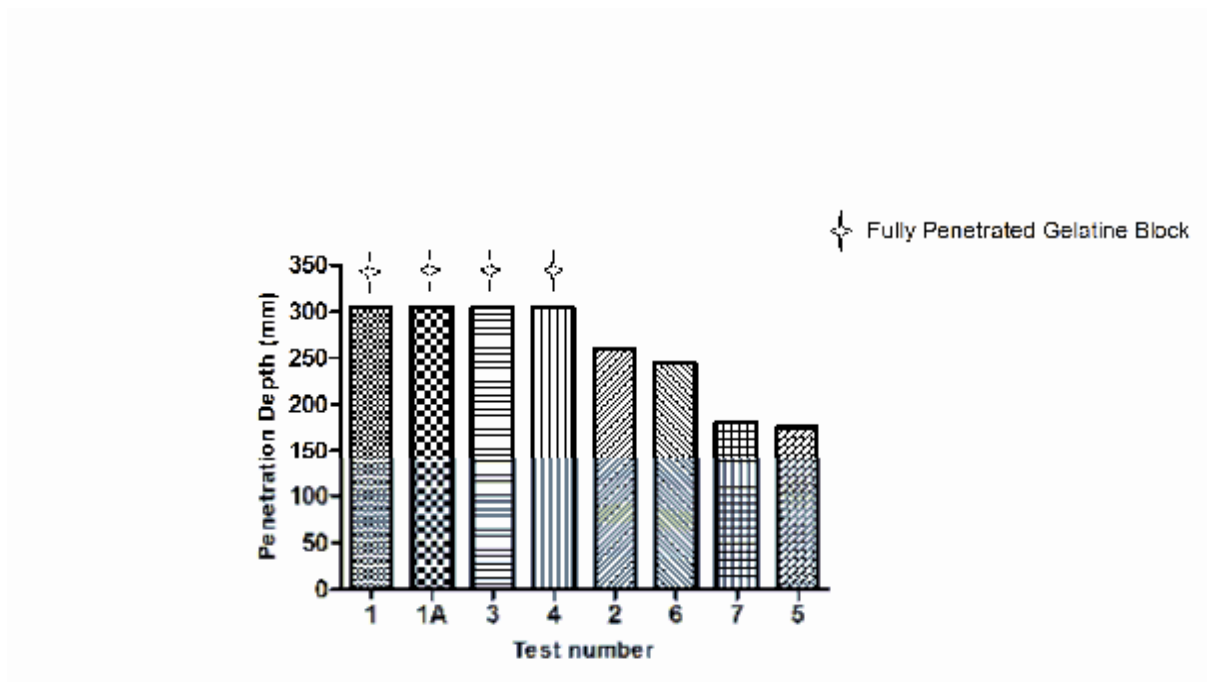
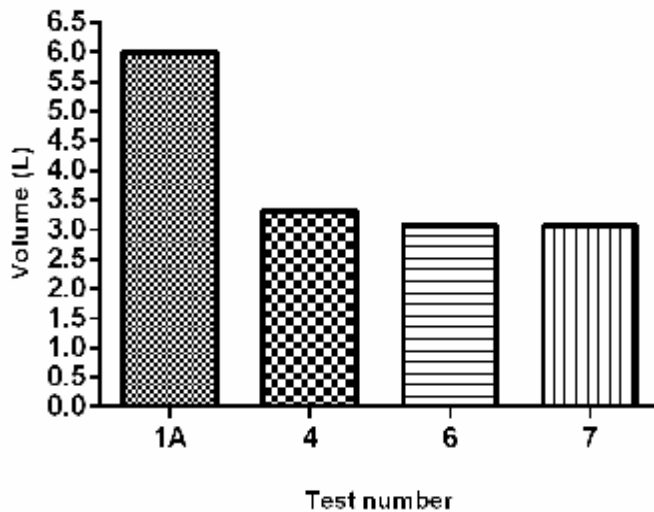


Figure 50. Bullet penetration depths for each of the anatomical stimulant models compared to the two gelatine control blocks (Numbers 1 and 1A). Note: The result for Test 5 is less than expected for reasons explained in Section 7.3.6.



**Figure 51. Comparison of the volume of the temporary cavity, for those anatomical model tests where the volume could be determined, compared to gelatine control block 1A.**

#### 7.4 Discussion

The experimental tests in this chapter have attempted to address the question of how representative the results obtained from ballistic firings into FBI bare ordnance gelatine are when compared to a more representative model of a heterogeneous human thorax. This was achieved by the progressive addition of simulant materials. It is acknowledged that even the most detailed model used in Test 7 is not a complete representation of a human thorax. However, this is a pilot study and the materials used as well as the test rig dimensions, have been validated in various ways as detailed in Chapter 2. In addition, many of the damage patterns to the models and spent bullets were directly comparable to those seen in the homicide study in Chapter 3. This provides additional confidence in the results.

Figure 49 demonstrates that an ASF1 ball bullet fired into a bare ordnance gelatine block does not visually commence temporary cavitation until a substantial distance has been covered, namely 94mm for Test 1 and 74mm for Test 1A. However, by simply adding a gelatine plate to simulate subcutaneous tissue and fat followed by an air gap, cavitation commenced much sooner, namely 8 mm for Test 2 and 50 mm for Test 3.

The progressive addition of other simulant materials in Tests 4 to 7 caused temporary cavitation to commence immediately upon bullet impact because the bullets had yawed significantly, presenting a much greater frontal area and resistance to the media.

Figure 50 shows a comparison of bullet penetration depths for each of the tests. Maximum penetration depth values were not greatly affected until the introduction of additional simulant materials such as the bone composite. When this occurred, the penetration depths drop markedly, particularly for Tests 5 to 7. The drop in penetration depth, in most instances, corresponds to the immediate onset of temporary cavitation.

In this study, temporary cavitation volumes were determined to be a more appropriate measure of energy dissipation than the permanent cavity volumes. This is because Tests 1, 1A, 3 and 4 over penetrated the gelatine witness blocks and the bullet prematurely exited the block in Test 5.

Figure 51 shows temporary cavity volumes for the limited number of tests where results were available (Tests 1A, 4, 6 and 7). A linear decline in volumes occurs as additional simulants were added to the models. The residual volume (L) in the gelatine witness block for Test 4 was 55% of that recorded for control Test 1A, which means that the other 45% was expended within the anatomical model. Similarly the residual volume for Test 6 was 51% of that recorded for control Test 1A (49% expended within the model), and 50% for Test 7 (50% expended within the model). When compared holistically, the temporary cavity volume results together with the penetration depth results are a reflection of the fact that there is less residual kinetic energy and momentum available to do 'disruptive' work as the bullet negotiates a greater number of barriers in the form of the simulant materials. In addition, the onset of immediate temporary cavitation is a direct result of increased bullet yaw, which will have a significant retardation effect upon the velocity of the bullet. Therefore, the overall wounding potential can generally be expected to be less, but will occur immediately rather than deeper as indicated with the bare gelatine blocks. This could substantially alter the incapacitation or lethality potential of the 'wounds'.

It must be recognised that if a bullet strikes a major organ during its path, the resulting damage could still be fatal, regardless of the amount of kinetic energy or momentum delivered. An example of this is a fatal wound caused by a small calibre bullet such as 22 Rimfire. This reinforces the fact that bullet placement is still the single most important factor which determines incapacitation or lethality potential (21, 44, 45).

To understand why the ASF1 ball bullet behaves so differently when encountering additional simulants, we must examine the exterior ballistics performance of this type of bullet.

A Spitzer shaped bullet such as the ASF1 ball always exhibits some degree of yaw (non-zero yaw) throughout its entire flight range (see Chapter 1 for further details). There are a variety of aerodynamic forces acting upon the bullet during flight, the primary ones being gravity and air resistance. However, there are other forces too which act to a lesser degree, but are nevertheless important and warrant further discussion with respect to the onset of temporary cavitation.

Modern bullets are designed to be spin stabilized during flight by rotating on their longitudinal axis, which passes through their centre of mass. The helical rifling within a barrel provides this spin stabilisation. However, bullets and barrels commonly have slight manufacturing imperfections which cause the bullet to leave the barrel with some degree of instability (wobble) called ballistic yaw. The angle between the bullets direction of travel and the degree of yaw is known as the 'yaw of repose' or 'yaw angle'. After a bullet leaves the barrel it rotates (spins) either in a left or right direction, depending on whether the barrel has a left or right hand twist (angle and pitch of the rifling). This rotation occurs around the centre of mass, but aerodynamic forces also act upon the bullets centre of gravity and centre of pressure (Figure 1). If the bullet has no 'yaw of repose' then both the centre of mass and the centre of pressure are perfectly aligned. However, when the centre of mass and centre of pressure are not perfectly aligned, the bullet will yaw slightly because of pressure differences around the bullet. This is known as the 'Magnus effect' and causes the tip of the bullet to angle slightly away from the direction of travel and drift (deviate), even when no wind is present. The

direction of the drift is consistent with the direction of spin and is also commonly referred to as 'spin drift'. Therefore, a bullet such as the ASF1 ball with a right twist will drift off to the right and a bullet with a left hand twist will drift off to the left. The destabilising force created by the 'Magnus effect' can cause a bullet to tumble if the centre of pressure is located far enough in front of the centre of mass. However, if the centre of pressure is located behind the centre of mass, it can help to stabilise the bullet. The deflection caused by the 'Magnus effect' becomes more apparent as the range from the muzzle of the rifle or handgun increases (249, 250). In this series of tests, the bullet was fired from a distance of 50m in an indoor range and so wind was not a factor.

Due to the aerodynamic forces and characteristics described, bullets like the ASF1 ball are already predisposed to increased yaw in aqueous media. This is because they exhibit non-zero yaw and are not completely stable. Their frontal area may have increased because they are not flying completely straight and true. Therefore when striking gelatine, which has a higher density (ca 1,000 fold) compared to air, the bullet will be subjected to even greater yaw and drag, resulting in larger permanent and temporary cavitation (1). This translates into greater tissue damage earlier within both the permanent and temporary cavities. This effect was magnified in the anatomical model tests when the bullet encountered skin, lung and bone simulant because the bullet yawed significantly and deformed, as was best seen in Tests 6 and 7. Yawing causes the bullet to present a larger cross-sectional area, which increases drag and the dissipation of the bullets kinetic energy. This often results in the bullet expending its energy fully within the medium and remaining within it (16, 27, 45, 53, 251, 252). Tests 6 and 7 demonstrated this. The effects described here are similar to a spring board diver entering a pool of water. If the diver enters the water head first and cleanly there will be a negligible splash or disruption to the water. However, if the diver enters the water with their body in a slightly angled position, a significant splash and disruption of the water will occur.

Figure 43 (Test 7) was of particular interest with respect to the bullet's exit point through the posterior skin simulant. The exit hole was very large as a result of the bullet losing all stability and yawing at 90° just prior to the point of exit. It produced a keyhole type

pattern into the gelatine block. In this orientation the bullet can be expected to cause significant tissue damage, provided the majority of its energy has not been consumed during the passage through the anterior and posterior gelatine plates. A large exit wound of this kind is common for military style high velocity bullets that have lost gyroscopic stability in tissue (32, 75).

At this stage it is too early to make any definitive comment on the wounding potential of the ASF1 ball round with respect to a human thorax without an advanced anatomical model being developed. Ideally such a model would include materials like Simulant 'A' (refer Chapter 5) and others that are yet to be developed. This type of model, combined with an appropriate injury scoring system, should allow for more definitive analyses to be made. However, the models used in this study showed a number of wounding features that were directly comparable to the homicide study. Among them were the damage correlations for the bullets of calibre 5.56x45mm (Figures 46, 47, 48), the shape and size of the entry hole in the skin simulant (Figure 29), the splintering effect on the bone simulant and projection of these splinters and other bone fragments further into the thorax (Test 5, 6), as well as bullet ricochet within the thorax following impact with the bone simulant (Test 5). These effects can be expected to cause additional wounding. Also, the key hole exit wound seen in the skin simulant (Test 7) (Figure 43) was consistent with published literature (2, 56), as was the remote damage to the bone simulant (Test 7) resulting from temporary cavitation and shock wave effects (248).

## 7.5 Conclusion

This study demonstrates that by combining skin, bone and other simulant materials with ordnance gelatine, the behaviour of the ASF1 ball bullet changes compared to that in bare ordnance gelatine. Most significantly, temporary cavitation will occur almost immediately as the bullet yaws and presents a larger frontal area. The corresponding loss of velocity and momentum resulting from negotiating a greater number of simulant barriers, combined with the increased resistance from bullet yaw, will reduce the total penetration depth that is achieved. While this can be expected to cause tissue injury sooner, the severity of that injury is very much dependent upon what organs and tissues are affected. Those deep within the body may not be affected to a significant degree,

particularly by the permanent wound cavity. The effects of the temporary wound cavity are much less predictable as discussed in Chapter 1. In addition, bullet impact with bone can often result in ricochet of the bullet into another area of the body, and splintered bone and other fragments are likely to cause secondary injuries. All of these factors will impact significantly upon injury severity in realistic tactical scenarios.

The anatomical models created for these experiments are limited by their basic construction and small number of experimental results. Nevertheless, they clearly demonstrate the benefit of using simulants that are more representative of the heterogeneous nature of human organs and tissues, because many of the wounding features were comparable to the homicide study. An advanced anatomical model of the thorax and abdomen using the data obtained in Chapter 5 to create additional temperature stable simulants, would provide the platform to perform a number of test firings using different engagement scenarios into various quadrants of the torso to determine the resulting wound trauma. This combined with a suitable injury scoring system such as AIS 2005/2008 and MAXAIS, would enable critical analyses of the severity of the trauma and survivability outcomes. While incapacitation potential is the optimum measure, at this point it would appear that lethality is still the easiest measure to assess, even with the proposed model and scoring system.

This study combined with those in Chapters 3 and 5, and the analyses of injury scoring systems in Chapter 1, support the hypothesis that an anatomical model would be a more reliable and accurate method of evaluating the lethality potential of ammunition in a weapons system than FBI specification bare ordnance gelatine alone.



**8. CONCLUSIONS**

## 8. **Conclusions**

### 8.1 **An Analysis of the Characteristics of Thoracic and Abdominal Injuries and Ballistic Data in Gunshot Homicides in Israel**

This study provided the foundation for establishing which critical organs/tissues most often sustain bullet wound trauma in the torso, namely the heart, lungs, liver, aorta, spleen and kidneys in decreasing order of incidence. In addition, ribs were struck by most bullets that entered the thorax. It also identified the specific characteristics of injuries caused by military and commercial FMJ ammunition fired from semi-automatic pistols in calibre 9mm Luger and assault rifles in calibres 5.56x45mm and 7.62x39mm Soviet. Although much of the data are specific to cases that were autopsied in Tel Aviv, Israel, generalisations can be made allowing extrapolation of the results to assist in comparing and developing simulants of the critical organs/tissues and rib. Once this is achieved, complex models may evolve where a range of different simulant materials are used to more accurately simulate the human torso. Such models can be used to further study and evaluate the mechanisms and effects of ballistic injuries for a wide range of purposes, including ammunition development and advanced ballistic protection.

### 8.2 **Unpredictable Tensile Strength Biomechanics May Limit Thawed Cadaver Use in Wound Ballistics Research**

Human cadavers have traditionally been a source of bio-mechanical data for the study of soft tissue/organ injuries. One of the most important properties is tensile strength, and this data would appear useful for the development of simulant materials. Ideally, fresh un-embalmed average age cadavers should be used, but they are not available in many countries. The alternative is stored cadavers which have often been frozen and thawed a number of times. This study has shown that freezing and thawing cadaveric organs/tissues may alter the physical properties in ways that are not predictable, with both increases and decreases in tensile strength. Therefore, data of this nature may not be reliable for the development of simulants designed to analyse ballistic effects on normal human tissues.

### 8.3 Porcine Organ Energy Loss Comparison Experiments Using BB Rifle Pellets

This study used fresh porcine organs/tissues that were identified as 'critical' for modelling purposes, based on the homicide data. The primary aims were to establish which of these were similar to each other at both room temperature and 37°C (human body temperature), as well as to determine if the FBI/NATO gelatine formulations and Simulant 'A' are suitable simulants to model specific organs and tissues. It provides a method to measure and compare their mechanical response to low velocity projectile impact using BB air rifle pellet energy loss figures.

The most significant conclusions were that heart and lung, hindquarter muscle and kidney, and hindquarter muscle and spleen are comparable paired organs/tissues. FBI 10% gelatine at 4°C is a suitable simulant for both heart and lung, NATO 20% gelatine at 10°C is a suitable simulant for spleen, and Simulant 'A' is a suitable simulant for both hindquarter muscle and kidney. A separate simulant would be required for liver, fat and aorta as they cannot be grouped together with any of the other organs or tissues tested at the respective temperatures.

Bare hindquarter muscle was shown to be statistically different ( $p < 0.001$ ) to FBI 10% gelatine at 4°C. This appears different to the data published by Facker and Malinowski (29) who indicate that it was comparable. However, Fackler and Malinowski conducted their tests using porcine hindquarter muscle with the skin attached. As discussed in Chapter 5, the difference in results can most likely be attributed to a greater amount of energy being required to perforate the combination of pig skin, subcutaneous tissue and fat.

This study has identified the limitations of both standard ordnance gelatine formulations with respect to what they are anatomically comparable to. It has also indicated a promising alternative option in Simulant 'A' because it is temperature stable and much easier to work with. These energy loss results provide the basis for manufacturing additional temperature stable simulants to cover the range of 'critical organs' required. One option is to vary the ratio of synthetic materials used in the manufacture of Simulant 'A' as appropriate.

#### **8.4 Ballistics Ordnance Gelatine – How Different Concentrations, Temperatures and Curing Times Affect Calibration Results**

This study showed how different concentrations, including Bloom strength, as well as temperature and curing times, might affect BB pellet calibration results (penetration depth) in FBI and NATO specification ballistics ordnance gelatine.

It was determined that temperature and curing times may have a direct effect on projectile penetration. However, using different water types during the manufacturing process had no significant effect on projectile penetration.

Neither the NATO formulation, nor a 20% concentration of 285 Bloom gelatine at 10°C, met the same calibration standard as the FBI formulation. However, the Chapter 5 study showed that the NATO formulation is comparable to porcine spleen at both room temperature and 37°C. As there is currently no calibration standard mentioned in the literature for the NATO formulation, a separate standard is required. The porcine spleen energy loss values could be used to create one.

The penetration depths achieved for 10% concentrations of 250 Bloom at both 3° and 4°C were closest to the recommended calibration standard after 3 weeks of curing time, but increasing curing time beyond the accepted 3 to 4 day period is not recommended by Cronin and Falzon (247). A 20% concentration of 285 Bloom at 20°C met the same calibration standard as the FBI formulation after 100 hours of curing, and can be classed as comparable.

The limitations of using ballistics ordnance gelatine were also highlighted. Significant variability in calibration results occurred when temperature and curing times were altered. Therefore, if the manufacture of this homogeneous simulant is not carefully controlled and precisely standardized, interpretation and comparison of ballistics results may not be possible.

#### **8.5 Anatomical Model Pilot Study**

The anatomical models created for this pilot study are limited by their basic construction and the small number of experimental results. However, they clearly demonstrate the benefit of using simulants that are more representative of the heterogeneous nature of human organs and tissues, because many of the wounding features were comparable

to the homicide study. By combining skin, bone and other simulant materials with FBI formulation ordnance gelatine, the behaviour of the ASF 1 ball bullet was shown to change significantly regarding the onset of temporary cavitation, total penetration depth and the degree of bullet yaw compared to bare ordnance gelatine. These factors impact significantly upon injury severity simulations and their interpretation to real tactical scenarios.

The porcine organ energy loss study can be used to manufacture additional temperature stable simulants to cover the range of 'critical organs' required for an advanced anatomical model of the thorax and abdomen. This platform would allow for a number of test firings to be conducted using different engagement scenarios. The resulting 'wound trauma' damage correlations could be examined for each quadrant of the torso, and the data from the homicide study can be used for additional validation purposes.

A suitable medical injury scoring system is required to be used in combination with each anatomical model wounding scenario. AIS 2005/2008 combined with MAXAIS has been identified as the simplest and best options for gunshot injuries, as discussed in Chapter 1, Section 1.8.12. This would enable critical analyses of the severity of the trauma sustained and determine survivability outcomes for each scenario.

Incapacitation is regarded as a superior measure to lethality, as discussed in Chapter 1, Section 1.8.3. However, it is very difficult to assess. At this point, lethality remains the easiest measure to use, even with the proposed model and scoring system.

If an advanced anatomical model is created, a finite element analysis (FEA) computer model could be developed based on the results of each engagement scenario chosen. FEA models offer many advantages for ballistics researchers including cost, practicality and functionality benefits.

## **8.6 Thesis Hypothesis Conclusion**

The thesis commenced with the hypothesis that an anatomical simulant model that replicates the heterogeneous nature of relevant human organs and tissues, will provide a more reliable and accurate method to evaluate the effects of ammunition than FBI or NATO specification bare ordnance gelatine. The experimental studies provide the

framework for the development of a heterogeneous model for bullet trauma simulations of the thorax and abdomen. This model would be more representative of actual wound trauma than bare ordnance gelatine alone. This conclusion was arrived at by identifying the most critical organs/tissues for modelling purposes (heart, lungs, liver, aorta, spleen and kidneys). Their energy loss values (J/m) were established and the method adopted allows for comparable temperature stable simulants to be developed.

Frozen and thawed cadaveric tissue was shown to produce unpredictable tensile strength data and is therefore unsuitable for simulant development. The limitations of using FBI and NATO specification ordnance gelatine was highlighted when changes to Bloom number, temperature and curing times altered calibration results.

The anatomical model pilot tests clearly demonstrated that the addition of simulant materials directly affects wound severity simulations compared with bare ordnance gelatine alone. This in turn affects interpretation to real life situations. Therefore, the original hypothesis has been validated.

This type of model could potentially have a number of applications. From a military and law enforcement perspective it could assist in the development of better performing ammunition and personal protective equipment. From a medical perspective it could assist not only battlefield surgeons, but also civilian medical personnel to better assess bullet wound injuries for triage, treatment and training purposes.

## **8.7 Future Directions**

The following work is planned to progress the development of two dimensional and three dimensional anatomical models to evaluate bullet wound trauma.

### **8.7.1 Anthropometric Data**

Establishing the average size of a male thorax and abdominal cavity from existing anthropometric data, as well as the average size of and dimensional relationship between the major organs and tissues within the thorax and abdomen, is required. It is proposed that 100 Computed Tomography (CT) scans of healthy males between the ages of 20 and 40 years will be obtained from a suitable hospital and an appropriate computer program used to measure the relevant organs. Those data will help address

human variation and provide the dimensional characteristics required to build an anatomically correct model.

### **8.7.2 High Velocity and Energy Retardation Tests**

Chapter 5 provided data relevant to low velocity/energy projectile impact. At this point it is unknown if the tissue grouping results from Chapter 5 will remain the same when a high velocity projectile is used. To establish this, it is proposed that the same tests are repeated using a non-deforming high velocity projectile. Enquiries with DSTO personnel indicate that steel ball bearings of calibre 5.56mm fired from a suitable gas operated firing system is an option. The aim is to achieve velocities similar to those of the ADF AUSTEYR model F88 ICW firing ASF1 ball ammunition. The average velocity achieved by this weapon system during the Chapter 7 tests was 880m/s. Subject to approval, these additional tests would be conducted at the DSTO indoor ballistic firing range.

Depending on the results of the above experiments, the next step would be to trial ASF1 ball ammunition, followed by a range of commercially manufactured handgun and rifle rounds. The aim would be to ascertain if different projectile geometry has an effect on tissue grouping results.

### **8.7.3 Develop Candidate Simulants**

To develop suitable temperature stable synthetic simulants for the 'critical' organs, candidate materials would be assessed using the same methodology employed in Chapter 5 and compared against the energy loss data already collected. It is proposed that the ratio of synthetic materials used to formulate Simulant 'A' is varied to meet the requirements of each of the organs.

If the tissue grouping results for the high velocity/energy retardation tests prove different, then this will need to be addressed at that time.

Once the average size of the critical organs has been established as described earlier, suitable moulds of each organ will need to be manufactured for a three dimensional model. A two dimensional model may only require 'organ plates' that are representative of a particular quadrant of the thorax or abdomen.

#### **8.7.4 Model Validation**

The wound trauma and forensic ballistics data outlined in Chapter 3 can be used as a further validation tool to compare the results achieved from test firings on the proposed anatomical model, against this real world shooting data. However, the test firings must replicate the type of firearm and ammunition combination used, anatomical site that was struck, as well as the relevant distance and angle involved. In addition, consultation with an appropriate pathologist will be required to establish the physiological results of each wound simulation under consideration.

#### **8.7.5 Scoring System**

As previously mentioned, a suitable medical injury scoring system will be required to grade the lethality potential of bullet trauma to particular regions of the simulated thorax and abdomen. Due to their international acceptance, the AIS 2005/2008 and MAXAIS scoring systems detailed in Chapter 1 are deemed appropriate.

#### **8.7.6 Finite Element Analysis Model**

A FEA model based on the results of each advanced anatomical model engagement scenario is the ultimate aim of this research, because of the potential benefits it offers.



## REFERENCES

1. Crucq JWB. Stochastic computer modeling of wound ballistics. Middelburg: Drukkerij Meulenberg; 1991.
2. Di Maio VJM. Gunshot Wounds, Practical Aspects of Firearms, Ballistics and Forensic Techniques. Florida: CRC Press; 1999.
3. Bussard ME, Wormley SL. NRA Firearms Sourcebook. Fairfax, VA: National Rifle Association of America; 2006.
4. Association of Firearm and Toolmark Examiners. Glossary [Internet]. 2004 [cited 2009 Aug 5]. Available from: <http://www.afte.org/MembersArea/AFTEGL/Glossary.shtml>.
5. Fackler ML, Dougherty PJ. Theodor Kocher and the Scientific Foundation of Wound Ballistics. Surg Gynecol Obstet. 1991;172(2):153-60.
6. Fackler ML. What's wrong with the wound ballistics literature and why. Wound Ballistics Review. 2001;5(1):37-47.
7. Kocher T. Neue beitraege zur kenntnis der wirkungsweise der modernen klein-gewehrgeschosse. Correspondenz-Blatt fuer Schweizer Aerzte. 1879;9:65-71, 133-7.
8. Post SM, Johnson TD. A survey and evaluation of variables in the preparation of ballistics gelatine. Wound Ballistics Review. 1995;2:9-20.
9. La Garde L. Gunshot injuries: how they are inflicted, their complications and treatment. London: John Lane Company; 1916.
10. Fackler ML. La Garde's gunshot injuries: An introduction. Wound Ballistics Review. 1992;1(2):26-30.
11. Fackler ML. Wound ballistics: A review of common misconceptions. Association of Firearm and Toolmark Examiners Journal. 1988;21:25-9.
12. Harvey EN, Korr IM, et al. Secondary damage in wounding due to pressure changes accompanying the passage of high velocity missiles. Surgery. 1947;21(2):218-39.
13. Harvey EN. The mechanism of wounding by high velocity missiles. Philadelphia: American Philosophical Society; 1948. 294-304 p.
14. Hollerman JJ, Fackler ML, Coldwell DM, Ben-Menachem Y. Gunshot wounds: Bullets, ballistics and mechanisms of injury. American Roentgen Ray Society. 1990;155:685-90.

15. Janzon B. Material interactions: simulants. In: Cooper GL, Dudley HAF, Gann DS, Little RA, Maynard RL, editors. *Scientific Foundations of Trauma*. Oxford: Butterworth Heinemann; 1997. p. 26-36.
16. Jussila J. Wound ballistic simulation: assessment of the legitimacy of law enforcement firearms ammunition by means of wound ballistic simulation. Academic Dissertation. University of Helsinki 2005.
17. MacPherson D. *Bullet Penetration: modeling the dynamics and the incapacitation resulting from wound trauma*. California: Ballistics Publications; 1994.
18. Ragsdale BD. Gunshot wounds: historical perspective. *Mil Med*. 1984;149:301-15.
19. Payne LD. Wound ballistics research before 1945. In: Cooper GJ, Dudley HAF, Gann DS, Little RA, Maynard RL, editors. *Scientific Foundations of Trauma*. Oxford: Butterworth Heinemann; 1997. p. 3-11.
20. Journee C. La Force Vive des Balles. *Revue d'Artillerie*. 1907;70:81-120.
21. Hatcher JS. *Textbook of Firearms Investigation, Identification and Evidence*. North Carolina: Small Arms Technical Publishing Company; 1935.
22. Garrison DH. Machine gunner: MG Julian S. Hatcher. *Association of Firearm and Toolmark Examiners Journal*. 1988;20:129-30.
23. Karger B. Penetrating gunshots to the head and lack of immediate incapacitation. I. Wound ballistics and mechanisms of incapacitation. *Int J Legal Med*. 1995;108(2):53-61.
24. Karger B. Penetrating gunshots to the head and lack of immediate incapacitation. II. Review of case reports. *Int J Legal Med*. 1995;108(3):117-26.
25. Karger B. Forensic Ballistics. In: Tsokos M, editor. *Forensic pathology reviews*. 5. NJ: Humana Press; 2008. p. 141-57.
26. Patrick UW. Handgun wounding factors and effectiveness. In: FBI, editor. Quantico, VA: FBI training publication; 1989. p. 2-16.
27. Sellier KG, Kneubuehl BP. *Wound ballistics and the scientific background*. Amsterdam: Elsevier; 1994.
28. Fackler ML. Gunshot wound review: wound ballistics and the scientific background. *Ann Emerg Med*. 1996;28(2):194-203.

29. Fackler ML, Malinowski JA. The wound profile: a visual method for quantifying gunshot wound components. *J Trauma*. 1985;25(6):522-9.
30. Fackler ML, Kneubuehl BP. Applied wound ballistics, what's new and what's true. *Journal of Trauma China*. 1990;6:32-7.
31. Fackler ML. Wound profiles. *Wound Ballistics Review*. 2001;5(2):25-38.
32. Fackler ML. The wound profile and the human body: damage pattern correlation. *Wound Ballistics Review*. 1994;1(4):12-3.
33. Fackler ML. Review of bullet penetration. *Fight Firearm*. 1995:10-3.
34. Pollak S, Rothschild MA. Gunshot injuries as a topic of medicolegal research in the German-speaking countries from the beginning of the 20th century up to the present time. *Forensic Sci Int*. 2004;144(2-3):201-10.
35. Haag L. *Shooting Incident Reconstruction*. Burlington, MA: Academic Press; 2006.
36. Glattstein B, Vinokurov A, Levin N, Zeichner A. Improved method for shooting distance estimation. Part 1. Bullet holes in clothing items. *J Forensic Sci*. 2000;45(4):801-6.
37. Karger B, Nusse R, Schroeder G, Wustenbecker S, Brinkmann B. Backspatter from experimental close-range shots to the head. I. Macrobackspatter. *Int J Legal Med*. 1996;109(2):66-74.
38. Karger B, Billeb E, Koops E, Brinkmann B. Autopsy features relevant for discrimination between suicidal and homicidal gunshot injuries. *Int J Legal Med*. 2002;116(5):273-8.
39. Thali MJ, Kneubuehl BP, Dirnhofer R, Zollinger U. Body models in forensic ballistics: reconstruction of a gunshot injury to the chest by bullet fragmentation after shooting through a finger. *Forensic Sci Int*. 2001;123(1):54-7.
40. Thali MJ, Kneubuehl BP, Zollinger U, Dirnhofer R. The "skin-skull-brain model": a new instrument for the study of gunshot effects. *Forensic Sci Int*. 2002;125(2-3):178-89.
41. Thali MJ, Kneubuehl BP, Zollinger U, Dirnhofer R. A study of the morphology of gunshot entrance wounds, in connection with their dynamic creation, utilizing the "skin-skull-brain model". *Forensic Sci Int*. 2002;125(2-3):190-4.

42. Thali MJ, Kneubuehl BP, Zollinger U, Dirnhofer R. A high-speed study of the dynamic bullet-body interactions produced by grazing gunshots with full metal jacketed and lead projectiles. *Forensic Sci Int.* 2003;132(2):93-8.
43. Wehner HD, Sellier K. Compound action potentials in the peripheral nerve induced by shock-waves. *Acta Chir Scand Suppl.* 1982;508:179-84.
44. Davis JH. Forensic pathology in firearms cases. *Wound Ballistics Review.* 1998;3(4):7-12.
45. Roberts GK. The wounding effect of 5.56mm/.223 law enforcement general purpose shoulder fired carbines compared to 12 GA. shotguns and pistol calibre weapons using 10% ordnance gelatine as a tissue simulant. *Wound Ballistics Review.* 1998;3:26-8.
46. Newgard K. The physiological effects of handgun bullets: the mechanisms of wounding and incapacitation. *Wound Ballistics Review.* 1992;1:12-7.
47. Fackler ML. Incapacitation time, questions and comments. *Wound Ballistics Review.* 1999;4(1):4-8.
48. Aviado DM. Reflexes from stretch receptors in blood vessels, heart and lungs. *Physiol Rev.* 1955;35:247-300.
49. Kumada M, Schmidt RM, Sagawa K, Tan KS. Carotid sinus reflex in response to hemorrhage. *Am J Physiol.* 1970;219(5):1373-9.
50. Westaby S, Blaisdell FW. Ballistic injury to the chest. In: Ryan JM, Rich NM, Dale RF, Morgans BT, Cooper GJ, editors. *Ballistic Trauma, Clinical Relevance in Peace and War.* London: Arnold; 1997. p. 193-206.
51. Janzon B, Hull JB, Ryan JM. Projectile, material interactions: soft tissue and bone. In: Cooper GJ, Dudley HAF, Gann DS, Little RA, Maynard RL, editors. *Scientific Foundations of Trauma.* Oxford: Butterworth Heinemann; 1997. p. 37-52.
52. Amato JJ, Rich NM. Temporary cavity effects in blood vessel injury by high velocity missiles. *J Cardiovasc Surg (Torino).* 1972;13(2):147-55.
53. Ryan JM, Rich NM, Burris DG, Ochsner MG. Biophysics and pathophysiology of penetrating injury. In: Ryan JM, Rich NM, Dale RF, Morgans BT, Cooper GJ, editors. *Ballistics trauma, clinical relevance in peace and war.* London: Arnold; 1997. p. 31-46.
54. Janzon B, Seeman T. Muscle devitalization in high-energy missile wounds, and its dependence on energy transfer. *J Trauma.* 1985;25(2):138-44.

55. Fackler ML. Wound ballistics research of the past twenty years: A giant step backwards. *Wound Ballistics Review*. 2000;4(4):39-40.
56. Di Maio VJM. *Gunshot Wounds, Practical Aspects of Firearms, Ballistics and Forensic Techniques*. New York, Amsterdam, Oxford: Elsevier; 1985.
57. Yamada H. *Strength of biological materials*. Baltimore, Maryland: Williams & Wilkins Company; 1970.
58. Amato JJ, Billy LJ, Lawson NS, Rich NM. High velocity missile injury. An experimental study of the retentive forces of tissue. *Am J Surg*. 1974;127(4):454-9.
59. Holmes Sellors T. Penetrating wounds of the chest. *Postgrad Med J*. 1940;16:89-97.
60. Fackler ML. Handgun bullet performance. *Association of Firearm and Toolmark Examiners Journal*. 1988;20(4):446-8.
61. Fackler ML. Police handgun selection. *Wound Ballistics Review*. 1992;1(3):32-7.
62. Kolsky H. The role of stress waves in penetration processes. In: Labile RC, editor. *Ballistic materials and penetration mechanics*. New York: Elsevier; 1980. p. 185-223.
63. Settles GS. High speed imaging of shock wave, explosions and gunshots. *Am Sci*. 2006;94:22-31.
64. Fackler ML, Peters CE. The shock wave myth (and comment). *Wound Ballistics Review*. 1991;1(1):38-40.
65. Fackler ML. Wound ballistics and the scientific background: Book review. *Wound Ballistics Review*. 1994;2:46-8.
66. Ming L, Yu-Yuan M, Ring-Xiang F, Tian-Shun F. The characteristics of pressure waves generated in the soft target by impact and its contribution to indirect bone fractures. *Journal of Trauma*. 1988;28(1) Supplement:S104-S9.
67. Berlin R. Energy transfer and regional blood flow changes following missile trauma. *J Trauma*. 1979;19(3):170-6.
68. Moss GM. Projectiles: types and aerodynamics. In: Cooper GJ, Dudley HAF, Gann DS, Little RA, Maynard RL, editors. *Scientific Foundations of Trauma*. Oxford: Butterworth Heinemann; 1997. p. 12-25.

69. Rockert H, Berlin R, Dahlgren B, Rybeck B, Seeman T. Cell damage at different distances from wound channels caused by spherical missiles with high impact velocity 1 - 12 hours after injury. *Acta Chir Scand Suppl.* 1979;489:151-8.
70. Rybeck B, Janzon B. Absorption of missile energy in soft tissue. *Acta Chir Scand.* 1976;142(3):201-7.
71. Tikka S, Cederberg A, Rokkanen P. Remote effects of pressure waves in missile trauma. The intra-abdominal pressure changes in anesthetized pigs wounded in one thigh. *Acta Chir Scand Suppl.* 1982;508:167-73.
72. Suneson A, Hansson HA, Seeman T. Peripheral high-energy missile hits cause pressure changes and damage to the nervous system: experimental studies on pigs. *J Trauma.* 1987;27(7):782-9.
73. Suneson A, Hansson HA, Seeman T. Central and peripheral nervous damage following high-energy missile wounds in the thigh. *J Trauma.* 1988;28(1 Suppl):S197-203.
74. Courtney A, Courtney M. Links between traumatic brain injury and ballistic pressure waves originating in the thoracic cavity and extremities. *Brain Inj.* 2007;21(7):657-62.
75. Fackler ML. Wounding patterns of military rifle bullets. *International Defence Review.* 1989;1:59-64.
76. Dutton G, Lyons, T., Roach, S., Dickinson, J. A review of the wounding effects of the Colt AR-15 and FN FAL rifles used by Martin Bryant in the Port Arthur shooting incident April 26 1996, Tasmania, Australia. . *Wound Ballistics Review.* 1998;3(4):41-3.
77. Hays Parks W, Fackler ML. Third international workshop on wound ballistics: Thun, Switzerland, March 28-29. *Association of Firearm and Toolmark Examiners Journal.* 2001;5:17-20.
78. Barnes C. *Cartridges of the world.* 11th ed. Wisconsin: Krause Publications; 2006.
79. Arvidsson PG. NATO Infantry Weapons Standardization, Chairman Weapons and Sensors Working Group, Land and Capability Group 1 - Dismounted Soldier NATO Army Armaments Group [Internet]. 2008 [cited 2012 Jul 18]. Available from: [www.dtic.mil/ndia/2008intl/arvidsson.pdf](http://www.dtic.mil/ndia/2008intl/arvidsson.pdf).
80. Haag LC. 5.56x45mm SS109/M855 bullets: design, exterior and terminal ballistic performance. *Association of Firearm and Toolmark Examiners Journal.* 2001;33:20-3.

81. Janzon B. High Energy Missile trauma - A study of the mechanisms of wounding of muscle tissue. Sweden: University of Goteborg; 1983.
82. Frost GE. Ammunition Making. Washington DC: National Rifle Association of America; 1992.
83. Knudsen PJ, Sorensen OH. The initial yaw of some commonly encountered military rifle bullets. *Int J Legal Med.* 1994;107(3):141-6.
84. Coupland RM, Kneubuehl BP, Rothchild MA, Thali M. Wound ballistics: Basics and Applications. Berlin: Springer; 2011.
85. Fackler ML, Brown AJ, Johnston D. Effect of distance of fire on deformation of the M16A2 M855 bullet in shots penetrating ordnance gelatin tissue simulant. *Wound Ballistics Review.* 2000;4(3):27-9.
86. Killicoat P. World bank post-conflict working paper No. 10. Weaponomics: The global market for assault rifles. Oxford: Oxford University, 2007.
87. Fackler ML. The U.S. M-16 rifle versus the Russian AK-74 rifle. *Am Surg.* 1984;50(9):515-6.
88. Fackler ML, Surinchak JS, Malinowski JA, Bowen RE. Wounding potential of the Russian AK-74 assault rifle. *J Trauma.* 1984;24(3):263-6.
89. Reese M. Luger Tips. 2nd ed. Union City, TE: Pioneer Press; 1992.
90. Hogg IV. Military Small Arms of the 20th Century 7th edn. Wisconsin: Krause Publications; 2000.
91. MacPherson D. The dynamics of tissue simulations. *Wound ballistics review.* 1997;3(1):21-3.
92. Janzon B. Soft soap as a tissue simulant medium for wound ballistic studies investigated by comparative firings with assault rifles Ak 47 and M16A1 into live, anesthetized animals. *Acta Chir Scand Suppl.* 1982;508:79-88.
93. Janzon B. Edge, size and temperature effects in soft soap block simulant targets used for wound ballistic studies. *Acta Chir Scand Suppl.* 1982;508:105-22.
94. Berlin RH, Janzon B, Rybeck B, Schantz B, Seeman T. A proposed standard methodology for estimating the wounding capacity of small calibre projectiles or other missiles. *Acta Chir Scand Suppl.* 1982;508:11-28.
95. Berlin RH, Janzon B, Liden E, Nordstrom G, Schantz B, Seeman T, et al. Terminal behaviour of deforming bullets. *J Trauma.* 1988;28(1 Suppl):S58-62.

96. Schantz B. Aspects on the choice of experimental animals when reproducing missile trauma. *Acta Chir Scand Suppl.* 1979;489:121-30.
97. Salisbury CP, Cronin DS. Mechanical properties of ballistic gelatin at high deformation rates. *Experimental Mechanics.* 2009;49:829-40.
98. North Atlantic Treaty Organisation. Specific tests for kinetic munition: personal vulnerability to small arms fire. AC/225(LG/3-SG1) Section 4.1 [Internet]. NATO Publications; n.d. [cited 2013 Nov 2]. Available from: <http://www.gobooke.org/search.php?q=nato+ac+225+lq%2F3-SG1>.
99. Yang WJ. Heat and mass transport in skin and subcutaneous tissues. In: Ghista DN, editor. *Applied Physiological Mechanics.* New York: Harwood Academic Publishers; 1979. p. 105-42.
100. Cronin DS, Salisbury CP, Horst C, editors. High rate characterization of low impedance materials using a polymeric split Hopkinson pressure bar. SEM Conference and Exposition on Experimental and Applied Mechanics; 2006 June 4-7; St. Louis, MI.
101. Cronin DS. Ballistics gelatin characterization and constitutive modeling. In: Proulx T, editor. *Dynamic Behaviour of Materials: Proceedings of the 2011 Annual Conference on Experimental and Applied Mechanics.* 1: The Society for Experimental Mechanics, Inc; 2011. p. 51-6.
102. Fackler ML. Ordnance gelatin for ballistic studies. *Association of Firearm and Toolmark Examiners Journal.* 1987;19:403-5.
103. Advani SH, Martin RB, Powell WR. Mechanical properties and constitutive equations of anatomical materials. In: Ghista DN, editor. *Applied physiological mechanisms.* New York: Harwood Academic Publishers; 1979. p. 31-96.
104. Nicholas NC, Welsch JR. *Ballistics gelatin.* Pennsylvania: Institute for Non-Lethal Defense Technologies, 2004.
105. Berlin R, Janzon B, Rybeck B, Sandegard J, Seeman T. Local effects of assault rifle bullets in live tissues. Part II. Further studies in live tissues and relations to some simulant media. *Acta Chir Scand Suppl.* 1977;477:5-48.
106. Haag LC. Ballistics gelatin: Controlling variances in preparation and a suggested method for the calibration of gelatin blocks. *Association of Firearm and Toolmark Examiners Journal.* 1989;21:483-9.
107. Berlin R, Gelin LE, Janzon B, Lewis DH, Rybeck B, Sandegard J, et al. Local effects of assault rifle bullets in live tissues. *Acta Chir Scand Suppl.* 1976;459:1-76.



108. Jussila J. Preparing ballistic gelatine--review and proposal for a standard method. *Forensic Sci Int.* 2004;141(2-3):91-8.
109. Fackler ML, Malinowski JA. Ordnance gelatin for ballistic studies: Detrimental effect of excess heat used in gelatin preparation. *Am J Forensic Med Pathol.* 1988;9:218-9.
110. Corzine AJ, Roberts GK. Correlation of ordnance gelatin penetration results between 20% gelatin at 10 degrees C and 10% gelatin at 4 degrees C. *Association of Firearm and Toolmark Examiners Journal.* 1993;25:2-5.
111. MacPherson D. A simplified penetration depth correlation for data taken in non-standard gelatine. *Association of Firearm and Toolmark Examiners Journal.* 1994;2:41-5.
112. Amick DD. Perma-Gel [Internet]. 2009 [cited 2012 Mar 26]. Available from: URL currently inactive & under development.
113. Juliano TF, Forster AM, Drzal PL, Weerasooriya T, Moy P, VanLandingham MR. Multiscale mechanical characterization of biomimetic physically associating gels. *Journal of Material Research.* 2006;21:2084-92.
114. Moy P, Weerasooriya T, Juliano TF, VanLandingham MR, Chen W, editors. Dynamic response of an alternative tissue simulant, physically associating gels (PAG). *Society for Experimental Mechanics Conference*; 2006; St.Louis, MI.
115. Uzar AL, Dakak M, Ozer T, Ogunc G, Yigit DT, Kayaham C, et al. A new ballistic simulant "transparent gel candle" (experimental study). *Turkish Journal Trauma & Emergency Surgery.* 2003;9:204-6.
116. Cook RD, Malkus DS, Plesha ME. *Concepts and applications of finite-element analysis.* New York: Wiley and Sons; 1989.
117. Moaveni S. *Finite Element Analysis: Theory and application with Ansys.* New Jersey: Prentice Hall; 1999.
118. Strait DS, Wang Q, Dechow PC, Ross CF, Richmond BG, Spencer MA, et al. Modeling elastic properties in finite-element analysis: how much precision is needed to produce an accurate model? *Anat Rec A Discov Mol Cell Evol Biol.* 2005;283(2):275-87.
119. Widas P. Introduction to finite element analysis [Internet]. 1997 [cited 2012 Mar 31]. Available from: [www.sv.vt.edu/classes/MSE2094](http://www.sv.vt.edu/classes/MSE2094).
120. Biermann PJ, Ward EE, Cain RP, Carkhuff B, Merkle AC, Roberts JC. Development of a physical human surrogate torso model for ballistic impact and blast. *Journal of Advanced Materials.* 2006;38:3-12.

121. Roberts JC, Biermann PJ, O'Connor JV, Ward EE, Cain RP, Carkhuff BG, et al. Modeling non-penetrating ballistic impact on a human torso. Johns Hopkins APL Technical Digest. 2005;26:84-92.
122. Roberts JC, Merkle AC, Biermann PJ, Ward EE, Carkhuff BG, Cain RP, et al. Computational and experimental models of the human torso for non-penetrating ballistic impact. J Biomech. 2007;40(1):125-36.
123. Footner MJ, Bergeron DM, Swinton RJ. Development and calibration of a frangible leg instrumented for compression and bending. Edinburgh, SA: Defence Science and Technology Organisation, 2006.
124. Bir CA. The evaluation of blunt ballistic impacts of the thorax: Wayne State University, MI; 2000.
125. TNE Systems. Frangible Surrogate Leg [Internet]. 2006 [cited 2012 Apr 2]. Available from: [www.tnesystems.com/fs/html](http://www.tnesystems.com/fs/html).
126. Cronin DS, Williams K, Salisbury C. Physical surrogate leg to evaluate blast mine injury. Mil Med. 2011;176(12):1408-16.
127. Johns Hopkins University. Human surrogate head model testing reveals brain's response to blast [Internet]. 2011 [cited 2012 Apr 3]. Available from: [www.jhuapl.edu/newscenter/stories/st111104.asp](http://www.jhuapl.edu/newscenter/stories/st111104.asp).
128. Bir C, Viano D, King A. Development of biomechanical response corridors of the thorax to blunt ballistic impacts. J Biomech. 2004;37(1):73-9.
129. Silver FH. Biological Materials: Structure, mechanical properties and modeling of soft tissues. New York and London: New York University press; 1987.
130. Tortora GJ, Grabowski SR. Principles of Anatomy and Physiology. New York: John Wiley & Sons Inc.; 2000.
131. Haag MG, Haag LC. Skin perforation and skin simulants. Association of Firearm and Toolmark Examiners Journal. 2002;34:268-81.
132. Powell WR. Pulmonary mechanics. In: Ghista DN, editor. Applied Physiological Mechanics. New York: Harwood Academic Publishers; 1979. p. 483-529.
133. Lee GC, Tai RC. Structural mechanics of the lung. In: Ghista DN, editor. Applied Physiological Mechanics. New York: Harwood Academic Publishers; 1979. p. 381-446.

134. Romanes GJ. Cunningham's Manual of Practical Anatomy: Thorax and Abdomen. Fifteenth ed. New York: Oxford University Press, Inc; 1986.
135. Fung YC. Biomechanics: Mechanical properties of living tissues. 2nd Edition. New York: Springer; 2004.
136. Sinnatamby CS. Last's Anatomy Regional and Applied. 10th edn. UK: Churchill Livingstone; 1999.
137. Valentinuzzi ME, Ghista DN, Nichols WW. Vascular elasticity: Its homeostatic role, simplified parametric characterisation and determination. In: Ghista DN, editor. Applied Physiological Mechanics. New York: Harwood Academic Publishers; 1979. p. 309-72.
138. Gray H. Anatomy of the Human Body. Philadelphia: Lea & Febiger; 1908.
139. Abbrecht PH, Palatt PJ. Function mechanics of the kidney In: Ghista DN, editor. Applied physiological mechanisms. New York: Harwood Academic Publishers; 1979. p. 595-654.
140. Viano DC, King AI. Biomechanics of chest and abdomen impact. In: Bronzino JD, editor. The Biomedical Engineering Handbook 3rd edn. Connecticut: CRC Press; 2006. p. 53-.13.
141. Dale RF, Leppaniemi, A.K., Wetherall, A.P., Peyton, J.W.R., Mattox, K.L. . Abdomen and pelvis. In: Ryan JM, Rich, N.M., Dale, R.F., Morgans, B.T., Cooper, G.J., editor. Ballistics Trauma, Clinical Relevance in Peace and War. London: Arnold; 1997. p. 167-8.
142. DeMuth WE, Jr. High velocity bullet wounds of the thorax. Am J Surg. 1968;115(5):616-25.
143. Kokinakis W, Neades D, Piddington M, Roecher E. A gelatin energy methodology for estimating vulnerability to military rifle systems. Acta Chir Scand Suppl. 1979;489:35-55.
144. Law AM, Kelton WD. Simulation Modeling and Analysis. New York: McGraw Hill; 1991.
145. Committee on Medical Aspects of Automotive Safety. Rating the severity of tissue damage. The abbreviated scale. J Am Med Assoc. 1971;215:277-80.
146. Dillon B, Wang, W., Bouamra, O. A comparison study of the injury score models. Eur J Trauma Emerg Surg. 2006;32:538-47.

147. Stevenson M, Segui-Gomez M, Lescohier I, Di Scala C, McDonald-Smith G. An overview of the injury severity score and the new injury severity score. *Inj Prev*. 2001;7(1):10-3.
148. Champion HR. Mapping of WDMET in AIS 2005 and AIS 2005 Military. Final report for Tech Med Inc. In: Inc TM, editor. VA: Defence Technical Information Center; 2007. p. 1-10.
149. Eberius N, Gillich, P. Survivability analysis for the evaluation of personnel in body armor. Report ARL-RP-304. PASS; Quebec City, CA2010.
150. Baker SP, O'Neill B. The injury severity score: an update. *J Trauma*. 1976;16(11):882-5.
151. Gennarelli TA, Wodzin E, editors. *The Abbreviated Injury Scale 2005 - Update 2008*. Barrington, IL Association for the Advancement of Automotive Medicine; 2008.
152. Gennarelli TA, Wodzin E. AIS 2005: a contemporary injury scale. *Injury*. 2006;37(12):1083-91.
153. Skago NO, Eken T, Hestnes M, Jones JM, Steen PA. Scoring of anatomic injury after trauma: AIS 98 versus AIS 90 - do the changes affect overall severity assessment? *Injury International Journal of the Care of the Injured*. 2007;38:84-90.
154. Tohira H, Jacobs I, Matsuoka T, Ishikawa K. Impact of the version of the abbreviated injury scale on injury severity characterization and quality assessment of trauma care. *J Trauma*. 2011;71(1):56-62.
155. Tohira H, Jacobs I, Mountain D, Gibson N, Yeo A. Comparisons of the Outcome Prediction Performance of Injury Severity Scoring Tools Using the Abbreviated Injury Scale 90 Update 98 (AIS 98) and 2005 Update 2008 (AIS 2008). *Ann Adv Automot Med*. 2011;55:255-65.
156. Tohira H, Jacobs I, Mountain D, Gibson N, Yeo A, Ueno M, et al. Validation of a modified table to map the 1998 Abbreviated Injury Scale to the 2008 scale and the use of adjusted severities. *J Trauma*. 2011;71(6):1829-34.
157. Barnes J, Hassan A, Cuerden R, Cookson R, Kohlhofer J. Comparison of injury severity between AIS 2005 and AIS 1990 in a large injury database. *Ann Adv Automot Med*. 2009;53:83-9.
158. Copes WS, Lawnick M, Champion HR, Sacco WJ. A comparison of Abbreviated Injury Scale 1980 and 1985 versions. *J Trauma*. 1988;28(1):78-86.
159. Palmer C. Adoption of new AIS version by Victoria State Trauma Registry. Melbourne: Royal Children's Hospital, 2010.

160. Palmer CS, Niggemeyer LE, Charman D. Double coding and mapping using Abbreviated Injury Scale 1998 and 2005: identifying issues for trauma data. *Injury*. 2010;41(9):948-54.
161. Palmer CS, Franklyn M. Assessment of the effects and limitations of the 1998 to 2008 Abbreviated Injury Scale map using a large population-based dataset. *Scand J Trauma Resusc Emerg Med*. 2011;19(1):1.
162. Salottolo K, Settell A, Uribe P, Akin S, Slone DS, O'Neal E, et al. The impact of the AIS 2005 revision on injury severity scores and clinical outcome measures. *Injury*. 2009;40(9):999-1003.
163. Baker SP, O'Neill B, Haddon W, Long WB. The injury severity score: a method for describing patients with multiple injuries and evaluating emergency care. *J Trauma*. 1974;14:187-96.
164. Moore L, Lavoie A, Le Sage N, Bergeron E, Emond M, Abdous B. Consensus or data-derived anatomic injury severity scoring? *J Trauma*. 2008;64(2):420-6.
165. Baker SP, O'Neill B, Haddon W, Long W, editors. The injury severity score: development and potential usefulness. 18th Annual Conference of the American Association for Automotive Medicine; 1974.
166. Chawda MN, Hildebrand F, Pape HC, Giannoudis PV. Predicting outcome after multiple trauma: which scoring system? *Injury*. 2004;35(4):347-58.
167. Kilgo PD, Meredith JW, Hensberry R, Osler TM. A note on the disjointed nature of the injury severity score. *J Trauma*. 2004;57(3):479-85; discussion 86-7.
168. MacKenzie EJ. Injury severity scales: overview and directions for future research. *Am J Emerg Med*. 1984;2(6):537-49.
169. MacKenzie EJ, Steinwachs DM, Shankar B. Classifying trauma severity based on hospital discharge diagnoses. Validation of an ICD-9CM to AIS-85 conversion table. *Med Care*. 1989;27(4):412-22.
170. Rutledge R. The Injury Severity Score is unable to differentiate between poor care and severe injury. *J Trauma*. 1996;40(6):944-50.
171. Meredith JW, Evans G, Kilgo PD, MacKenzie E, Osler T, McGwin G, et al. A comparison of the abilities of nine scoring algorithms in predicting mortality. *J Trauma*. 2002;53(4):621-8; discussion 8-9.
172. Sacco WJP, MacKenzie EJP, Champion HR, Davis EG, Buckman RF. Comparison of alternative methods of assessing injury based anatomic descriptors. *J Trauma*. 1999;47:441-6.

173. Stephenson SCR, Langlely JD, Civil ID. Comparing measures of injury severity for use with large databases. *J Trauma*. 2002;53:326-32.
174. Hannan EL, Waller CH, Farrell LS, Cayten CG. A comparison among the abilities of various injury severity measures to predict mortality with and without accompanying physiologic information. *J Trauma*. 2005;58(2):244-51.
175. Osler T, Baker SP, Long W. NISS: A modification of the injury severity score that both improves accuracy and simplifies scoring. *J Trauma*. 1997;43(6):922-5; discussion 5-6.
176. Di Bartolomeo S, Ventura C, Marino M, Valent F, Trombetti S, De Palma R. The counterintuitive effect of multiple injuries in severity scoring: a simple variable improves the predictive ability of NISS. *Scand J Trauma Resusc Emerg Med*. 2011;19:26.
177. Balogh ZJ, Offner PJ, Moore EE, Biffl WL. NISS predicts post injury multiple organ failure better than the ISS. *J Trauma*. 2000;48:624-7.
178. Balogh ZJ, Varga E, Tomka J, Suveges G, Toth L, Simonka JA. The new injury severity score is a better predictor of extended hospitalization and intensive care unit admission than the injury severity score in patients with multiple orthopaedic injuries. *J Orthop Trauma*. 2003;17(7):508-12.
179. Brenneman FD, Boulanger BR, McLellan BA, Redelmeier DA. Measuring injury severity: time for a change? *J Trauma*. 1998;44(4):580-2.
180. Harwood PJ, Giannoudis PV, Probst C, Van Griensven M, Krettek C, Pape HC, et al. Which AIS based scoring system is the best predictor of outcome in orthopaedic blunt trauma patients? *J Trauma*. 2006;60(2):334-40.
181. Husum H, Strada G. Injury Severity Score versus New Injury Severity Score for penetrating injuries. *Prehosp Disaster Med*. 2002;17(1):27-32.
182. Lavoie A, Moore L, LeSage N, Liberman M, Sampalis JS. The New Injury Severity Score: a more accurate predictor of in-hospital mortality than the Injury Severity Score. *J Trauma*. 2004;56(6):1312-20.
183. Lavoie A, Moore L, LeSage N, Liberman M, Sampalis JS. The Injury Severity Score or the New Injury Severity Score for predicting intensive care unit admission and hospital length of stay? *Injury*. 2005;36(4):477-83.
184. Streng M, Tikka S, Leppaniemi A. Assessing the severity of truncal gunshot wounds: a nation-wide analysis from Finland. *Ann Chir Gynaecol*. 2001;90:246-51.
185. Sullivan T, Haider A, DiRusso SM, Nealon P, Shaukat A, Slim M. Prediction of mortality in pediatric trauma patients: new injury severity score

outperforms injury severity score in the severely injured. *J Trauma*. 2003;55(6):1083-7; discussion 7-8.

186. Tay SY, Sloan EP, Zun L, Zaret P. Comparison of the New Injury Severity Score and the Injury Severity Score. *J Trauma*. 2004;56:162-4.

187. Aharonson-Daniel L, Givon A, Stein M, Israel Trauma G, Peleg K. Different AIS triplets: Different mortality predictions in identical ISS and NISS. *J Trauma*. 2006;61(3):711-7.

188. Copes WS, Champion HR, Sacco WJ, Lawnick MM, Keast SL, Bain LW. The Injury Severity Score revisited. *J Trauma*. 1988;28(1):69-77.

189. Russell R, Halcomb E, Caldwell E, Sugrue M. Differences in mortality predictions between Injury Severity Score triplets: a significant flaw. *J Trauma*. 2004;56(6):1321-4.

190. Boyd CR, Tolson MA, Copes WS. Evaluating trauma care: the TRISS method. Trauma Score and the Injury Severity Score. *J Trauma*. 1987;27(4):370-8.

191. Cayten CG, Stahl WM, Murphy JG, Agarwal N, Byrne DW. Limitations of the TRISS method for interhospital comparisons: a multihospital study. *J Trauma*. 1991;31(4):471-81; discussion 81-2.

192. Morris JA, Jr., MacKenzie EJ, Edelstein SL. The effect of pre-existing conditions on mortality in trauma patients. *JAMA*. 1990;263(14):1942-6.

193. Healey C, Osler TM, Rogers FB, Healey MA, Glance LG, Kilgo PD, et al. Improving the Glasgow Coma Scale score: motor score alone is a better predictor. *J Trauma*. 2003;54(4):671-8; discussion 8-80.

194. Teasdale G, Murray G, Parker L, Jennett B. Adding up the Glasgow Coma Score. *Acta Neurochir Suppl (Wien)*. 1979;28(1):13-6.

195. Osler T, Rutledge R, Deis J, Bedrick E. ICISS: an international classification of disease-9 based injury severity score. *J Trauma*. 1996;41(3):380-6; discussion 6-8.

196. Kilgo PD, Osler TM, Meredith W. The worst injury predicts mortality outcome the best: rethinking the role of multiple injuries in trauma outcome scoring. *J Trauma*. 2003;55(4):599-606; discussion -7.

197. Rutledge R, Fakhry S, Baker C, Oller D. Injury severity grading in trauma patients: a simplified technique based upon ICD-9 coding. *J Trauma*. 1993;35(4):497-506; discussion -7.

198. Rutledge R. Injury severity and probability of survival assessment in trauma patients using a predictive hierarchical network model derived from ICD-9 codes. *J Trauma*. 1995;38(4):590-7; discussion 7-601.
199. Rutledge R, Hoyt DB, Eastman AB, Sise MJ, Velky T, Canty T, et al. Comparison of the Injury Severity Score and ICD-9 diagnosis codes as predictors of outcome in injury: analysis of 44,032 patients. *J Trauma*. 1997;42(3):477-87; discussion 87-9.
200. Rutledge R, Osler T, Emery S, Kromhout-Schiro S. The end of the Injury Severity Score (ISS) and the Trauma and Injury Severity Score (TRISS): ICISS, an International Classification of Diseases, ninth revision-based prediction tool, outperforms both ISS and TRISS as predictors of trauma patient survival, hospital charges, and hospital length of stay. *J Trauma*. 1998;44(1):41-9.
201. Osler TM, Cohen M, Rogers FB, Camp L, Rutledge R, Shackford SR. Trauma registry injury coding is superfluous: a comparison of outcome prediction based on trauma registry International Classification of Diseases-Ninth Revision (ICD-9) and hospital information system ICD-9 codes. *J Trauma*. 1997;43(2):253-6; discussion 6-7.
202. Meredith JW, Kilgo PD, Osler T. A fresh set of survival risk ratios derived from incidents in the National Trauma Data Bank from which the ICISS may be calculated. *J Trauma*. 2003;55(5):924-32.
203. Rutledge R, Osler T, Kromhout-Schiro S. Illness severity adjustment for outcomes analysis: validation of the ICISS methodology in all 821,455 patients hospitalized in North Carolina in 1996. *Surgery*. 1998;124(2):187-94; discussion 94-6.
204. Wong SS, Leung GK. Injury Severity Score (ISS) vs. ICD-derived Injury Severity Score (ICISS) in a patient population treated in a designated Hong Kong trauma centre. *McGill J Med*. 2008;11(1):9-13.
205. Medicaid. ICD-10 Changes from ICD-9 [Internet]. Baltimore, MD: US Federal Government; n.d. [cited 2014 Apr 19]. Available from: <http://www.medicaid.gov/Medicaid-CHIP-Program-Information/By-Topics/Data-and-Systems/ICD-Coding/ICD-10-Changes-from-ICD-9.html>.
206. Copes WS, Champion HR, Sacco WJ, Lawnick MM, Gann DS, Gennarelli T, et al. Progress in characterizing anatomic injury. *J Trauma*. 1990;30(10):1200-7.
207. Heard BJ. *Handbook of Firearms and Ballistics: Examining and Interpreting Forensic Evidence*. West Sussex, UK: John Wiley & Sons Inc.; 2008.
208. Jason A. The roots of bad data: The RII revisited. *Wound ballistics review*. 1992;1(2):11.



209. Marshall EP, Sanow EJ. Handgun Stopping Power: The definitive study. Colorado: Paladin Press; 1992.
210. Marshall EP, Sanow EJ. Street Stoppers: The latest handgun stopping power street results. Colorado: Paladin Press; 1996.
211. MacPherson D. Relative incapacitation ballistics. *Wound Ballistics Review*. 1992;1:12-4.
212. Karger B, Kneubuehl BP. On the physics of momentum in ballistics: can the human body be displaced or knocked down by a small arms projectile? *Int J Legal Med*. 1996;109(3):147-9.
213. Fackler ML. Street Stoppers, the latest handgun stopping power results: Book review. *Wound Ballistics Review*. 1997;3(1):27-31.
214. MacPherson D. Sanow strikes out again: literature review. *Wound Ballistics Review*. 1997;3(1):32-3.
215. Roberts GK, Wolberg EJ. Handgun stopping power: The definitive study. *Association of Firearm and Toolmark Examiners Journal*. 1992;24:383-6.
216. Van Maanen M. Discrepancies in the Marshall & Sanow data base: An evaluation over time. *Wound Ballistics Review*. 1999;4:5-7.
217. Glattstein B, Zeichner A, Vinokurov A, Levin N, Kugel C, Hiss J. Improved method for shooting distance estimation. Part III. Bullet holes in cadavers. *J Forensic Sci*. 2000;45(6):1243-9.
218. Glattstein B, Zeichner A, Vinokurov A, Shoshani E. Improved method for shooting distance determination. Part 2--bullet holes in objects that cannot be processed in the laboratory. *J Forensic Sci*. 2000;45(5):1000-8.
219. Hounsfield Test Equipment Ltd. H25KM Operating Instructions Manual. Surrey, UK1987.
220. Competitive Edge Dynamics Ltd. CED M2 Chronograph. China2009.
221. Krstic AR, inventorA surrogate. Australian Patent PQ14241999.
222. Krstic AR, inventor A surrogate. Australian Patent AUPQ89432000.
223. Krstic AR, inventorA surrogate. United States of America Patent 0183025-A12003.

224. Krstic AR, Bergon DM, Bourget D, Softley I, Neades D. Development of a lower leg physical model for enhanced soldier survivability against landmines. The Technical Cooperation Program Technical Report. Edinburgh, SA: Defence Science and Technology Organisation 2002.
225. Krstic AR, Wang JJ, Atkinson RN, Netherway D, Abbott A, Chehade M. Protection against ballistic trauma, the human surrogate: Abstract. External Publications. Edinburgh, SA: Defence Science and Technology Organisation, 2003.
226. Chehade MN, Krstic AR, Henneberg M, Netherway D, Abbott A, Atkinson RN. Human surrogate technology. *J Bone Joint Surg Br.* 2002;84-B:209.
227. Central Bureau of Statistics Israel. Census - Population and Demography [Internet]. 2012 [cited 2012 Apr 5]. Available from: [http://www1.cbs.gov.il/reader/?Mlval=cw\\_usr\\_view\\_SHTML&ID=705](http://www1.cbs.gov.il/reader/?Mlval=cw_usr_view_SHTML&ID=705).
228. Mazur P. Freezing of living cells: mechanisms and implications. *Am J Physiol.* 1984;247(3):C125-42.
229. Mazur P, Rall WF, Leibo SP. Kinetics of water loss and the likelihood of intracellular freezing in mouse ova. Influence of the method of calculating the temperature dependence of water permeability. *Cell Biophys.* 1984;6(3):197-213.
230. Baraibar MA, Schoning P. Effects of freezing and frozen storage on histological characteristics of canine tissues. *J Forensic Sci.* 1985;30(2):439-47.
231. Venkatasubramanian RT, Grassl ED, Barocas VH, Lafontaine D, Bischof JC. Effects of freezing and cryopreservation on the mechanical properties of arteries. *Ann Biomed Eng.* 2006;34(5):823-32.
232. Wang MC, Pins GD, Silver FH. Collagen fibres with improved strength for the repair of soft tissue injuries. *Biomaterials.* 1994;15(7):507-12.
233. Ng BH, Chou SM, Lim BH, Chong A. The changes in the tensile properties of tendons after freeze storage in saline solution. *Proc Inst Mech Eng H.* 2005;219(6):387-92.
234. Huang H, Zhang J, Sun K, Zhang X, Tian S. Effects of repetitive multiple freeze-thaw cycles on the biomechanical properties of human flexor digitorum superficialis and flexor pollicis longus tendons. *Clin Biomech (Bristol, Avon).* 2011;26(4):419-23.
235. Woo SL, Orlando CA, Camp JF, Akeson WH. Effects of postmortem storage by freezing on ligament tensile behavior. *J Biomech.* 1986;19(5):399-404.

236. Hongo M, Gay RE, Hsu JT, Zhao KD, Ilharreborde B, Berglund LJ, et al. Effect of multiple freeze-thaw cycles on intervertebral dynamic motion characteristics in the porcine lumbar spine. *J Biomech.* 2008;41(4):916-20.
237. Gottsauner-Wolf F, Grabowski JJ, Chao EY, An KN. Effects of freeze/thaw conditioning on the tensile properties and failure mode of bone-muscle-bone units: a biomechanical and histological study in dogs. *J Orthop Res.* 1995;13(1):90-5.
238. Leitschuh PH, Doherty TJ, Taylor DC, Brooks DE, Ryan JB. Effects of postmortem freezing on tensile failure properties of rabbit extensor digitorum longus muscle tendon complex. *J Orthop Res.* 1996;14(5):830-3.
239. Giannini S, Buda R, Di Caprio F, Agati P, Bigi A, De Pasquale V, et al. Effects of freezing on the biomechanical and structural properties of human posterior tibial tendons. *Int Orthop.* 2008;32(2):145-51.
240. Venkatasubramanian RT, Wolkers WF, Shenoi MM, Barocas VH, Lafontaine D, Soule CL, et al. Freeze-thaw induced biomechanical changes in arteries: role of collagen matrix and smooth muscle cells. *Ann Biomed Eng.* 2010;38(3):694-706.
241. Rathman GA. The effect of shape on BB and pellet penetration. *Association of Firearm and Toolmark Examiners Journal.* 1987;4:426-31.
242. Wang SC, Bednarski B, Patel S, Yan A, Kohoyda-Inglis C, Kennedy T, et al. Increased depth of subcutaneous fat is protective against abdominal injuries in motor vehicle collisions. *Annu Proc Assoc Adv Automot Med.* 2003;47:545-59.
243. Barnes HA. Thixotropy - a review. *Journal of Non-Newtonian Fluid Mechanics.* 1997;70:1-33.
244. Dewangan KN, Shahmire A, Rakheja S, Marcotte P, editors. Gender effect on the seated body apparent mass response to vertical whole body vibration. *Fourth American Conference on Human Vibration; 2012; Hartford, Connecticut.*
245. Geerligs M, Peters GW, Ackermans PA, Oomens CW, Baaijens FP. Does subcutaneous adipose tissue behave as an (anti-)thixotropic material? *J Biomech.* 2010;43(6):1153-9.
246. Rosen J, Brown JD, De S, Sinanan M, Hannaford B. Biomechanical properties of abdominal organs in vivo and postmortem under compression loads. *J Biomech Eng.* 2008;130(2):210-20.
247. Cronin DS, Falzon, C. Characterization of 10% ballistics gelatin to evaluate temperature, aging and strain rate effects. *Experimental mechanics.* 2011;51:1197-206.

248. Kieser DC, Carr DJ, Leclair SC, Horsfall I, Theis JC, Swain MV, et al. Remote ballistic fractures in a gelatine model--aetiology and surgical implications. *J Orthop Surg Res.* 2013;8:15.
249. Janzon B, Berlin R, Nordstrand I, Rybeck B, Schantz B. Drag and tumbling behaviour of small calibre projectiles in tissue simulant. *Acta Chir Scand Suppl.* 1979;489:57-70.
250. Nennstiel R. How do bullets fly? [Internet]. 2013 [cited 2013 Jan 28]. Available from: [www.nennstiel-ruprecht.de/bullfly/](http://www.nennstiel-ruprecht.de/bullfly/).
251. Tikka S, Bostman O, Marttinen E, Makitie I. A retrospective analysis of 36 civilian gunshot fractures. *J Trauma.* 1996;40(3 Suppl):S212-6.
252. Haag LC. Wound production by ricocheted and destabilized bullets. *Am J Forensic Med Pathol.* 2007;28(1):4-12.